Master's Thesis

Master's Program in Biomedicine

May 2020

Combination Treatments with Regorafenib in Preclinical Models of Colorectal Cancer

Suzanne Perregaard Munch Jørgensen

MABIO5900

60 credits

Faculty of Health Sciences

OSLO METROPOLITAN UNIVERSITY
STORBYUNIVERSITETET

Combination Treatments with Regorafenib in Preclinical Models of Colorectal Cancer

Suzanne Perregaard Munch Jørgensen

Master's Program in Biomedicine

Master thesis, 60 credits

Faculty of Health Sciences, Department of Life Sciences and Health

OSLO METROPOLITAN UNIVERSITY
STORBYUNIVERSITETET

The thesis was carried out at:

Department of Tumor Biology, Institute for Cancer Research

The Norwegian Radium Hospital

Supervisors:

Karianne Giller Fleten

Christin Lund-Andersen

Annette Torgunrud

Kjersti Flatmark

Oslo University Hospital
Norwegian Radium Hospital

PREFACE

Acknowledgements

This project was performed at the Department of Tumor Biology, Institute for Cancer Research, Radium Hospital in the period of August 2019 to May 2020. The financial support for this project was given by Kreftforeningen (Norwegian Cancer Society) and the research group led by Kjersti Flatmark.

Firstly, I would like to thank my main supervisor Karianne Giller Fleten for all the interesting conversations we have had regarding this project, her scientific training and stimulation for me to develop to become an independent researcher in this field. Thanks to my co-supervisors Christin Lund-Andersen and Annette Torgunrud for all the guidance throughout this project. I am also grateful to Kjersti Flatmark, for allowing me to write my master thesis in this research group and letting me be a part of such a great and social research environment. It has been inspiring to study beside everyone at the department, sharing all the knowledge and enthusiasm. I have enjoyed being included in so many ways and for the opportunity to learn and extend my knowledge in cancer biology.

I would also like to thank my family for providing all their support when needed.

Suzanne P. M. Jørgensen

Abstract

Introduction. Colorectal cancer (CRC) is the second most common cancer type in Norway in both genders. Active chemotherapy is used in first-line treatment regimens for patients with metastatic CRC (mCRC), which includes irinotecan and oxaliplatin. Regorafenib is a new promising drug that has demonstrated efficient anticancer activity against mCRC and is currently approved for third line treatment of mCRC, but the clinical use is limited since the effect of regorafenib is short lasted and patients develop resistance over time. Currently there are no other treatment options for mCRC patients with disease recurrence after treatment with all available standard therapies. Drug resistance that affect the tumors sensitivity is still the major cause of treatment failure. Combination treatment with various drugs might improve the response and could also lead to regorafenib being implemented in mCRC treatment at an earlier stage. **Methods**. We examined the drug sensitivity when co-administering regorafenib in combination with irinotecan or oxaliplatin in HCT-116 and SW-620 cell lines, in addition to PDX-models. Combination treatment experiments were performed to identify potential synergistic effects due to interactions between these drugs. Western Blot Immunoassay was performed to investigate the expression of selected proteins and phospho-proteins in different signaling pathways that are influenced by regorafenib and irinotecan, in an attempt to elucidate a possible mechanistic reason for synergistic effects at the protein level. In addition to this, differences in MUC-2 in a PDX-model and topoisomerase-1 expression in cell lines were investigated using RT-qPCR and immunofluorescence respectively. **Results**. Regorafenib, irinotecan and oxaliplatin exhibited anti-proliferative effects as single agents in HCT-116 and SW-620 cell lines. Regorafenib and irinotecan target signaling pathways such as MAPK, PI3K-Akt and JAK/STAT, in addition to inducing apoptosis by interfering with intracellular DNA damage signaling pathways. Combined treatment with regorafenib and irinotecan induced a synergistic anti-proliferative effect in HCT-116 and SW-620 cell lines, while oxaliplatin tended to show additive or antagonistic effects in combination with regorafenib. The synergistic drug effects to regorafenib and irinotecan in the cell lines tended to be reflected in the PMCA-2 model, which also suggests a beneficial outcome with this treatment combination. No mechanistic explanation for the synergistic interactions between regorafenib and irinotecan was observed by performing protein analysis with Western Blotting. Both HCT-116 and SW-620 cells exhibited nuclear expression of topoisomerase-1, but exhibited a cell type dependent reduction of the enzyme after drug treatment. **Conclusions**. While the favorable synergistic actions observed with regorafenib in

combination with irinotecan may suggest this as a promising treatment option, which could improve survival among mCRC patients, the combination with oxaliplatin would not. Further investigation is needed to draw a solid conclusion, and to improve our knowledge about the mechanistic explanation behind the synergistic effects.

Sammendrag

Introduksjon. Kolorektal kreft (CRC) er en av de vanligste kreft formene i Norge for begge kjønn. Aktiv kjemoterapi blir brukt i førstelinjebehandlings regimer for pasienter med metastatisk CRC (mCRC) som inkluderer irinotecan og oxaliplatin. Regorafenib er et nytt lovende medikament som har demonstrert effektiv anti-cancer aktivitet imot mCRC og er i øyeblikket godkjent som tredjelinjebehandling mot mCRC, men den kliniske verdien er begrenset siden effekten av regorafenib er kortvarig og fordi at pasientene utvikler resistens over tid. For øyeblikket er det ingen alternative behandlingsmuligheter for mCRC pasienter med tilbakefall etter behandling med alle tilgjengelige standard terapier. Medikament resistens som reduserer tumor sensitivitet er fremdeles den største årsak til uvirksom behandling. Kombinasjonsbehandling med ulike medikamenter vil muligens kunne forbedre responsen og kan også lede til at regorafenib blir implementert tidligere i behandling imot mCRC. **Metoder**. Vi studerte medikament sensitivitet av regorafenib i kombinasjon med irinotecan eller oxaliplatin i HCT-116 og SW-620 cellelinjer, i tillegg til PDX-modeller. Kombinasjon behandlings eksperimenter ble utført for å identifisere potensielle synergistiske effekter forårsaket av interaksjon mellom disse medikamenter. Western Blot Immunoassay ble utført for å studere uttrykk av utvalgte proteiner og fosforylerte proteiner i forskjellige signalveier som er påvirket av regorafenib og irinotecan, i et forsøk på å belyse potensielle mekanistiske årsaker til synergistiske effekter på protein nivå. I tillegg til dette ble det studert forskjeller i MUC-2 i PDX-modell og topoisomerase-1 uttrykk i celle linjer ved å bruke RT-qPCR og immunofluorescence. **Resultater**. Regorafenib, irinotecan og oxaliplatin utviste anti-proliferende effekter enkeltvis i cellelinjene, HCT-116 og SW-620. Regorafenib og irinotecan påvirker MAPK, PI3K-Akt og JAK/STAT signalveiene, i tillegg til å indusere apoptose ved å interferere med intracellulære DNA skade signalveier. Kombinasjon behandling med regorafenib og irinotecan induserte synergistisk anti-proliferende effekter i HCT-116 og SW-620 cellelinjene, mens oxaliplatin hadde tendens til å utvise additive eller antagonistiske effekter i kombinasjon med regorafenib. De synergistiske effekter med regorafenib og irinotecan i cellelinjene så ut til å bli gjenspeilet i PMCA-2 modellen, som igjen impliserer fordelene ved bruk av denne behandlingen. Ingen mekanistisk forklaring på den synergistiske interaksjonen mellom regorafenib og irinotecan ble observert ved å utføre proteinanalyse med Western Blotting. Både HCT-116 og SW-620 cellene utviste nukleært uttrykk av topoisomerase-1, men utviste celle type avhengig reduksjon av enzymet etter medikament behandling. **Konklusjon**. Mens de ønskede synergistiske effekter observert med

regorafenib kombinert med irinotecan kan implisere dette som en lovende alternativ til behandling, som kan forbedre overlevelse blant mCRC pasienter, så tyder det på at kombinasjon med oxaliplatin ikke vil dette. Videre undersøkelser er nødvendig for å komme fram til en solid konklusjon, og for å få bedre forståelse av de mekanistiske forklaringene som står bak synergistiske effekter.

Abbreviations

ANOVA	Analysis of Variance
APC	Adenomatous polyposis coli
ATM	Ataxia Telangiectasia Mutated
ATCC	American Type Culture Collection
BCA	Bicinchoninic Acid
BSA	Bovine Serum Albumin
CCD	Charge-Coupled Device
cDNA	Complementary DNA
CI	Combination index
CMS	The consensus molecular subtypes
CPT	Camptothecin
CRC	Colorectal Cancer
CRS	Cytoreductive surgery
DACH	1,2-diaminocyclohexane
DAPI	4´,6-diamidino-2-phenylindole
DMSO	Dimethyl Sulfoxide
dNTP	Deoxynucleotide triphosphate
DSB	DNA double strand break
DTT	Dithiothreitol
ECL	Enhanced Chemiluminescence
EDTA	EthyleneDiamineTetraacetic Acid
EGFR	Epidermal growth factor receptor
EMT	Epithelial mesenchymal transformation
EtOH	Ethanol
5-FU	5-fluorouracil

FAP	Familiar Adenomatous Polyposis coli
FBS	Fetal bovine serum
FDA	Food and Drug Administration
FGFR	Fibroblast growth factor receptor
FOLFIRI	5-fluorouracil/leucovorin/irinotecan
FOLFOX	5-fluorouracil/leucovorin/oxaliplatin
FOTS	Forsøksdyrforvaltningens Tilsyns og Søknadssystem
GPCR	G-protein coupled receptor
H&E	Hematoxylin and Eosin
HCC	Hepatocellular carcinoma cells
HIPEC	Hyper-thermic intraperitoneal chemotherapy
HNPCC	Hereditary Non-polyposis Colorectal Cancer
HRP	Horseradish Peroxidase
HSD	Honest Significant Difference
IF	Immunofluorescence
JAK/STAT	Janus kinase/ Signal Transducer and Activators of Transcription
kDa	Kilodalton
LAF	Laminar Air Flow
LDS	Lithium Dodecyl Sulfate
LV	Leucovorin
MAPK	Mitogen Activated Protein Kinase
MCA	Mucinous colorectal adenocarcinoma
mCRC	Metastatic colorectal cancer
MEP	Median effect principle
MOPS	3-(N-morpholino) propanesulfonic acid
MSI	Microsatellite instability

MTS	(3-(4,5-dimethylthiazol-2-yl)-5-(3-carboxymethoxyphenyl)-2-(4-sulfophenyl)-2H-tetrazolium)
mTOR	Mammalian Target of Rapamycin
OS	Overall Survival
PARP	Poly ADP-ribose Polymerase
PBS	Phosphate Buffered Saline
PDK	Phosphoinositide dependent kinase
PDGFR	Platelet-derived growth factor receptor
PDX	Patient derived xenograph
PFA	Paraformaldehyde
PFS	Progression free survival
PIAS	Protein inhibitor of activated STAT's
PIK3CA	Phosphatidylinositol-4,5-Bisphosphate 3-Kinase Catalytic Subunit Alpha
PI3K	Phosphatidylinositol 3-kinase
PM	Peritoneal metastasis
PTEN	Phosphatase and tensin homologue
PTP	Protein-tyrosine phosphatase
PUMA	p53-upregulated modulator of apoptosis
RAF	Rapidly accelerated fibrosarcoma
REK	Regional Committees for Medical and Health Research Ethics
Rpm	Revolutions per minute
RPMI	Roswell Park Memorial Institute
RR	Response rate
RT	Room temperature
RTK	Receptor tyrosine kinases
RT-qPCR	Real Time Quantitative Polymerase Chain Reaction

SEM	Standard Error of the Mean
SDS-PAGE	Sodium dodecyl sulfate polyacrylamide gel electrophoresis
SH2	Src-homology-2
SHP-1	SH2 domain containing phosphatase 1
SOCS	Suppressors of cytokine signaling
SPSS	Statistical Package for The Social Sciences
SSB	Single strand breaks
STR	Short Tandem Repeat
TBST	Tris Buffered Saline with Tween 20
TNM	Tumor Node Metastasis
UGT	Uridine diphosphate glucuronosyl-transferase
VEGF	Vascular endothelial growth factor
WT	Wildtype

Table of contents

1 INTRODUCTION 1

1.1. Cancer 1

1.2. Colorectal cancer 2

1.2.1. Classification of colorectal cancer staging 3

1.2.2. Epidemiology 4

1.2.3. Metastasis in colorectal cancer 4

1.2.4. Treatment of colorectal cancer 6

1.3. Chemotherapeutics drugs and targeted therapy 7

1.3.1. Regorafenib 7

1.3.2. Irinotecan 10

1.3.3. Oxaliplatin 10

1.3.4. Drug interaction 11

1.4. Signaling pathways 11

1.4.1. MAPK and PI3K-Akt signaling pathways 12

1.4.2. JAK/STAT signaling pathway 13

1.4.3. DNA damage signaling pathway 14

2 AIM OF THE PROJECT 16

3 MATERIALS AND METHODS 17

3.1. Cell lines 17

3.1.1. Cell cultures 17

3.1.2. Passaging of cells 18

3.1.3. Cell counting 19

3.1.4. Cell thawing and freezing 19

3.1.5. Drugs 19

3.1.6. Mycoplasma testing 20

3.2. Ex vivo culture 20
3.3. Measurement of cell viability 21
3.4. Protein analysis 22
3.4.1. Harvesting of cells 22
3.4.2. Protein isolation 23
3.4.3. Measurement of protein concentration 23
3.5. Western Blot Immunoassay 24
3.5.1. NuPAGE Bis-Tris gel electrophoresis 25
3.5.2. Transfer and immunostaining 26
3.6. Gene expression analysis 27
3.6.1. RNA extraction 27
3.6.2. NanoDrop 28
3.6.3. cDNA synthesis 28
3.6.4. Real Time Quantitative Polymerase Chain Reaction 29
3.7. Immunohistochemistry 30
3.8. Immunofluorescence 31
3.9. Data and statistical analysis 32
4 RESULTS 33
4.1. Single drug sensitivity in HCT-116 and SW-620 cells 33
4.1.1. Regorafenib mono-treatment in HCT-116 33
4.1.2. Regorafenib mono-treatment in SW-620 35
4.1.3. Irinotecan mono-treatment in HCT-116 37
4.1.4. Irinotecan mono-treatment in SW-620 39
4.1.5. Oxaliplatin mono-treatment in HCT-116 41
4.1.6. Oxaliplatin mono-treatment in SW-620 42
4.2. Sensitivity of HCT-116 and SW-620 to combination treatments 43
4.2.1. Combination treatment with regorafenib and irinotecan in HCT-116 43

4.2.2. Combination treatment with regorafenib and irinotecan in SW-620 46
4.2.3. Combination treatment with regorafenib and oxaliplatin in HCT-116 49
4.2.4. Combination treatment with regorafenib and oxaliplatin in SW-620 50
4.3. Morphological changes in HCT-116 and SW-620 cells induced by drug treatment 51
4.4. Combination experiments in mucinous PDX- models 53
4.4.1. Combination experiments with regorafenib and irinotecan 53
4.4.2. MUC-2 gene expression in drug exposed mucin 55
4.5. Microscopy of tissue sections from mucin 56
4.6. Nuclear topoisomerase-1 expression visualized by immunofluorescence 57
5 DISCUSSION 60
5.1. Regorafenib inhibits cell growth in both cell lines and induces apoptosis in SW-620 cells 60
5.2. Regorafenib combined with irinotecan exerted synergistic effects in HCT-116 and SW-620 cells 62
5.3. Combination therapy with regorafenib and oxaliplatin in HCT-116 and SW-620 cells 64
5.4. Heterogeneous combination therapy response in PDX-models 64
5.5. Combination therapy may result in additional reduction of MUC-2 expression in PDX-model 65
5.6. Regorafenib combined with irinotecan may results in additional reduction of topoisomerase-1 activity in HCT-116 cells 66
5.7. Methodological discussion 68
6 CONCLUDING REMARKS 70
7 REFERENCES 71
8 APPENDIX i
Appendix A: Materials and equipment i
Appendix B: Reagent preparation iii
Appendix C: Antibodies used for Western Blotting iv
Appendix D: Results from ID testing of cell lines v

Appendix E: Determination of cell density for experiments..... vi

Appendix F: Combination index and cut-off values..... vii

Appendix G: Cell viability measurement with MTS vii

1 INTRODUCTION

1.1. Cancer

Cancer is a term that comprises a large group of diseases with unregulated abnormal proliferation of cells which form tumors. Tumors are called benign when the cells remain confined to original location without invading surrounding tissue or having the ability to spread. Malignant tumors, however, have this invading capability and can metastasize to other parts of the body. Benign and malign tumors are classified depending on which type of cells they arise from. Carcinomas are malignancies of epithelial cells, sarcomas are solid tumors of connective tissue and leukemias or lymphomas are from blood forming cells and cells of the immune system. Cancer arises when cells do not respond to signals controlling normal cell behavior [1]. For normal human cells to develop into a neoplastic disease they require multiple molecular changes, like the accumulation of somatic genetic mutations [2]. The cells need selection for certain capabilities known as the hallmarks of cancer, proposed by Hanahan and Weinberg (Figure 1) [3], where genomic instability is one of the mentioned cancer hallmarks. Genes with mutational changes are classified according to their functional effect on encoded proteins. Proto-oncogenes are genes involved in regulation of proliferation and cell growth, and by dominant gain-of-function mutations, it can change into an oncogene. Tumor suppressor genes are involved in inhibition of proliferation or promote apoptosis, which through recessive loss-of-function mutations, can lose their function and become oncogenic. Together, these genes drive disease progression [4]. Both genetic alterations, and epigenetics like DNA methylation and histone modifications, can contribute to cancer development [2]. Even though there are many different forms of cancer, there are certain types that are more frequent than others [1].

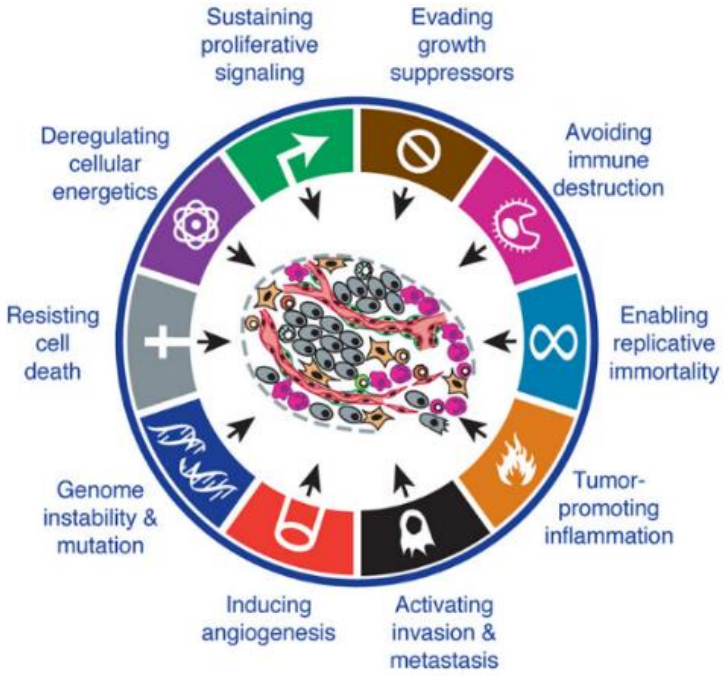

Figure 1: Overview of the proposed Hallmarks of cancer [3]. Modified and reprinted with permission from Elsevier.

1.2. Colorectal cancer

Colorectal cancer (CRC) are dysplastic adenocarcinomas which typically develops from focal changes within benign, precancerous polyps that protrude into the epithelial lining of the colon or rectum in the digestive system [5, 6]. CRC is caused by progressive disruption of intestinal epithelial cell proliferation. Most cases of CRC are sporadic, but it can also develop because of inheritance in the family, like familiar adenomatous polyposis coli (FAP) caused by a single dominant inherited germline mutation in the adenomatous polyposis coli (APC) tumor suppressor gene, and hereditary non-polyposis colorectal cancer (HNPCC (Lynch syndrome)) caused by a DNA mismatch repair gene mutation [7]. Aging is the biggest risk factor for sporadic CRC [5]. The fact that the incidence of CRC in Europe increases is largely due to the ageing of the population, but could also indicate that lifestyle and environmental factors have an impact [5]. There are many other known risk factors related to development of CRC such as gender, smoking, obesity, nutritional practice with high consumption of red and processed meat, ethnical background, family or personal history of colorectal cancer and polyps, inflammatory conditions like Crohn disease and ulcerative colitis [8].

Inactivation of tumor suppressor genes, DNA repair systems and oncogene activation can give advantageous growth conditions for the tumor, which can results in normal epithelium developing to adenomatous polyps to become invasive CRC [5]. CRC has high genetic heterogeneity, and clinical consequences of individual mutations are therefore difficult to determine [9]. In order of decreasing frequencies *TP53*, *KRAS*, *PIK3CA*, *BRAF* and *PTEN* are the most commonly altered genes in CRC [10]. The consensus molecular subtypes (CMS) classification is considered the best system available for CRC [11]. This is a gene-expression based system that classifies CRC into four subtypes with distinct biological characteristics; the CMS1 subtype having microsatellite instability (MSI), increased immune activation and hypermutations; the CMS2 termed canonical subtype with prominent upregulation of WNT-MYC signaling pathways; the CMS3 subtype with distinct epithelial and metabolic dysregulation, and CMS4 displaying epithelial mesenchymal transformation (EMT), stromal invasion and angiogenesis [11].

1.2.1. Classification of colorectal cancer staging

The development of CRC happens in different growth stages, where the stage of disease at time of diagnosis is related to survival rate [6]. Even though screening techniques have been improved, many cases of colorectal cancer are detected at advanced stage of the disease [12]. The Tumor Node Metastasis (TNM) system is the preferred classification for CRC staging and is done according to local primary tumor growth into intestinal wall (T), regional lymph node metastasis (N) and distant metastasis (M) [13]. The system categorizes the cancer into stages dependent on the tumor progression or its characteristics (Table 1). Once the patients are diagnosed, the staging of the disease is an important factor, which affects choice of therapy and treatment planning. Patients diagnosed with stage I CRC are treated with surgery alone. Stage II involves no lymph node metastasis, and adjuvant chemotherapy has not shown to have any beneficial effects at this stage. In stage III, the cancer cells have spread to the lymph nodes and are treated with both surgery and chemotherapy. Stage IV involves metastasis to distant organs and is usually incurable [13].

Table 1: Simplified overview of the TNM classification system for CRC including sub-categories of the different stages. Zero refers to no presence of lymph node or distant metastasis. The CRC is metastatic if it is classified as stage IV [14].

Stage	T	N	M
I	T1, T2	N0	M0
II	T3, T4	N0	M0
III	Any T	N1, N2	M0
IV	Any T	Any N	M1

1.2.2. Epidemiology

In 2018, the estimated amount of new CRC cases was 1.8 million and caused 880.000 deaths on a global basis [15]. In Norway there were 34.190 new cases of cancer in 2018, where the total incidence for CRC were 4428 cases [16]. CRC constitutes the second most common type of cancers in Norway for both genders after prostate and breast cancer. In Norway, the incidence and mortality rates of CRC are among the highest in the world. In 2017, there were 11.016 deaths from cancer in Norway with colorectal cancer accounting for 14% (new data for 2018 was not available from The Cancer Registry of Norway) [16]. In the last 30 years the incidence of colon cancer has increased, while the incidence of rectal cancer has declined slightly, but remained relatively stable. The 5-year survival rate in Norway for colon cancer is 65% for men and 68% for women while for rectal cancer it is 69% for both genders. The overall survival (OS) tends to be lower with increased age at diagnosis. Furthermore, the cases of colon cancer are equally distributed among men and woman, while rectal cancer is more commonly found in men [16]. The highest incidence rates of CRC are in developing countries, which are thought to be related to lifestyle factors. The incidence of CRC varies worldwide, where Africa and Asia have the lowest, and Europe and North America have the highest [15].

1.2.3. Metastasis in colorectal cancer

CRC is one of the leading causes of cancer associated mortality globally, due to tumor recurrence and metastatic disease, which is closely related to the tumor cells proliferative and invasive capabilities [17]. In mCRC patients, the cancer will spread to other organs like the liver, lung and peritoneum [18], where liver metastasis is the most common and peritoneal metastasis (PM) is the second most common metastatic site [19]. Most of the patients that

develop metastases have unresectable tumors [20]. The cancer cells spread lymphatic, through the blood or transcoelomic to the peritoneum by dissociating from primary tumor [21]. PM develops in 5-15% of patients at time of CRC diagnosis (synchronous metastasis) and is associated with poor prognosis and life quality [19]. For patients with CRC, the overall 5-year survival rate is 64%, while for patients with metastatic CRC the rate is decreased to 12% after diagnosis [22]. Figure 2 illustrates that the survival differs between the metastatic sites.

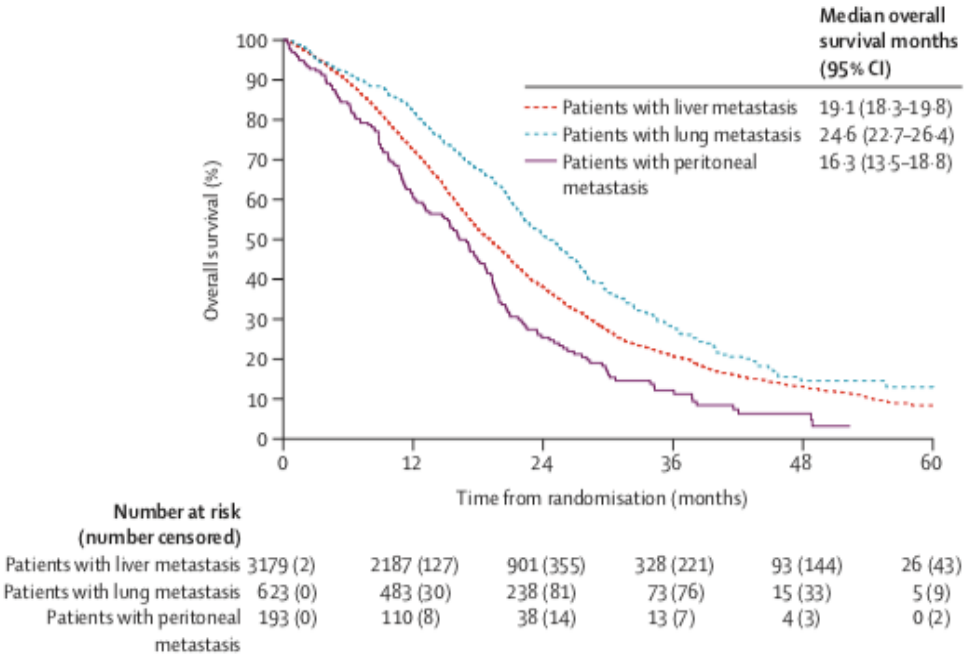

Figure 2: Overall survival (OS) for patients with colorectal cancer and only one-site metastasis. Patients with peritoneal metastasis have lower OS compared to patients with liver and lung metastasis [23]. Printed with permission from Elsevier.

Peritoneal metastases are metastatic diseases confined to the peritoneum [24]. Mucinous colorectal adenocarcinoma (MCA), which represents a distinct subtype of CRC, frequently develops metastatic disease, limited to the peritoneum. Patients with MCA accumulate extracellular mucin produced by secreting cells and are more frequently diagnosed at an advanced stage [24], which increases the need for specialized treatment for these patients. Mucins are membrane-associated or secretory high-molecular weight glycoproteins, where the secretory mucins MUC-2 and MUC-5AC are the most predominant glycoproteins in mucinous colorectal adenocarcinoma. The mucin encoded gene MUC-2 is one of the best characterized, where overexpression of MUC-2 is the most evident distinction between mucinous and non-mucinous adenocarcinoma [25]. Mucins normally form a physical

protective barrier for epithelia in the gastrointestinal tract, where different mucin types are synthesized and expressed dependent on location. Mucin has been used as a target for molecular therapy, but the overexpression of MUC-2 might form a mucous layer as a protective shield, so the antitumor therapy does not lead to any effect and promotes tumor progression. It is still contradictory if the expression of MUC-2 has any impact on tumor development and the underlying mechanism for extensive mucin production in tumors are still unknown [26].

1.2.4. Treatment of colorectal cancer

Colorectal cancer is a highly treatable and often curable disease, if detected early enough [27]. The treatment prognosis for early stage CRC are approximately 90% cure rate, while it is reduced to below 10% for advanced stage CRC [28]. Today there is no alternative treatment for patients with unresectable metastatic colorectal cancer, which result in progression after all currently available conventional therapies. It is therefore important to find new treatment options for long-term survival among the patients with disease progression, since many of the patients maintain a good performance status and can be responsive to further treatment [20]. Chemotherapy with 5-fluorouracil (5-FU)/ leucovorin (LV) in combination with either irinotecan (FOLFIRI), oxaliplatin (FOLFOX) and targeting therapy are used in standard management against mCRC [29]. Targeting agents against mCRC like anti-vascular endothelial growth factor (VEGF) monoclonal antibodies (bevacizumab) and monoclonal antibodies (cetuximab), blocking the activity of epidermal growth factor receptor (EGFR) for patients without *KRAS* mutations (*KRAS* wildtype (WT)), are used [20]. Even though CRC with PM are categorized as metastatic, it is considered as a locoregional disease which has a specific spreading pattern, often localized in the abdomen [30]. Local disease of CRC with PM is treated with cytoreductive surgery (CRS) and hyper-thermic intraperitoneal chemotherapy (HIPEC) [30].

Cytoreductive surgery involves removal of all visible tumor tissue in the abdomen. Microscopic tumor cells might be left behind and can lead to recurrence of the cancer. Therefore, the abdominal cavity of the patient is filled up with heated chemotherapy by using a perfusion device, which circulates it throughout the abdomen, as part of the same operative procedure. Treatment with hyper-thermic intraperitoneal chemotherapy (HIPEC) with temperatures between 40°C and 44°C becomes cytotoxic for cancer cells in tumors with low blood perfusion, since the drugs have easier access to such areas [31]. Several drugs like

mitomycin C also have an enhanced effect when increasing the temperature [31]. The patients that receive this treatment are selected according to their likeliness of having any beneficial effect, which depends on factors like age, general condition and tumor biology [30]. HIPEC is now considered as standard treatment for selected patients with peritoneal cancer, mesothelioma and pseudomyxoma peritonei, but also peritoneal cancer from gastric and ovarian cancer [30].

1.3. Chemotherapeutics drugs and targeted therapy

Conventional chemotherapeutic drugs like 5-FU [32], irinotecan [33], and oxaliplatin [34] and targeted therapy with regorafenib [20, 35] have shown promising results by increasing the median overall survival and median progression free survival (PFS) of advanced CRC patients. Combination therapy is used widely in treatment for cancer diseases. The reason behind this approach in chemotherapeutic research is to achieve a synergetic effect between drugs, which can lead to dose and systematic toxicity reduction and minimize or delay induction of drug resistance. Combination therapy is also used because multiple drugs have effects on multiple targets and cell subpopulations [36]. But the efficacy of these drugs is limited due to preexisting intrinsic resistance mechanisms, the cancer cells' ability to become resistant [12], and the side effects of treatments are substantial due to a lack of specificity [37]. In this project we examine how regorafenib and irinotecan in combination and as single agents, affect the MAPK (Mitogen-activated protein kinase), PI3K-Akt (phosphatidylinositol 3- kinase), JAK/STAT (Janus kinase/Signal Transducer and Activators of Transcription) and DNA-damage signaling pathways. Each of these signaling pathways are described separately in section 1.4.

1.3.1. Regorafenib

Regorafenib (Stivarga) is a relative new drug and was approved in 2013 by the Food and Drug Administration (FDA) for treatment of advanced mCRC and gastrointestinal stromal tumors after the patients had progressed from first and second line of treatment [38]. This approval was based on the publication of the international CORRECT trial study, where the efficacy of regorafenib was compared with a placebo group [20, 39] (Figure 4). The fact that these patients do not respond to chemotherapy makes more efficient treatment options and the need to understand the molecular mechanisms for resistance to anticancer therapies very

important. Regorafenib is a multi-tyrosine kinase inhibitor for a wide range of tyrosine kinases, which is activated in tumor cells such as VEGFR, platelet-derived growth factor receptor (PDGFR), fibroblast growth factor receptor (FGFR), rapidly accelerated fibrosarcoma (B-RAF), that facilitate angiogenesis, oncogenesis, tumor growth and cancer cell survival (Figure 3) [22].

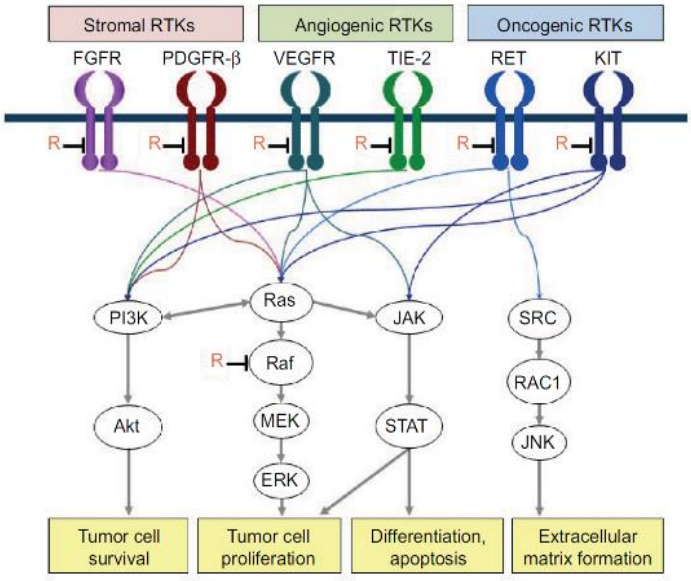

Figure 3: Illustration of the broad-spectrum activity of regorafenib in the cells. Regorafenib is active against different membrane bound receptor tyrosine kinases (RTK's), but also inhibits intracellular signaling kinases such as RAF [40]. Printed with permission from Dove Medical Press.

These kinases are a part of various signaling pathways and can influence important functions in the cells. Regorafenib is associated with pro-apoptosis activity, synergistic anti-proliferation and suppression of tumor angiogenesis mediator inhibition [38, 41].

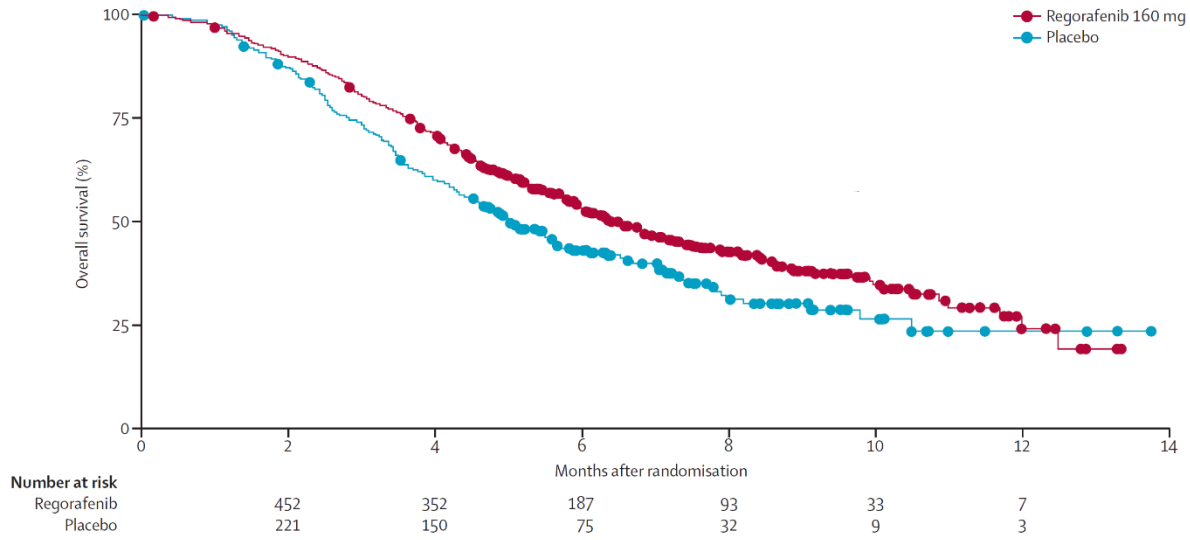

Figure 4: Overall survival by administration of regorafenib as monotherapy **[20]**. Modified and printed with permission from Elsevier.

New trials have been initiated to figure out if regorafenib can treat other cancers in liver, lung and esophageal for instance [37]. Unfortunately, the clinical use is limited because the effect of regorafenib is short lasted and the patients develop resistance over time [42]. As monotherapy regorafenib has extended patients survival by 1-2 months [20]. This makes regorafenib the first novel small-molecule multi-kinase inhibitor with survival benefits for mCRC patients with disease progression after treatment failure with all available therapies [20]. The main effect of regorafenib appears to be cytostatic rather than cytotoxic, where regorafenib monotherapy leads to disease stabilization and less tumor shrinkage [43]. This treatment is also associated with a mild severity of adverse events, where the most frequently seen is pain, fatigue, hand-foot skin reaction, diarrhea, decreased appetite, hypertension, infection and liver dysfunctions with elevated liver enzymes. Based on current evidence, regorafenib is a valuable treatment option in resistant mCRC patients with poor prognosis [43].

1.3.2. Irinotecan

Irinotecan (Camptosar) is a topoisomerase-1 interacting agent and a key molecularly targeted anticancer drug in mCRC treatment regimen [44]. It is a semisynthetic analogue to camptothecin (CPT), which is an extract from the Chinese tree *Camptotheca acuminate*. The active metabolite of irinotecan is 7ethyl-10-hydroxycamptothecin (SN-38) and its conversion is done by the enzyme carboxylesterase in the body. Irinotecan exerts antitumor activity by binding to and inhibiting catalytic activity of nuclear DNA topoisomerase I enzyme, which results in an inhibition of cell division of the cancer cells. Its catalytic activity results in formation of enzyme-DNA cleavage complexes with DNA double stand breaks [44]. DNA synthesis cannot be completed, which activates DNA damage checkpoint responses involving Ataxia Telangiectasia Mutated (ATM) kinase activation. It induces cell cycle arrest to prevent further replication of damaged DNA and eventually causes cell death [45]. Normally the function of the topoisomerase enzyme is to maintain and modulate the DNA structure. The enzyme avoids supercoiling of the DNA by cutting the double stranded DNA and splicing it back together. There are two members of the topoisomerase family; topo I and topo II, with involvement in DNA replication, transcription and repair [46]. Earlier studies in patients not responding, or with disease progression after 5-FU monotherapy treatment, showed increased survival among these patients when combining their treatment with irinotecan [47].

1.3.3. Oxaliplatin

Oxaliplatin (Eloxatin) is a third-generation platinum compound characterized by a 1.2-diaminocyclohexane (DACH) [48]. This drug is a cisplatin analog developed to overcome the significant side toxicity caused by cisplatin in anticancer treatment and to retain the widespread spectrum of activity. Oxaliplatin was launched in 1999 in Europe and is the first platinum-based drug with anticancer effect in mCRC. It produces inter- and intra-strand platinum-DNA adducts by crosslinking with specific base sequences in the DNA. DACH will prevent the mismatch repair enzyme complex and thus prevent DNA replication and transcription. It is thought that it reduces cell viability via apoptosis induction caused by this DNA damage. This has made oxaliplatin exert a higher cytotoxic and DNA synthesis inhibitory effect, compared to cisplatin [48]. Oxaliplatin as a single agent has shown modest activity against CRC, but in oxaliplatin based combination regimens with other drugs, the antitumor activity got higher in metastatic colorectal cancer patients [49]. Furthermore, oxaliplatin has exerted biochemical synergism in combination with irinotecan [33]. In a phase

II study, the addition of oxaliplatin in triplet combination regimen for pretreated patients with resistance against leucovorin and 5-FU demonstrated a high response rate (RR) of 46% to this treatment. 5-FU as a single agent produced a RR of 10-15% [50].

1.3.4. Drug interaction

Sometimes, drug interactions may improve or inhibit the efficacy of the each other. In some cases, it can therefore be beneficial to combine different drugs in cancer treatment to improve the outcome of treatment in patients. If the combination of drugs is more effective than the sum of the individual effects of each drug alone, it is defined as synergism, where one drug improves the action of the second drug [36]. The effect of the drug combination is defined as additive when the combined effect of the drugs is equal to the sum of the effect of each of the agents alone. Antagonism is the opposite of synergism and is defined as when the combination of the drugs becomes less effective together because one of the drugs counteracts the actions of the second drug [36]. CalcuSyn software can be used to evaluate the effects of such drug interactions.

1.4. Signaling pathways

Cells communicate and respond to environmental changes through signal transduction pathways [51]. In CRC, many different extracellular signaling regulated pathways have been implicated to contribute to disease development and progression. Signaling cascades in pathways such as MAPK and PI3K-Akt (involving ribosomal protein S6 kinase) are frequently involved in CRC [52], in addition to the JAK/STAT pathway [53].

1.4.1. MAPK and PI3K-Akt signaling pathways

Regorafenib targets the MAPK transduction pathway network, belonging to a family of many serine/threonine kinases [40]. The MAPK pathway is located downstream of many growth-factor receptors, where one of these receptors include epidermal growth factor, which is often seen to be overexpressed in CRC [54]. The downstream substrates of this pathway regulate and control key physiological functions of cells such as proliferation, differentiation and apoptosis [54]. The cell cycle is a regulatory system affected by external signals such as growth factors activating signal transduction cascades by binding to membrane receptors or internal signals caused by mutations in genes like *RAS*. Earlier studies have shown the importance of the MAPK pathway in pathogenesis, progression, oncogenic behavior of human CRC [54] and a link between the p38 MAPK signal pathway and sensitivity to irinotecan have been reported [55]. *KRAS* represents about 86% and *NRAS* 14% of *RAS* oncogene mutations in CRC [56].

The PI3K-Akt signal pathway can be activated through different mechanisms like tyrosine kinase growth receptors, cell adhesion molecules (integrins), G-protein coupled receptors (GPCR) and oncogenes (*RAS*) [51]. This pathway has a central role in the regulation of cellular processes such as cell survival, proliferation and differentiation [57]. Phosphatidylinositol-4,5-Bisphosphate 3-Kinase Catalytic Subunit Alpha (*PIK3CA*) mutations is observed in 10-20% of cases and is associated with *KRAS* mutations in CRC [56]. A simplified overview of the MAPK and PI3K-Akt signal transduction pathway and their downstream mediators can be seen in Figure 5.

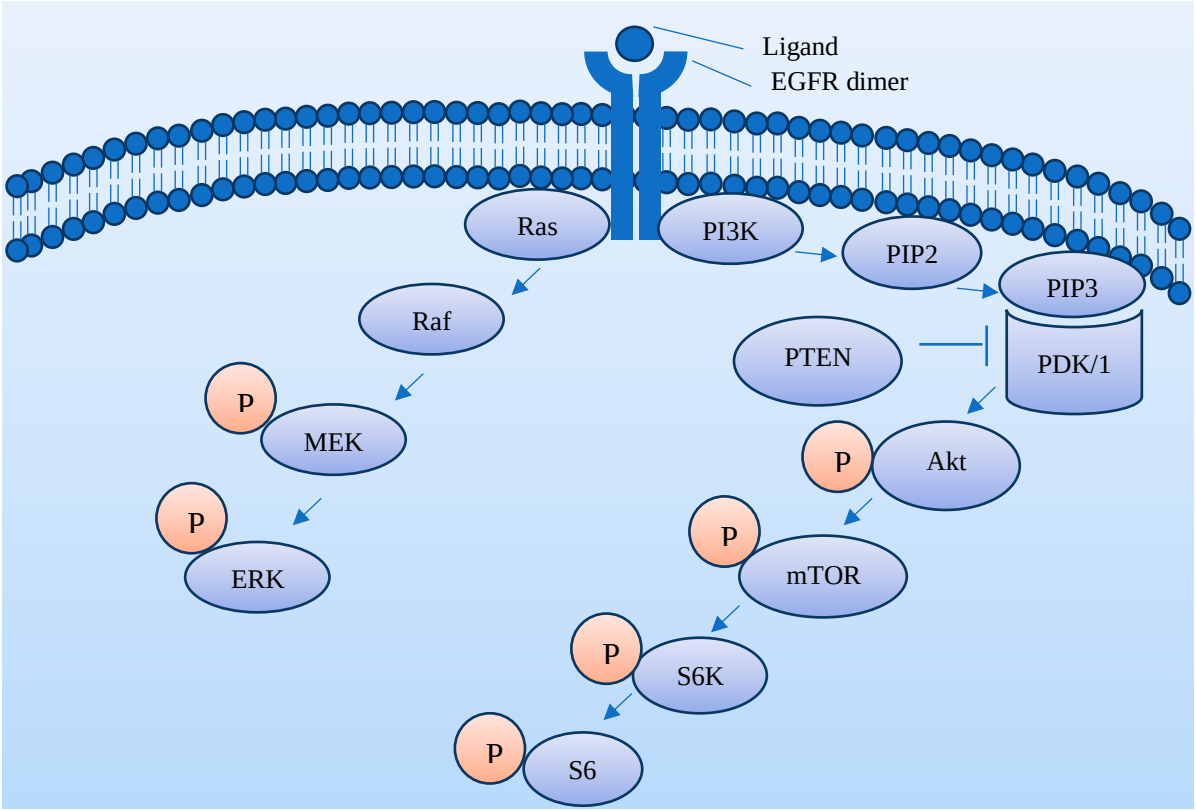

Figure 5: Simplified overview of the mitogen-activated protein kinase (MAPK) and phosphatidylinositol-3 kinase/Akt (PI3K/Akt) signaling pathway involved in CRC. Signal transmission through *Ras* activates *Raf* kinase which serine phosphorylates MEK followed by initiation of ERK pathway signaling [54]. The PI3K/Akt signaling pathway is triggered by activated PI3K, which catalyze the conversion of phosphatidylinositol-4-5-biphosphate (PIP2) to generate phosphatidylinositol-3-4-5-triphosphate (PIP3). The PIP3 will bind to domains of phosphoinositide dependent kinase 1 (PDK1) and Akt and cause their translocations to the plasma membrane. PDK-activation by PIP3 phosphorylates Akt at its catalytic domain and becomes active. Akt activates mTOR which in turn activates its downstream substrate S6 kinase (S6K). The phosphatase and tensin homologue (PTEN) is a tumor suppressor that functions as negative regulator of PI3K by dephosphorylation [51].

1.4.2. JAK/STAT signaling pathway

The Janus kinase/ Signal Transducer and Activators of Transcription (JAK/STAT) signaling pathway is crucial to mediate certain cellular responses to different cytokines and studies suggest that this is one of the major oncogenic pathways activated in CRC [53]. Constitutive STAT3 activation in CRC is associated with invasion, survival and growth of CRC cells [53]. The STAT family of transcription factor proteins consists of seven members with their own unique function in signal transduction, STAT3 being one of them [58]. A simplified overview of the JAK/STAT signaling pathway can be seen in Figure 6.

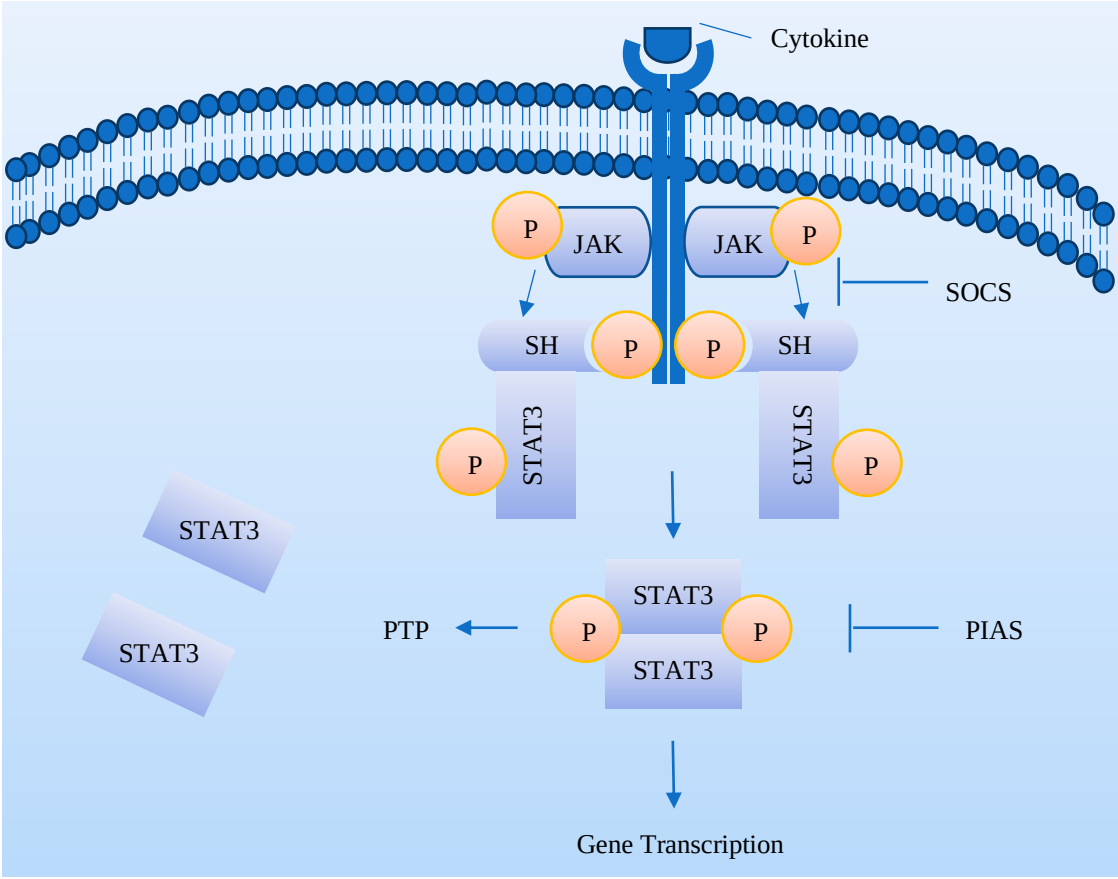

Figure 6: Simplified overview of Janus kinase /signal transducer and activators of transcription (JAK/STAT) signaling pathway involved in CRC. The JAK contains src-homology-2 (SH2) domains and the activation of this kinase leads to initiation of a phosphorylation cascade. Upon extracellular ligand binding to cytokine cell surface receptors, the intracellular JAKs associated with these receptors fully trans-phosphorylate each other on tyrosine, which again will phosphorylate the receptors to generate binding sites for SH2 domains of STAT proteins. The JAK also recruit and phosphorylate the STAT, which disassociate from the receptors. The activation of the STATs leads them to translocate from cytosol to enter the nucleus, where they form dimers that regulate transcription of genes in the cell. Proteins of the protein inhibitor of activated STAT's (PIAS) and suppressors of cytokine signaling (SOCS) family can directly interfere with STAT3 activation by competing with STAT3 at binding sites at the activating receptor or prevent dimerization and translocation to the nucleus. Protein- tyrosine phosphatase (PTP) can also prevent the formation of STAT3 dimers by dephosphorylation [58].

1.4.3. DNA damage signaling pathway

Many of the drugs used in treatment of mCRC induce DNA damage, which can lead to increased levels of phospho-H2AX and PARP cleavage. H2AX phospho-Ser139 and cleaved PARP1 provide biomarkers for DNA double strand break (DSB) and level of apoptotic cell death respectively. Induction of DSB in the cells is followed by histone protein H2AX phosphorylation at serine 139, where H2AX recruits DNA repair proteins to DSB damage

sites. This modified version is termed gamma-H2AX (γH2AX). This phosphorylation is caused by ATM proteins which are members from PI3K kinase family [59]. Poly (ADP-ribose) polymerase (PARP) is a family of related nuclear DNA binding repair enzymes able to catalyze transfer of ADP-ribose to target proteins. During apoptosis PARP is cleaved by activated caspases, which impair its function. PARP has an important function in DNA damage repair, where it is autoactivated and involved in repair of single strand breaks (SSBs) in the DNA by binding to DNA breaks to initiate auto-poly ADP-ribosylation. PARP inhibitors will lead to genome instability and damaged cells in cell cycle arrest, and due to these characteristics of PARP, it has become an attractive target in cancer therapy [60].

2 AIM OF THE PROJECT

In order to improve the survival in patients with mCRC, new treatments and drug combinations are necessary to establish. Regorafenib is currently approved to be used in third line treatment of mCRC, however the effect is limited, and adverse events are associated with the use of regorafenib in patients. If there are beneficial effects of combining it with other drugs commonly used in treatment of mCRC, it might be implemented in earlier lines of treatment, which could lead to improved response and survival for patients with this disease. The main aim of this thesis was to investigate if a synergistic effect would be observed when combining regorafenib with irinotecan or oxaliplatin, and if so try to elucidate the underlying mechanism behind this effect. This will be studied with the following approach:

- Evaluate the effect of mono therapy with regorafenib, irinotecan and oxaliplatin in HCT-116 and SW-620 cell lines
- Investigate the efficacy of combination therapy of regorafenib with irinotecan or oxaliplatin in HCT-116 and SW-620 cell lines.
- Study patient derived xenographs (PDX material) from mucinous peritoneal metastasis to investigate if similar results are obtained as in cell line experiments. Evaluate the drug response in the PDX-models using protein and mRNA analysis.
- Elucidate which signaling pathways might be involved in a potential synergistic effect, by investigating changes in protein expression and protein phosphorylation by using Western Blot Immunoassay.
- Investigate if topoisomerase-I expression in cell lines, the target of irinotecan, will be affected by regorafenib or combination treatment.

3 MATERIALS AND METHODS

3.1. Cell lines

The cell lines used for this project were HCT-116 and SW-620 human colon cancer cell lines from Horizon Discovery and ATCC respectively. More information about each cell line can be seen below in Table 2. An overview of all used material and equipment are listed in appendix A.

Table 2: Overview of where HCT-116 and SW-620 cell lines are derived from. These cell lines have distinct mutation profiles [10].

Cell line	Organ	Disease	Derived from	Patient	Mutation
HCT-116	Colon ascendens	Colorectal carcinoma	Primary tumor	48-year old male	*KRAS, PIK3CA*
SW-620	Colon	Colorectal adenocarcinoma	Lymph node metastasis	51-year old male	*KRAS, TP53*

To authenticate and to be certain that the right cell lines were used, both of them were ID tested by Genetica Cell Line Testing before being included in experiments (Table D1 and D2, Appendix D) and were confirmed to be the correct cell lines. The ID testing creates a short tandem repeat (STR) profile of each cell line and looks after matching sequences by comparing this STR profile with already published STR profiles (reference) for the cell lines from different databases such as ATCC. This makes it possible to determine if one is using the correct cell lines [61-63].

3.1.1. Cell cultures

HCT-116 cells and SW620 tumor cells were cultured as a monolayer in Nunclon^{TM} 75 cm^2 culturing flasks with Roswell Park Memorial Institute 1640 (RPMI) standard medium supplemented with heat inactivated 10% fetal bovine serum (FBS) and 1% glutamax. RPMI medium contains glucose, amino acids, mineral salts and vitamins essential for cell growth, but no growth factors. FBS was therefore added to stimulate cell proliferation. Glutamax is a stabilized form of L-glutamine that minimizes toxic ammonia accumulation and improves cell viability and growth. The cells were incubated in a humid atmosphere at 37°C without antibiotics. Since RPMI-1640 medium has a sodium bicarbonate system, they were incubated

at 5% CO_2 to maintain physiological pH. All lab work with these cells was performed under sterile conditions in laminar air flow (LAF) benches. It was necessary to passage the cell cultures twice weekly, to avoid the cells growing too densely and become less viable. All experiments performed used cells in the exponential growth phase. Pilot-experiments with different cell densities were performed to determine how many cells are needed to seed out for further experiments for each cell line (Appendix E). This was done to ensure that the cell confluence at the end of the experiment was not too dense as this would make it challenging to get reliable drug effect results.

3.1.2. Passaging of cells

Ethylene-Diamine-Tetra-acetic Acid (EDTA) or trypsin-EDTA was used to detach adhesive cells from the growth surface, when necessary. EDTA is a metal chelator for calcium and magnesium ions. It acts for instance on calcium dependent adhesion molecules such as cadherins, which cause the cells to lose their interactions. Trypsin is a proteolytic enzyme that cleave peptides, and by combining it with EDTA, the activity is enhanced. Using trypsin-EDTA solution instead of EDTA makes it easier to get homogenous single cell suspensions and a more reliable cell count.

Protocol

Old medium was discarded, and five mL of PBS was added to wash the surface and remove dead cells, which was then discarded. Two mL of trypsin-EDTA was added and incubated for three minutes and then eight mL medium were added to inactivate the trypsin. Since trypsin can cause cell membrane damage and eventually kill the cells, it was removed and disabled with medium immediately after cell detachment. The cell suspension was transferred to 15 mL tube and was centrifugated at 1000 revolutions per minute (rpm) for five minutes before all medium was removed, so only the pellet was left. The cells were diluted with medium dependent on the cell confluence in culture examined with microscopy before detachment. One mL of this cell suspension was transferred to a new 75 cm^2 flask, nine mL of medium was added and incubated to be used for later experiments.

3.1.3. Cell counting

The counting of cells was necessary so that the right amounts of cells required for a specific experiment were seeded out. Viable and dead cells were counted with standard Trypan blue assay by using Countess Automated cell counter from NanoEntek. This is a dye exclusion assay where dead cells with porous cell membrane becomes blue since the dye gets into the cell, while the viable cells with an intact cell membrane remain uncolored.

Protocol

After cell detachment, 10 µL of the cell suspension was transferred to small Eppendorf tubes, 10 µL of trypan blue dye was added, and mixed together. 10 µL of the sample was put into one of the chambers of a counting slide and counted.

3.1.4. Cell thawing and freezing

When the cell lines reached about 26 passages they were discarded, and a new tube of frozen cells was taken out of the nitrogen tank and defrosted. When the cells were almost completely thawed, the suspension was transferred to a 75 cm^2 flask and 10 mL medium was added. The next day, when cells had attached to the growth surface, the medium with dimethyl sulfoxide (DMSO), which the cell lines were stored in, was removed and new medium added and incubated. Following this, the cells were split two times a week. The new cell lines could not be used immediately and were split a few times before usage. After splitting and seeding out the cell line the first time, the rest of the cells were frozen down in nunc tubes if needed later. The cell suspension was centrifugated, four mL of freezing medium (10% DMSO, 90% FBS) added to the cells and one mL allocated in nunc tubes. The tubes were stores in a -80°C freezer to acclimatize and slowly freeze before they were put into nitrogen tanks some days later. DMSO is added to the freezing medium to prevent ice crystal formations upon freezing that would cause cell damage and eventually kill the cells.

3.1.5. Drugs

Stock solution of the regorafenib drug was diluted in DMSO for storage. 9.7 g of regorafenib and 1005 µL DMSO was used to make a 20 mM stock solution of this drug, whereas irinotecan and oxaliplatin was ordered as solutions ready for usage. For experiments, the drugs (regorafenib, irinotecan and oxaliplatin) where diluted with medium to achieve the different selected concentrations (Table 3). The same dilution of sterile DMSO as for the

highest drug concentration was used as a control for both regorafenib monotreatment experiments and combination experiments, while RPMI medium was the control for experiments with irinotecan and oxaliplatin. Work with cytostatic drugs like irinotecan and oxaliplatin, as well as all use of biological material, was handled after certified restrictions and considered as risk waste.

Table 3: Overview of the different drugs used and their specified concentrations.

Drug name	Molar mass (g/mol)	Stock concentration	Used concentration
Regorafenib	482.82	20 mM	0.01- 5 µM
Irinotecan	677.20	20 mg/mL	1-100 µM
Oxaliplatin	397.29	5 mg/mL	0.1-50 µM

3.1.6. Mycoplasma testing

Cell lines used in these experiments were tested for mycoplasma infection by using a Mycoplasma detection kit for conventional PCR with c1000 Touch^{TM} Thermal cycler from Bio-Rad, and all tested samples were negative. The mycoplasma testing was demonstrated and performed by an authorized technician at the lab. Mycoplasma is prokaryotic organisms and is a major cause of contamination of cell cultures. This can remain undetected for a long time and leads to changes in gene expression and cell behavior [64].

3.2. Ex vivo culture

As a part of this project, PDX material from mice was used. This is patient-derived colorectal cancer xenograft models established from patients with peritoneal metastasis. Only mucinous tumor tissue from the mice was used, without any direct experiments using the animals. The mice are regularly checked and euthanized when necessary. Research experiments which involve animals happens according to the Norwegian law of animal welfare and are approved by Forsøksdyrforvaltningens Tilsyns- og Søknadssystem (FOTS) (application number 18209). Regional committees for medical and health research ethics (REK) approval was not necessary for the experiments in this project, but had received acceptance by the Norwegian food safety authority. The PDX- models used were PMCA-1 and PMCA-2 that have been previously described [65] and approved by REK when established.

Protocol

Using 18G, 21G and 23G syringes, the samples of mucin harvested from the peritoneal cavity of the mice were made homogenous. The mucin was then diluted in 1:4 ratio with medium. This medium contained antibiotic (Penicillin Streptomycin) to prevent bacterial growth as the mucin was unsterile. 100 µL mucin suspension was seeded out in each well of 96 well plates for MTS measurement (see 3.3. MTS section) and one ml mucin suspension in 6 well plates for Western Blotting. Regorafenib and irinotecan were added the same day, incubated for 24 hours before MTS measurement or cells harvesting were performed. In the 96 well plates, 50 µL drug and RPMI was added to a total volume of 200 µL. When using 6 well plates to make protein lysates for Western Blot Immunoassay analysis and Real Time Quantitative Polymerase Chain Reaction (RT-qPCR), 500 µL drug and RPMI was added to a total of two mL. Harvesting of the mucin after drug treatment was done by using a cell scraper to detach any cells that might have attached to the surface before it was transferred to 15 mL tubes and 10 mL PBS was added. The tubes were centrifugated at 2000 rpm for ten minutes, and most of the liquid removed. The remaining suspension was transferred to small Eppendorf tubes and centrifugated again at 13.000 rpm for 15 minutes. The remaining liquid was removed, and the pellets stored at -80°C for later protein or RNA extraction. The procedure for making protein lysate for Western blotting was the same as for the cells.

3.3. Measurement of cell viability

Measurement with both MTS and IncuCyte instrument were both used to determine cell viability and assess the effects after drug treatment. MTS (3-(4.5-dimethylthiazol-2-yl)-5-(3-carboxymethoxyphenyl)-2-(4-sulfophenyl)-2H-tetrazolium) is a colorimetric method which was used to determine the amount of viable cells. Tetrazolium is bio-reduced by cells into a brown colored product, formazan. This conversion presumably occurs because of NAD(P)H, which is produced by dehydrogenase enzymes in metabolic active cells [66]. IncuCyte is an incubator with a live cell imaging system (10x phase objective), where images are taken every 3 hours to monitor growth by measuring confluence and changes in cellular morphology over time. The results were compared with MTS assays.

Protocol

After splitting and cell counting, 100 µL of cell suspension with 3000 HCT-116 cells or 10’000 SW-620 cells were seeded out in 96 wells plates and incubated for 24 hours in the IncuCyte. Drugs were added 24 hours later, to a total volume of 200 µL in each well and incubated in IncuCyte for approximately 72 hours before analysis. The viability of the cells was measured with MTS assay after 72 hours incubation for some of the experiments. 20 µL of MTS reagent (1:10 volume ratio) were added to each well and incubated at 37°C until the medium had developed a visible brown color. The viability of the cells was analyzed by using multimode plate reader colorimeter (VICTOR X3) where the absorbance at 490 nm was measured. The measured color intensity represents the relative amount of viable cells compared to the control. In these in vitro experiments, the effect on the drug combination treatment was evaluated with CalcuSyn software. CalcuSyn is a computer software that uses the median effect principle (MEP) with CI algorithm to evaluate drug interactions. The median drug effect analysis method was first described by Chou and Talalay. The software calculates a combination index (CI) to quantify and determine if the detected effect was synergistic, additive or antagonistic from a cytotoxicity or growth inhibition curve. Cutoff values from literature were used to determine what type of effect the combination treatment had [36].

3.4. Protein analysis

3.4.1. Harvesting of cells

Western Blot Immunoassay was used to study the cells’ protein expression after drug treatment. 250’000 HCT-116 cells /5 mL or 350’000 SW-620 cells/5 mL were seeded in small 25 cm^2 flasks. The medium was removed the following day and five mL of medium with different drug concentrations were added to the flasks. After incubating with drugs for 72 hours, the cells were harvested. Harvesting of the cells was achieved with a cell scraper and the cell suspension was transferred to 15 ml tubes. The tubes were centrifugated at 2000 rpm for three minutes and the supernatant was removed. The pellet was resuspended by adding 100 µL of cold PBS, transferred to small eppendorf tubes and centrifugated again at 2000 rpm for three minutes, supernatant was removed, and pellets stored at -80°C prior to cell lysis. PBS is a physiological buffer with osmolarity and pH that does not damage the cells, which is used to wash the cells.

3.4.2. Protein isolation

Prior to protein analysis, the cells needed to be lysed, a process where the cell membrane is disintegrated, and all intracellular content released. 50 µL of protease inhibitor and 50 µL of phosphatase inhibitor was added to 900 µL lysis buffer (for a complete list of reagents in lysis buffer see appendix B), so both inhibitors were diluted in 1:20 ratio. Keeping the samples at low temperature and using protease and phosphatase inhibitor prevents protein degradation. Protein extraction was performed by adding a certain amount of lysis buffer to each sample. The samples were incubated on ice and mixed with vortexing briefly every 15 minutes for an hour, sonicated with Ultrasonic Homogenizer and spun down at 13'000 rpm at 4°C for 15 minutes to separate cell debris from protein. Sonication is high intensity sound waves used as a mechanical intervention to disrupt the cells in order to be able to extract the protein in the cells. The supernatant was stored at -80°C.

3.4.3. Measurement of protein concentration

Protein isolation was followed by quantitative measurement of protein concentration using a BCA™ protein assay kit from Thermo Fischer Scientific. Determining total amount of protein in each sample was necessary to be able to compare the samples on an equivalent basis. The kit consists of reagent A with bicinchoninic acid (BCA), sodium carbonate, sodium bicarbonate, sodium tartrate in alkaline 0.1M sodium hydroxide and reagent B with 4% cupric sulfate. The BCA assay involves two different reactions which makes measurement of total protein possible. The principle behind the first reaction is the "Biuret reaction" where peptides with three or more amino acid residues chelate with copper ions from copper (II) sulfate which is then reduced from Cu^{2+} to Cu^{+} in alkaline environment containing tartrate producing a light blue complex. The second reaction is chelation of two molecules of BCA with reduced copper cation from the first reactions and creates a purple complex, which the colorimetric instrument detects. There is a linear correlation with signal detected and protein concentrations in the range of 20-2000 µg/mL.

Protocol

Protein concentration was determined by making a standard curve from a dilution series with nine different standard solutions (0.25, 250, 500, 750, 1000, 1500, 2000 ng/mL) from a stock bovine serum albumin solution of 2 mg/mL according to the manufacturer. Both samples and standards were measured in two technical replicates. Reagent A and B from BCA kit were mixed in 50:1 ratio. 5 µL of all samples were diluted in 55 µL ddH_2O in 96 wells plate. In each well, 25 µL of diluted sample or standard was added in addition to 200 µL of BCA reagent followed by incubation at 37°C for 30 minutes. The absorbance of each lysate was measured at 540 nm using a multimode plate reader (VICTOR X3). Protein concentration in each sample was calculated based on plotting the standard measurements into a linear regression curve in Excel. This will provide a regression equation for sample value measurements which allow accurate quantification of unknown protein concentrations. The different protein lysate samples containing equal amount of protein were then next subjected to direct Western Blot analysis.

3.5. Western Blot Immunoassay

Western blotting is a frequently method used in cell and molecular biology to separate and detect specific proteins in the cells. The method is therefore also known as immunoblotting and consists of five steps; Protein separation by molecular weight with gel electrophoresis (1), protein transfer and immobilization to solid membrane (blotting) (2), incubation with primary antibody (3), incubation with secondary antibody (4), visualization of target proteins with specific antibody and signal detection (5). Primary antibody binds to target protein which again will bind to a labeled secondary antibody. The thickness and intensity of the band visualized indicates the amount of protein of interest present. These proteins have known molecular weight and the bands were identified based on this by using a ladder [67]. In this project Western Blot Immunoassay was performed to study the alterations in protein expression in HCT-116 and SW-620 cells after exposure to regorafenib and irinotecan treatments. Protein analysis for experiments involving oxaliplatin was not performed. Western Blotting is a semi-quantitative method since it only gives relative comparison of protein levels to the controls and not an absolute quantity measurement. For a complete list of preparations of reagents, see appendix B.

3.5.1. NuPAGE Bis-Tris gel electrophoresis

Sodium dodecyl sulfate polyacrylamide gel electrophoresis (SDS-PAGE) is a standard technique used in the laboratory. Polyacrylamide (4-12%) gels for broad molecular weight protein separation were used. It consists of a network with pores which allow smaller proteins to move more rapidly through the gel towards the positive electrode, compared to larger proteins. This gel has a neutral pH environment and minimizes protein modification and is formulated for denaturing gel electrophoresis. These gels do not contain SDS nor its analog lithium dodecyl sulfate (LDS), but they were added in the sample and running buffer. Prior to electrophoresis all samples were mixed with loading buffer containing dithiothreitol (DTT) reducing agent and sample buffer with LDS plus tracking dye. The DTT reduces disulfide bonds in proteins and disrupts the natural structure, causing them to unfold. SDS and LDS are anionic detergents that bind and denature native proteins. They affect protein solubility, interfere with non-covalent interactions to reduce globular structure into linearization of proteins and establish a uniform negative net charge so the proteins migrate at the same rate, allowing the separation to only be dependent on size of the proteins.

Protocol

Depending on the measured protein concentration using BCA assay, a certain volume of protein lysate was diluted with lysis buffer (15 µg protein was loaded). A calculated amount of loading buffer was added to the samples and the tubes heated at 75°C for 10 minutes to denature the structure of the proteins. The loading buffer contains glycerol which increase the density of the samples, so they sink into the wells of the gel and bromophenol blue tracking dye. All samples were stored on ice until they were applied on the gel. The proteins were separated by using 3-(N-morpholino) propanesulfonic acid (1x MOPS) SDS running buffer. The gel was placed in the electrophoretic chamber, all wells of the gel were washed and filled with 1x MOPS and the chamber connected to power supply. See Blue Plus2 standard ladder (marker) with defined molecular weight of protein bands was also included. 18 µL of samples and 2.5 µL ladder were applied, and the gel run at 150 V for approximately 90 minutes.

3.5.2. Transfer and immunostaining

Separation of proteins on gel was followed up by transfer of protein to a nitrocellulose membrane. iBlot 2 Gel Transfer Device preprogrammed optimized transfer program was used to perform rapid dry-blotting of proteins from gel with nitrocellulose stack with high affinity for proteins for high quality transfer. The transfer stack consists of bottom stack and top stack with a pre-run gel, nitrocellulose membrane (the blotting membrane on the anode side and gel on cathode side), copper-coated electrode and gel matrices with incorporated transfer buffer. Electric current (electroblotting) makes the negatively charged proteins move from gel towards positively charged anode into the membrane. Binding of proteins to membrane happens through hydrophobic and electrostatic interactions.

Protocol

By using iBlot 2 Gel Transfer Device the gel was assembled in a ”gel-membrane transfer sandwich”, where the membrane was placed between the gel and the positive electrode and run for seven minutes. This was the recommended transfer time for most proteins (30-150 kDa). With this technique, the bands on the gel are transferred to the membrane (termed electrophoretic transfer) when exposed to an electric field.

Afterwards the membrane was washed with Tris Buffered Saline and Tween 20 (TBST) solution and blocked with either 5% nonfat dry milk or 5% Bovine Serum Albumin (BSA) in TBST for an hour on a rotation device and then washed once more with TBST solution. Blockage with dry milk or BSA prevents non-specific protein binding and background noise. The membrane was divided into sections and cut if multiple parallels or experiments had been run simultaneously. Sections of membrane to be used later were air-dried and stored in an envelope in the fridge. Tween-20 in blocking solution is also a non-ionic detergent that remove antibodies and other proteins to prevent unwanted protein interactions. Primary antibodies purchased from Cell Signaling Technology were used: anti-phospho-ERK, anti-ERK, anti-phospho-S6 ribosomal protein, anti-S6 ribosomal protein, anti-phospho-STAT3, anti-STAT3, anti-PARP, anti-phospho-H2AX and anti-α-tubulin. The following secondary antibodies from Dako were used: polyclonal goat anti-rabbit and polyclonal rabbit anti - mouse. These antibodies were diluted in certain ratio with 5% BSA or nonfat dry milk according to manufacturer recommendations (Appendix C). Primary antibody was added to the membranes and underwent overnight incubation at low temperature (4°C) on a rotation

device. This was followed by rinsing the membrane with TBST and then washed 3x times for 10 minutes with TBST before secondary antibody was added for one hour. Washing with TBST removes unbound antibodies and background noise. Secondary antibody was diluted with the same as the primary antibody, either BSA or nonfat dry milk. BSA are preferred to be used with anti-phospho-protein antibodies, as the phospho-protein casein in dry milk will interfere with assay results. The membrane was washed 3x times with TBST, then 3x washing steps with TBST for 10 minutes were repeated before signal detection of immune complexes was performed. Supersignal® West Dura Extended Duration Substrate was used for signal detection with Chemidoc™ Imaging system from Bio-Rad, which is a CCD camera-based detection system. It is a luminol-based enhanced chemiluminescence (ECL) horseradish peroxidase (HRP) substrate and was diluted in 1:1 ratio. The secondary antibody is conjugated to HRP and antibodies targeting both mouse and rabbit was used. The visualized bands on the membranes were merged against the ladder using Image-Lab software from Bio-Rad to determine the size of the proteins and confirm that the right proteins had been detected. In addition, the intensity of each band was determined to check if the same amount of protein had been loaded equally across wells. For this purpose, α-tubulin (50 kDa) or histone 3 (H3, 17 kDa) was used as internal loading control. These proteins are ubiquitous and highly expressed in every cell.

3.6. Gene expression analysis

3.6.1. RNA extraction

The differences in MUC-2 gene expression levels were analyzed in the PDX-model with RT-qPCR after 24 hours of treatment with regorafenib and irinotecan as single agents and in combination. Prior to analysis, RNA had to be extracted from each sample and converted to cDNA by reverse transcription.

Protocol

Mucin samples were put in eppendorf tubes and 500 µL trizol were added which lyse the cells. The samples were incubated 5 minutes at room temperature (RT), before 100 µL chloroform were added and put shortly on a whirl mixer. The tubes were spun down at 13’000 rpm for 20 minutes at 4°C. The clear upper layer was carefully removed with a pipette and transferred to new eppendorf tubes, without touching the interlayer. Mucin consists of few

cells and 2 µL of linear acrylamide (5 mg/ml) was therefore added followed by 200 µL isopropanol and the tubes were mixed. Linear acrylamide is ideal for qPCR reactions for quantitative recovery of small amounts of nucleic acids in solution during alcohol precipitation. The tubes were incubated at RT for five minutes and centrifugated at 13'000 rpm for 20 minutes at 4°C. Almost all the liquid was removed, the remaining pellet was washed with 200 µL 70% ethanol (EtOH) and spun down at 13'000 rpm for five minutes. The ethanol was removed and the pellet air dried for approximately 10 minutes. 30-50 µL sterile water was added, dependent on pellet size and the tubes were stored at 4°C until the pellet was fully suspended in the water. Hereafter the samples were stored at -20ºC.

3.6.2. NanoDrop

To determine the purity and concentration (µg/µL) of RNA in the mucin samples, the NanoDrop 2000 Thermo Scientific instrument, which is a UV-spectrophotometer, was used. This was done in order to ensure that an equal amount of RNA was added to each reverse transcription reaction.

Protocol

Five µL of ddH_2O was first added to the pedestal to wash the surface before two µL of ddH_2O were measured as a blank sample. The RNA concentration of the different samples was measured and the 260/280 plus 260/230 ratios were noted. RNA absorbs at 260 nm, proteins at 280 nm and salts at 230 nm. The quality of the RNA can be determined based these ratios which can be seen as curves with wavelength as a function of absorbance.

3.6.3. cDNA synthesis

Prior to subsequent qPCR analysis, synthesis of complementary DNA (cDNA) from single stranded RNA template was performed as the initial step by using reverse transcription to catalyze the reaction. The cDNA is produced based on the pairing of RNA base pairs with their DNA complements. The enzyme reverse transcriptase uses RNA as template and a short primer complementary 3`end of RNA to initiate synthesis of cDNA strands in the presence of deoxynucleotide triphosphate (dNTP).

Protocol

All samples were prepared for cDNA synthesis by diluting 1 ug of RNA with water to a total volume of 15 µL, dependent on their measured RNA concentration. A buffer-enzyme solution was made by mixing 4 µL qScript™ Reverse Transcriptase and 16 µL qScript™ 5X Reaction Mix. Five µL of this solution was added to each sample and mixed thoroughly with a pipette. The samples were put into Bio-Rad Cycler and analyzed with a preinstalled program for approximately 40 minutes. Before storage at -20ºC, 80 µL sterile water were added to the samples.

3.6.4. Real Time Quantitative Polymerase Chain Reaction

Real Time quantitative Polymerase Chain Reaction (RT-qPCR) assay is a laboratory technique used in a variety of applications like quantitative gene expression analysis, in this case the MUC-2 gene. This technique can amplify and detect changes in amplicon concentration (how much specific mRNA that is present in the samples) by using fluorescence signal (FAM-490) from specific probes. A thermocycler and fluorometer modulate the temperature during amplification. In each cycle of the qPCR the reaction, progression is monitored by the increase and intensity of the fluorescence emitted from the probes, which create qPCR curves (cycles as function of relative fluorescence units). The instrument calculated quantification cycles values (Cq-values), which are used to determine absolute target quantities. In this reaction, DNA polymerase enzyme transcribes the complementary sequence for single stranded cDNA based on sequence specific primers that hybridize to cDNA that encodes specific proteins. The result is double stranded cDNA with one strand representing a sequence identical to the RNA of interest. The sample measurements were normalized against a reference gene, YARS, to gain mean Cq-values. These values were used to determine the relative alterations in gene expression.

Protocol

The samples with generated cDNA were prepared for q-PCR by diluting them in a certain ratio. The diluting agent (stock) was a suspension consisting of 345 µL Supermix, 34.5 µL probe/primermix and 195.5 µL water for the MUC-2 samples. For the YARS (reference gene) samples, 345 µL Supermix, 55.2 µL probe/primermix and 174.8 µL suspension were made. 10 µL of each cDNA sample were transferred to small qPCR tubes followed by 50 µL of either MUC-2 or YARS stock solution to a total volume of 60 µL. The samples were mixed carefully, and the samples transferred to a 96 well plate in replicates of 2x 25 µL. All samples were analyzed on Bio-Rad CFX Manager instrument with preinstalled protocol for approximately 80 minutes.

3.7. Immunohistochemistry

Histology of the mucinous tissue from mice were performed and stained with Hematoxylin and eosin staining (H&E-staining). The staining method is common for analyzing different cellular tissue structures and their composition. Hematoxylin targets nucleic acids in the nucleus staining it purple, while eosin stains the cytoplasmic components pink in the cells, which makes it possible to differentiate between these two. The slide with tissue from PMCA-1 mucin was imaged using color brightfield microscopy.

Preparation of the slide with mucinous tissue form mice was done by authorized employees working with the mice. It involves fixation of the tissue by using formalin and embedding the slides in paraffin blocks, where H&E-staining is performed on 4 µM thick slides. After formalin fixation for minimum 24 hours, the formalin fixed tissues were delivered to the Department of Pathology (OUS), for H&E-staining according to standard protocol at the Department of Tumor Biology.

3.8. Immunofluorescence

The immunofluorescence (IF) technique is used to visualize proteins with fluorophore-conjugated antibodies and for determination of cellular localization of the protein of interest with confocal microscopy. In this thesis we looked at topoisomerase-1 (topo-1) expression in HCT-116 and SW-620 cells following 72 hours treatment with regorafenib and irinotecan. This technique involves cell fixation, permeabilization and blocking steps. Cell fixation is important to maintain the cells native state, to stop cellular biochemical reactions and for optimal IF-imaging. Permeabilization of fixed cells facilitates antibody binding by disturbing the cell membrane, while blocking prevents non-specific binding of antibodies.

Protocol

20'000 HCT-116 or 40'000 SW-620 cells were seeded out in four small wells each (250 µL) of an 8 wells chamber slide plate. In addition, the same number of cells in 500 µL were seeded in 4 chamber slide plate for negative controls. The drugs regorafenib and irinotecan were added after 24 hours of incubation time. RPMI medium was used as negative controls. The cells were exposed to the drugs for three days. The drug/medium was removed, and the cells washed with 250 µL PBS. Then, 150 µL of 4% paraformaldehyde (PFA) solution was added to each well for cell fixation and incubated at RT for 15 minutes. PFA solution was made by adding 1 mL of 16% PFA and 3 mL of ice-cold PBS. This was removed and the cells washed two times with PBS. 200 µL of blocking solution was added to the chambers for blocking/permeabilization and incubated at RT for approximately 20 minutes. The blocking solution was made by adding 2 mL 5% BSA, 8 mL PBS and 100 µL 10% saponin. Topoisomerase antibody (1 mg/mL) was diluted by mixing 1.5 mL blockage solution and 1.5 µL antibody. 160 µL of this solution was transferred to each well. The chambers were stored in a moist environment overnight without upper lid. Antibody was removed and the cells washed with blocking solution three times. Secondary antibody (anti-rabbit 488) was diluted in 1:400 ratio with blocking solution. 400 µL of this solution was added to the negative controls. In addition, 2 mL of this antibody solution was mixed with 50 µL Alexa Fluor 546 phalloidin, where 200 µL of this was added to the smaller wells. They were incubated at RT for approximately one hour in darkness. Hereafter, PBS and saponin (10 mL PBS plus 100 µL 1% saponin) solution was added, removed and the cells washed 2x with PBS. A small droplet of Gold Antifade Reagent with DAPI (4´.6-diamidino-2-phenylindole) was put on top of the

slide with coverslip. The slides with fixed cells were viewed in a confocal microscope. The phalloidin is a fluorescent labelled probe with high affinity for F-actin (filamentous actin), while DAPI is a blue fluorescent DNA stain. Actin is a family of proteins that form microfilaments in the cells and are components of the cytoskeleton.

3.9. Data and statistical analysis

Data obtained from MTS and IncuCyte assay were analyzed with Microsoft Excel and SPSS. Measured background signal with MTS assay only consisting of medium was subtracted from each sample and control. Average and relative values of the technical replicates were calculated and then the results were plotted as graph with standard deviation error bars or standard error of the mean (SEM). SPSS software was used to perform one-way Analysis of Variance (ANOVA), which is a parametric test to compare means in confluence (dependent variable) between categorical treatment groups in this project and determine if there is a significant difference between the experimental results. Statistical significant differences ($p < 0.05$) are indicated by asterisks and were calculated using Tukey HSD (** = $p < 0.05$ against both mono-treatments or * = $p < 0.05$ against one mono-treatment).

4 RESULTS

4.1. Single drug sensitivity in HCT-116 and SW-620 cells

4.1.1. Regorafenib mono-treatment in HCT-116

The drug sensitivity of the cell lines was evaluated by exposing the cells to increasing concentrations of the drugs regorafenib (reg.), irinotecan (iri.) and oxaliplatin (ox.). This was done in order to observe how the drugs alone would influence cell viability in the cell lines HCT-116 and SW-620. Based on these results, concentrations to use in the combination treatments were chosen to determine if the interaction of the drugs combined, exerted a reduced or improved effect than the drugs as single agents. Regorafenib treatment as a single agent did not seem to affect the confluence of HCT-116 cells at concentrations below 0.5 µM after 72 hours of drug exposure (Figure 7). As the drug concentration of regorafenib increased, the cells' response to this treatment became gradually higher reducing the cell confluence (Figure 7). Regorafenib concentrations of 1, 2.5 and 5 µM were selected for the combination experiments, as these doses had some measurable effects, but did not kill all cells.

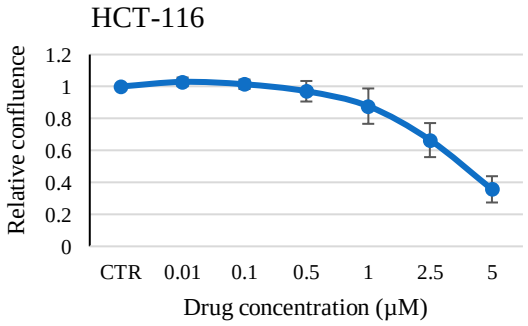

Figure 7: HCT-116 cells were grown as monolayer followed by cell confluence measurement with IncuCyte after 72 hours of exposure to selected doses of regorafenib. The cell sensitivity to the drug is presented as relative drug effect in comparison to untreated control (CTR). Error bars indicate standard deviation from three technical replicates (n=3).

Selected proteins in different pathways known to be influenced by the tested drugs were also investigated using Western Blot after 72 hours of drug exposure. Regorafenib mono-treatment in HCT-116 cells demonstrated increased pSTAT3 (JAK/STAT pathway) in the reg.1 group

compared to untreated control (CTR) (Figure 8), while at higher regorafenib concentrations, there was less pSTAT3 compared to the lowest dose, but still more than the CTR. Total STAT3 protein was upregulated in all treatment groups with the highest expression in the reg.5 group, while there was no difference between the two lowest concentration groups. The pS6 (PI3K-Akt signaling pathway) expression was reduced at regorafenib concentrations of 2.5 µM and higher. Dose dependent reduction of pERK (MAPK pathway) was observed, where treatment with 5 µM regorafenib resulted in a substantial reduction of pERK, while at lower drug concentrations, an increase was observed compared to the CTR. Total ERK protein were dose-dependently downregulated in all treatment groups with increasing regorafenib concentration, while the levels of S6 protein were dose-dependently upregulated compared to the CTR. Induction of apoptosis indicated by PARP cleavage (PARP cl.) was observed in the reg.1 treatment group, but at higher doses the apoptotic effect became lower than the CTR group. Total PARP protein was upregulation in all treatment groups, with the highest levels observed in the reg.1 and reg.5 groups. DNA damage indicated by γH2AX seemed to be reduced as the dose of regorafenib increased (Figure 8). This protein detection experiment was only performed once. Based on these results, a 2.5 µM dose was chosen to be used in later combination experiments for protein analysis as this dose had some, but not too strong effects on the protein levels. Experiments involving assessment of effects in the cell lines after 48 hours of drug exposure were also performed to investigate if there was a time dependent response in any of the proteins, but as the response did not differ much compared to a 72-hour exposure. These results were not included in the thesis.

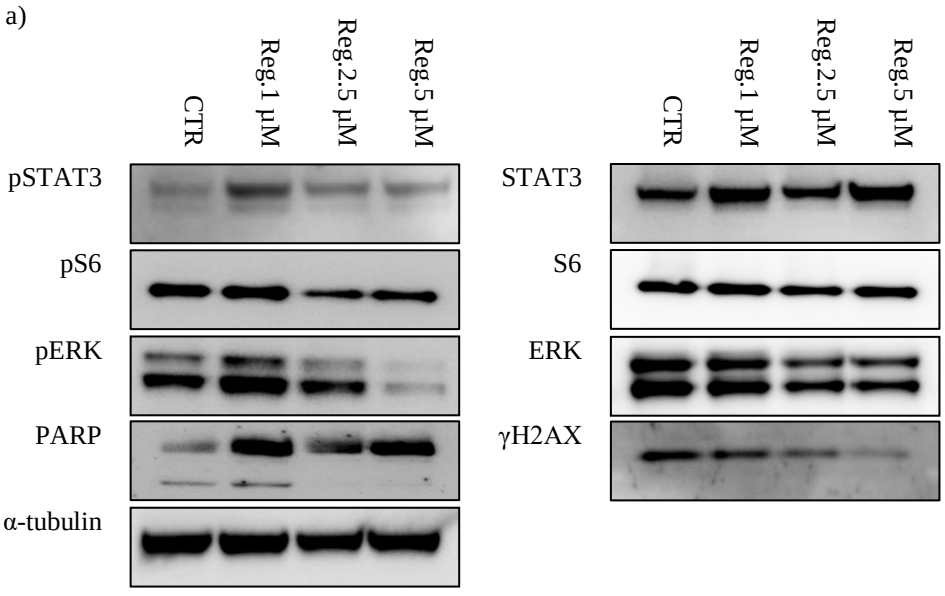

b)

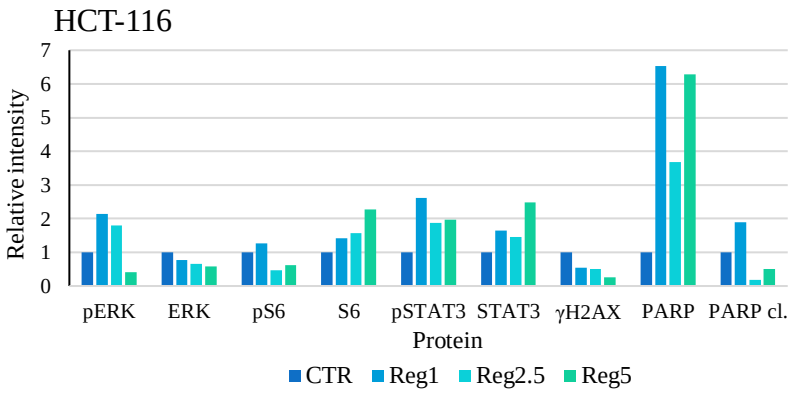

Figure 8: a) Representative Western Blot Immunoassay results for detection of relative protein expression levels in different signaling pathways in HCT-116 cells after 72 hours of mono-treatment with regorafenib. α-tubulin was used as internal loading control. b) Relative quantification of Western Blot protein bands with Image-Lab that show relative levels of protein expression in HCT-116 cells compared to the CTR after a 72-hour mono-treatment with regorafenib (n=1).

4.1.2. Regorafenib mono-treatment in SW-620

Regorafenib was also investigated in SW-620 cells. The result after 72 hours exposure of SW-620 cells to regorafenib was a marked drug induced growth inhibition as the drug concentration increased (Figure 9). It also demonstrated that these cells have a lower sensitivity to regorafenib than the HCT-116 cells at higher drug concentrations (> 1 µM), when comparing their relative confluence (Figure 7, Figure 9). The drug seems to have similar effect on confluence in the 0.5 and 1 µM groups for both cell lines, but as the doses increase to 2.5 µM, SW-620 become less responsive. Due to this, higher doses of regorafenib (1, 5, and 7.5 µM) were selected to be used in combination experiments.

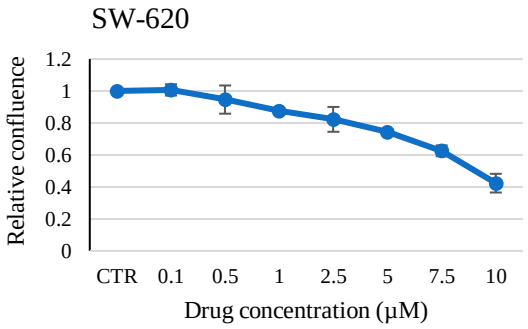

Figure 9: SW-620 cells were grown as monolayer followed by cell confluence measurement with IncuCyte after 72 hours of exposure to selected doses of regorafenib. The cell sensitivity to the drug is presented as relative drug effect in comparison to the CTR. Error bars indicate standard deviation from two technical replicates (n=2).

The Western Blot results from the regorafenib mono-treatment experiments in SW-620 cells showed a dose-dependent decrease in pS6 and pERK expression (Figure 10). The expression of these phospho-proteins was reduced at regorafenib concentrations of 5 µM or higher, compared to the CTR. The lowest drug concentration led to increased phosphorylation of these proteins compared to the CTR. Total S6 and ERK proteins were upregulated in all treatment groups, with the highest expression of ERK protein and the lowest expression of S6 protein seen with the two highest drug concentrations. In both cases the expression in the groups were similar. This cell line differed from HCT-116 as it was not possible to detect pSTAT3 expression. Both PARP cleavage and γH2AX expression increased dose-dependently. A similar increase in PARP cleavage was observed with the two highest concentrations, while γH2AX expression did not seems to be increase compared to the CTR. The reg5. and reg.7.5 groups exerted similar reduced levels of total PARP protein, but tended to increase at lower concentrations of regorafenib (Figure 10). For later combination experiments, a 5 µM dose was chosen.

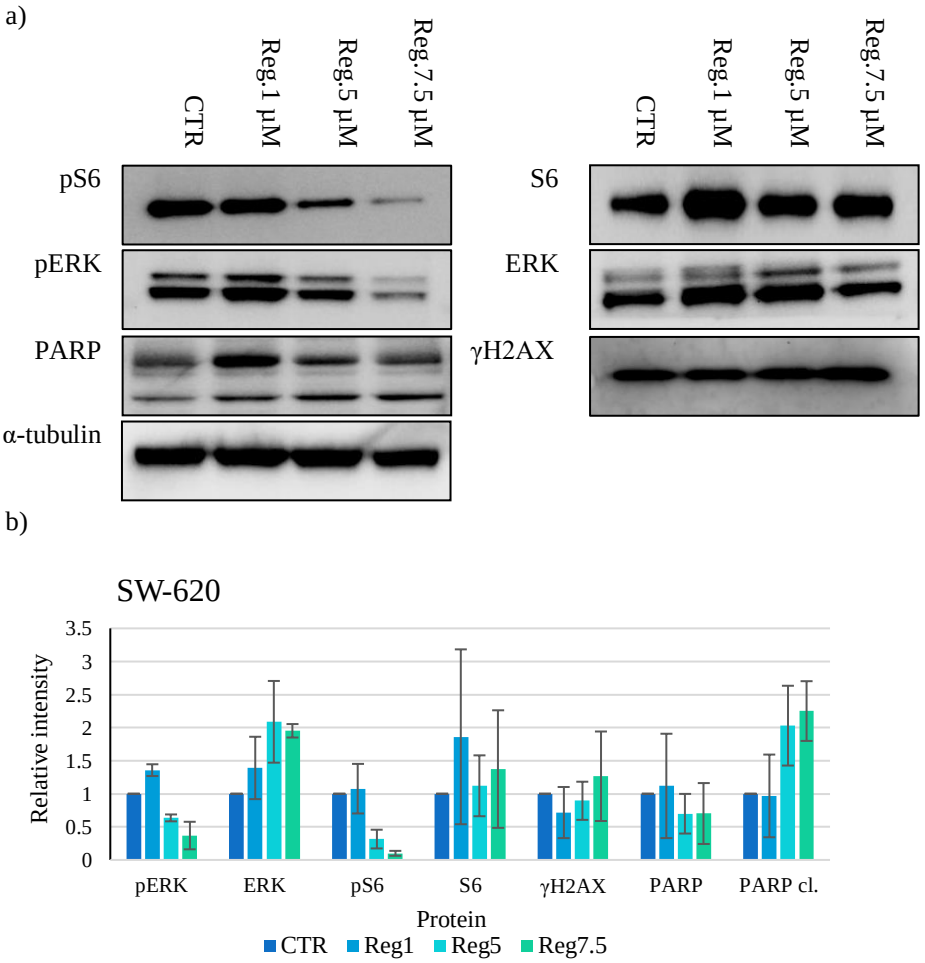

Figure 10: a) Representative Western Blot Immunoassay results for detection of relative protein expression levels in different signaling pathways in SW-620 cells after 72 hours of mono-treatment with regorafenib. α-tubulin was used as internal loading control. b) Relative quantification of Western Blot protein bands with Image-Lab that shows relative levels of protein expression in SW-620 cells compared to the CTR after a 72-hour mono-treatment with regorafenib. Error bars indicate standard deviation (n=2).

4.1.3. Irinotecan mono-treatment in HCT-116

The HCT-116 and SW-620 cells were also initially exposed to mono-treatment with increasing concentrations of irinotecan to be able to investigate the response to this drug and to select suitable concentrations for the combination treatments. Irinotecan induced a dose-dependent inhibition of growth in HCT-116 cells (Figure 11). Cell confluence decreased gradually from lowest irinotecan concentration to 50 µM. No additional effect was seen by increasing the concentration above 50 µM, probably due to no remaining viable cells (Figure 11). Concentrations of 1, 5 and 10 µM were selected for further combination experiments.

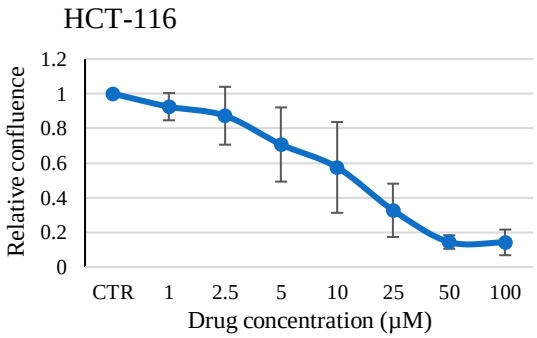

Figure 11: Measurement of HCT-116 cell confluence with IncuCyte after 72 hours of mono-treatment with different doses of irinotecan. Error bars indicate standard deviation (n=3).

The Western Blot results from mono-treatment with irinotecan in HCT-116 cells demonstrated a decrease of pSTAT3 in all treatment groups and a slight increase of pERK was seen compared to the CTR (Figure **12**). There was a tendency of dose dependent response with the two lowest concentrations investigated, while at doses of 5 and 10 µM, the level of pSTAT3 became asymptotic. Total STAT3 was upregulated with the two highest irinotecan doses, whereas total ERK protein became downregulated with increasing drug concentration. The same downregulated expression pattern as ERK protein was seen with total S6 protein. The reduction in pS6 expression was similar in the iri.0.5 and iri.10 group compared to the CTR, while iri.5 did not induce any reduction in pS6. γH2AX expression levels increased dose- dependently at irinotecan concentrations above 5 µM, compared to the iri 0.5 group and the CTR. The same increasing pattern as for γH2AX, was observed in PARP cleavage, while total PARP protein was upregulated in all treatment groups (Figure 12). For later combination experiments, a 5 µM dose was chosen. This protein detection experiment was only performed once.

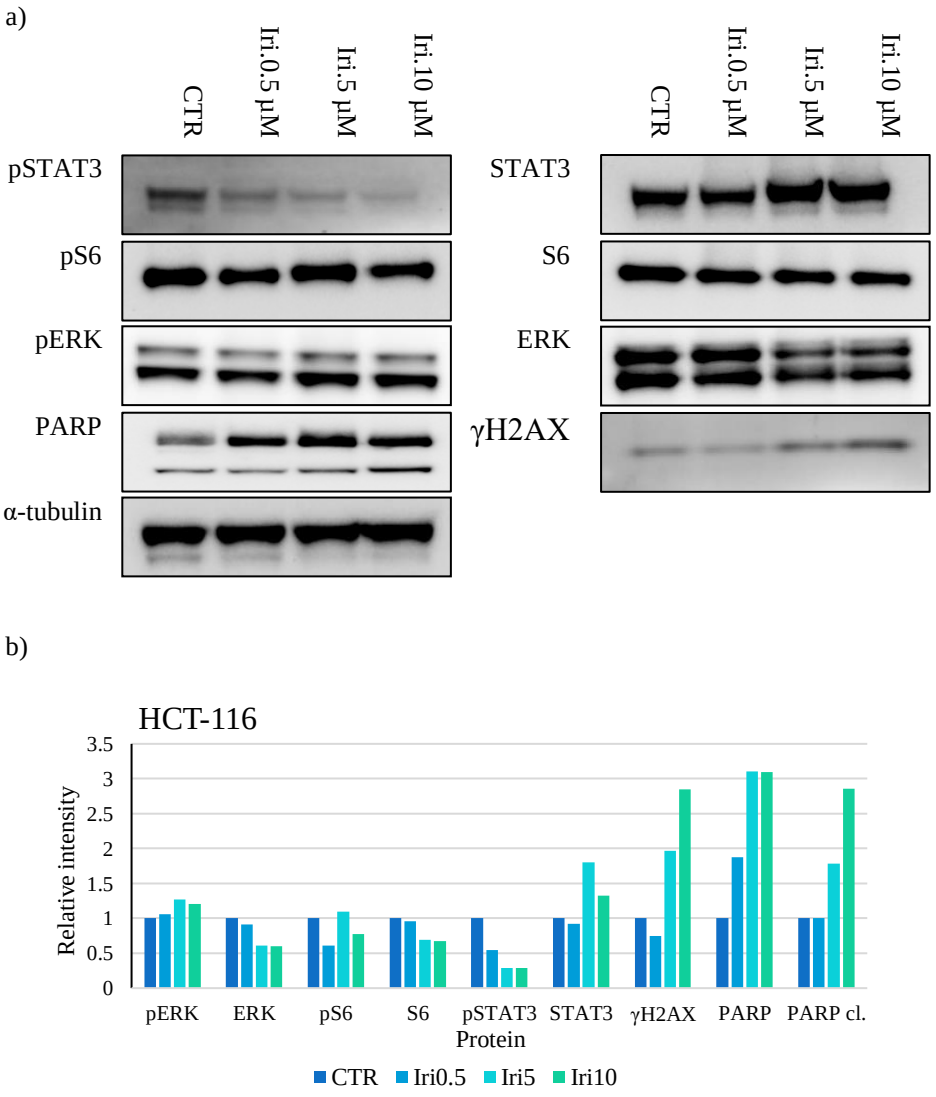

Figure 12: a) Representative Western Blot Immunoassay results for detection of relative protein expression levels in different signaling pathways in HCT-116 cells after 72 hours of mono-treatment with irinotecan. α-tubulin was used as internal loading control. b) Relative quantification of Western Blot protein bands with Image-Lab that shows relative levels of protein expression in HCT-116 cells compared to the CTR after a 72-hour mono-treatment with irinotecan (n=1).

4.1.4. Irinotecan mono-treatment in SW-620

SW-620 cells exposed to increasing doses of irinotecan from 1 µM to 25 µM resulted in a reduction in confluence (Figure 13). Thereafter the confluence became more asymptotic at higher concentrations, most likely due to no remaining viable cells. The SW-620 cells were exposed to the same concentrations as the HCT-116 cells, and the results indicate that SW-

620 are more sensitive to irinotecan than HCT-116 cells at concentrations between 2.5 and 10 µM (Figure 11, Figure 13). The doses 1, 2.5, 5 and 10 µM were selected for further combination experiments.

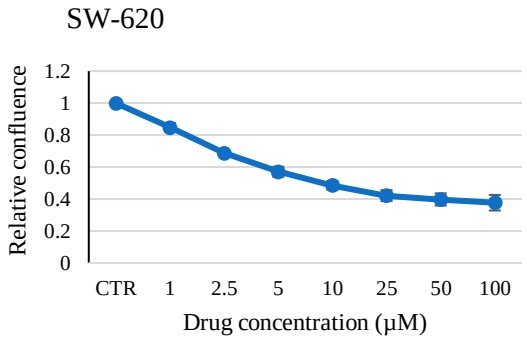

Figure 13: Measurement of SW-620 cell confluence with IncuCyte after 72 hours of mono-treatment with different doses of irinotecan. Error bars indicate standard deviation (n=4).

Protein analysis with Western Blot in SW-620 cells exposed to mono-treatment of irinotecan alone led to a slightly increased pERK and pS6 at the lowest concentration tested compared to the CTR (Figure 14). No marked effect on the total amount of ERK protein was observed, while S6 protein was slightly upregulated in all groups compared to the CTR. γH2AX expression was highly increased in all treatment groups, with the highest expression in the iri.5 group. The same expression pattern as for γH2AX, was seen in total PARP protein. A very weak signal of uncleaved PARP protein was detected in the CTR sample. Cleaved PARP was not observed in any of the treatment groups (Figure 14). The 5 µM dose was chosen for further combination experiments with regorafenib.

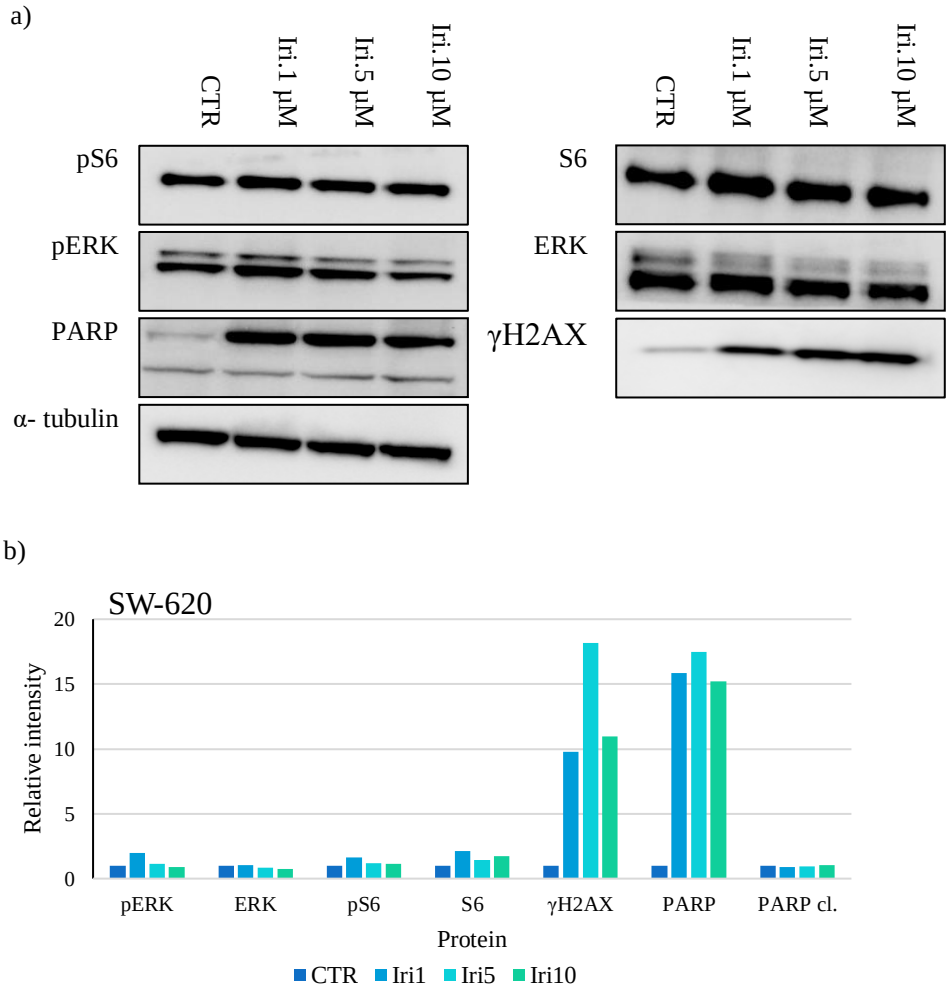

Figure 14: a) Representative Western Blot Immunoassay results for detection of relative protein expression levels in different signaling pathways in SW-620 cells after 72 hours of mono-treatment with irinotecan. α-tubulin was used as internal loading control. b) Relative quantification of Western Blot protein bands with Image-Lab that shows relative levels of protein expression in SW-620 cells compared to the CTR after a 72-hour mono-treatment with irinotecan (n=1).

4.1.5. Oxaliplatin mono-treatment in HCT-116

In the same way as for irinotecan we wanted to investigate the cellular drug response to oxaliplatin in combination with regorafenib in both cell lines, which potentially could result in synergistic interactions. Prior to this, we therefore performed single-agent experiments with oxaliplatin to determine suitable drug concentrations for the combination experiments. The response to oxaliplatin in HCT-116 indicated high cytotoxic effect already at the lowest concentrations tested (Figure 15). Mono-treatment with oxaliplatin as single agent led to a steep reduction in cell confluence in the 0.5 and 1 µM groups. No additional effect was observed by increasing the drug concentration, but the cell survival was already very low

(Figure 15). Concentrations of 0.1, 0.25 and 0.5 µM were selected for the combination experiments. It was necessary to use doses where the cells drug response was not too high, which would otherwise make it challenging to observe additional effects with the combination treatments. MTS measurement of cell viability for these experiments after the same mono-treatment with oxaliplatin can be seen in appendix G. The results showed the same tendency of reduction in viability in HCT-116 as the IncuCyte measurement. In contrast, the MTS measurements had a slightly more gradual reduction with higher confluence values at each concentration.

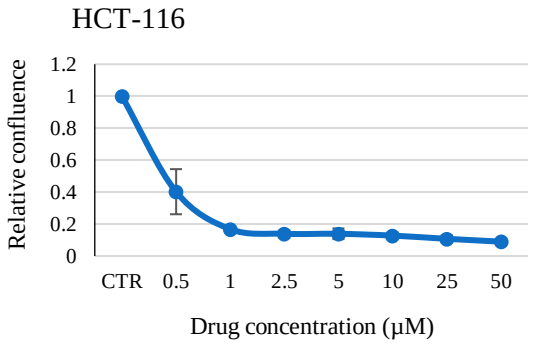

Figure 15: Measurement of HCT-116 cell confluence with IncuCyte after 72 hours of mono-treatment with different doses of oxaliplatin. Error bars indicate standard deviation (n=2).

4.1.6. Oxaliplatin mono-treatment in SW-620

In SW-620 cells, exposure of increasing oxaliplatin concentrations showed a steep reduction in confluence in the 0.5 µM group compared to the CTR group, where after the confluence became more asymptotic at higher doses (Figure 16). Both cell lines were treated with oxaliplatin doses up to 50 µM, where SW-620 seems to be less sensitive to oxaliplatin at the same respective doses than HCT-116 after 72 hours of exposure (Figure 15, Figure 16). Oxaliplatin concentrations of 0.1, 0.5 and 0.75 µM were selected for the combination experiments. The MTS measurement for this experiment also had approximately the same reduction pattern as the IncuCyte measurement. The viability was slightly higher with MTS measurements up to 5 µM, but lower at the highest concentrations (Appendix G).

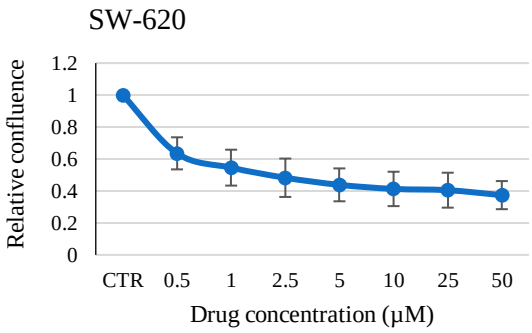

Figure 16: Measurement of SW-620 cell confluence with IncuCyte after 72 hours of mono-treatment with different doses of oxaliplatin. Error bars indicate standard deviation (n=2).

4.2. Sensitivity of HCT-116 and SW-620 to combination treatments

4.2.1. Combination treatment with regorafenib and irinotecan in HCT-116

The drug-effect relationship in each cell line was investigated by exposing the cells to selected concentrations of regorafenib in combination with either irinotecan or oxaliplatin. Based on the relative confluence data in all combination groups, a combination index value was calculated with CalcuSyn and the effect confirmed as synergistic with CI values below 0.9, additive with CI between 0.9-1.1 and antagonistic with CI values of 1.1 and above, by using cutoff values from the literature (Table F in appendix F). CalcuSyn software can only calculate combination indices with confluence values below 1.0. In a few cases, the relative confluence value for some mono-treatment groups had to be adjusted down to 0.999, due to confluence values slightly above one. Based on the experiments with mono-treatment it was expected that these values would be below 1.0. In general, the cell confluence data obtained demonstrated that treatment with regorafenib and irinotecan as single agents led to gradually reduced confluence with increasing drug concentration (Figure 17). In the combination groups, the most pronounced effects in confluence were seen up to 5 µM irinotecan concentration, to become more asymptotic at higher doses. A marked difference in confluence was observed in the iri5. group compared to the iri.5+reg.1 group (Figure 17). Synergistic effects were found in all combination groups, except from the iri.10 group combined with reg.2.5 and reg.5 in the HCT-116 cell line (Table 4). As the drug concentration was increased, the effect became additive. The obtained data for the combination treatments demonstrating synergism were chosen as points of interest for further statistical analysis. The statistical analysis was performed by comparing four of the groups together; the combination treatment,

the respective mono-treatments and the control. There was found statistical significance in the mean of confluence in all HCT-116 combination groups with the one-way ANOVA test, except for the iri.10+reg.1 group compared to the iri.10 group and iri.1+reg.5 group compared to the reg.5 group (Table 4).

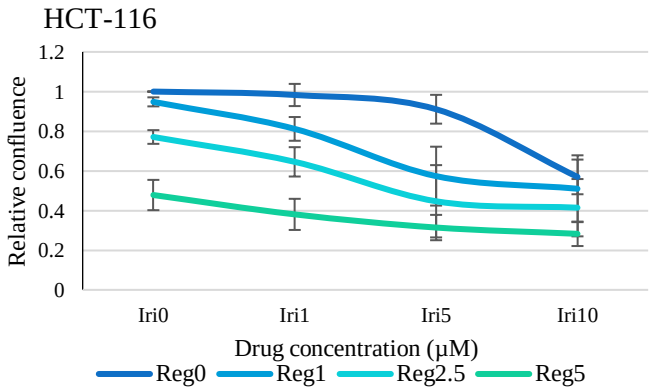

Figure 17: IncuCyte measurement of dose-effect relationship in HCT-116 cells with regorafenib and irinotecan as single agent and in combination after 72 hours of treatment. Error bars indicate standard deviation (n=4).

Table 4: Calculation of combination index for relative values from the HCT-116 combination experiment with regorafenib and irinotecan (Figure 17) by using CalcuSyn software. Statistical significance ($p < 0.05$) as obtained from Tukey HSD is indicated with asterisks (** = significant against both mono-treatments or * = significant against one mono-treatment).

	Irinotecan 1	Irinotecan 5	Irinotecan 10
Regorafenib 1	0.625**	0.634**	0.871*
Regorafenib 2.5	0.817**	0.745**	0.945
Regorafenib 5	0.851*	0.880**	0.983

The same proteins as with mono-treatment were also investigated in cells treated with the drug combinations. The Western Blot combination results in the HCT-116 cancer cells demonstrated increased pSTAT3 in the reg. group, while the expression was reduced in the other treatment groups compared to the CTR (Figure 18). Total STAT3 protein was upregulated in all treatment groups, with the highest levels in the iri. and combination group. Based on the quantification plot, there was no difference in phospho-ERK expression between the treatment groups. A reduction of pS6 was observed in the reg. and combination groups, but with less pS6 in the combination group compared to treatment with regorafenib alone.

Downregulation of total S6 protein and ERK protein were seen with combination of the drugs, whereas there were no visible changes in the mono-treatments compared to the CTR. γH2AX was increased in the combination and iri. groups, but no differences in expression was observed between these groups. There was a lot of variation between the replicate measurements of γH2AX though, which is indicated by the high standard deviation (SD=2.96-3.46). Regorafenib treatment alone did not result in increased γH2AX expression. All treatment groups exerted an upregulation of total PARP protein, with the highest expressions found in the iri. group and combination group. Cleaved PARP only seemed to be induced following mono-treatment with irinotecan compared to the CTR, but there was variation between the experiments and the same levels of cl. PARP was not observed consistently (Figure 18). In general, the expression patterns seen in these combination experiments correlated with the results from the single agent experiments with regorafenib and irinotecan at equivalent drug concentrations, with few divergences. There seems to be a larger irinotecan induced reduction in S6 protein in the mono-treatment experiments, in addition to increased pERK with regorafenib, which conflicts with the observations in the combination experiments (Figure 8, Figure 12).

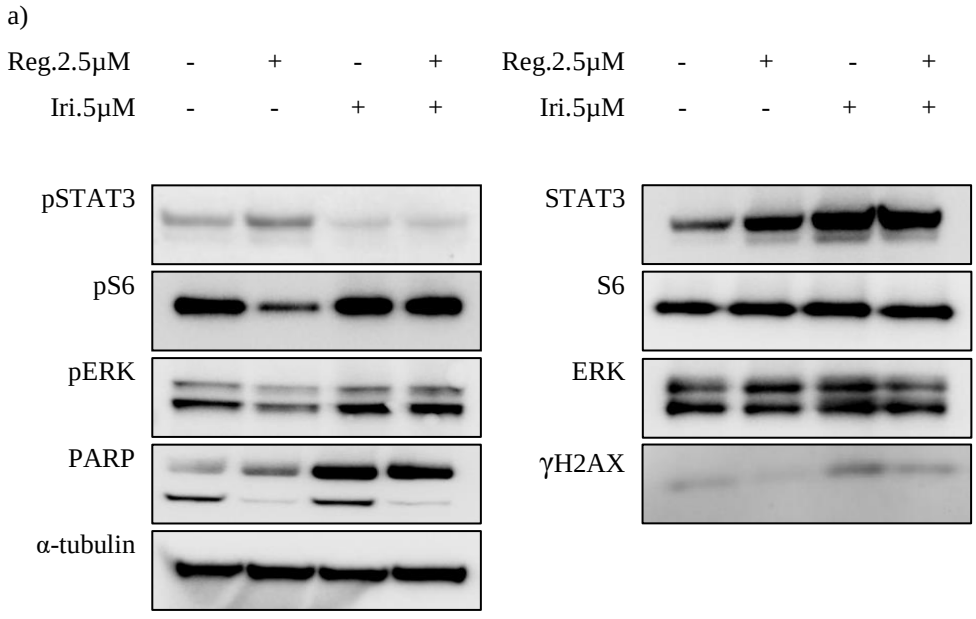

b)

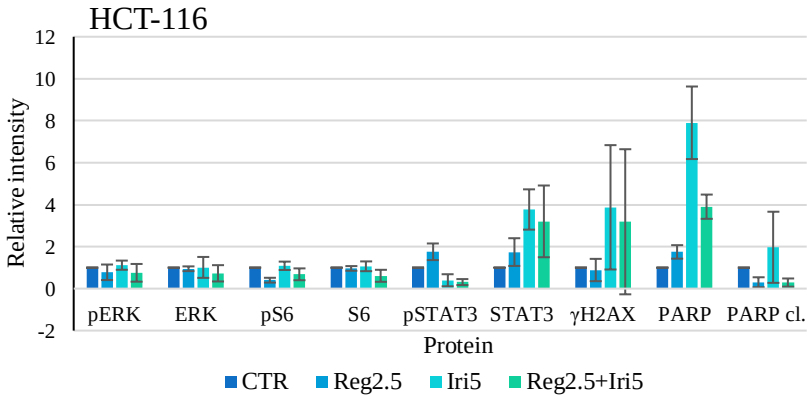

Figure 18: a) Representative Western Blot Immunoassay results for detection of protein expression levels in different signaling pathways in HCT-116 cells after 72-hour combination therapy with regorafenib and irinotecan. α-tubulin was used as internal loading control. b) Relative quantification of Western Blot protein bands with Image-Lab that shows relative levels of protein expression in HCT-116 cells compared to the CTR after 72-hour combination treatment with regorafenib and irinotecan. Error bars indicate standard deviation (n=3).

4.2.2. Combination treatment with regorafenib and irinotecan in SW-620

The same combination experiment was performed in SW-620 cells. Following mono-treatment with regorafenib and irinotecan, the confluence became lower as the drug concentration increased (Figure 19). In the treatment groups with iri.1 combined with the two highest regorafenib concentrations, the treatment seems to lead to a drop in cell confluence before the confluence tended to be less pronounced with 2.5 μM irinotecan. Thereafter the confluence kept reducing in a dose dependently manner at higher drug concentrations. The combination groups with reg.1 exerted a gradual decrease in confluence with increased irinotecan concentration (Figure 19). In SW-620 cells, the same tendency for combination treatment with regorafenib and irinotecan as for HCT-116 cells was observed, where synergism was found mostly at the lower drug concentrations (Table 5). In the SW-620 cells, synergism was demonstrated with all reg.1 combination groups in addition to the reg.5+iri.1 group. In the latter combination group, significance was found with ANOVA-test and Tukey HSD ($p < 0.05$). All four reg.1 combination groups were significant compared to reg.1 monotherapy, but not against equivalent irinotecan mono-treatment. With higher doses, additive and antagonistic effects were observed (Table 5).

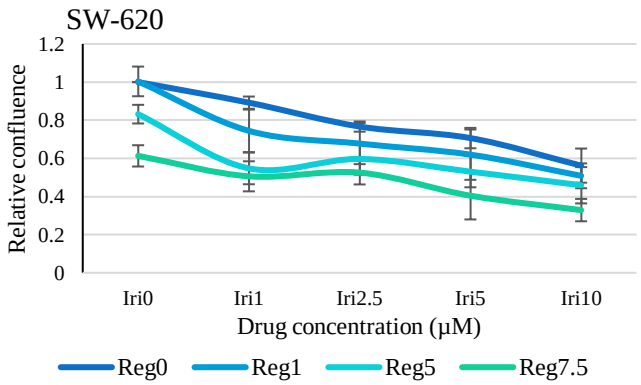

Figure 19: IncuCyte measurement of dose-effect relationship in SW-620 cells with regorafenib and irinotecan as single agent and in combination after 72 hours of treatment. Error bars indicate standard deviation (n=3).

Table 5: Calculation of combination index for relative values from SW-620 combination experiment (Figure 19) by using CalcuSyn software. Statistical significance ($p < 0.05$) as obtained from Tukey HSD is indicated with asterisks (** = significant against both mono-treatments or * = significant against one mono- treatment).

	Irinotecan 1	Irinotecan 2.5	Irinotecan 5	Irinotecan 10
Regorafenib 1	0.448*	0.620*	0.821*	0.887*
Regorafenib 5	0.763**	1.002	1.084	1.207
Regorafenib 7.5	1.037	1.192	1.104	1.112

The Western Blot results showed that phosphorylation of S6 and ERK was reduced in the regorafenib group and combination group, while the expression of pS6 and pERK tended to be slightly increased with irinotecan compared to the CTR (Figure 20). The reduced levels of these phospho-proteins were relatively similar in both groups. Both total S6 protein and ERK protein was slightly downregulated in the regorafenib and combination groups. All treatment groups induced increased expression of PARP protein, where the reg. group exerted the lowest expression level. The CTR sample had a very weak signal of PARP cleavage, while cleavage was detected in all the treatment groups, indicating apoptosis. The iri. group and combination group had similar and the highest levels of PARP cleavage, but the combination group had a lot of variation between replicate experiments. No differences in levels of γH2AX were observed in cells treated with irinotecan and the combination of drugs, but there was a clear increase in the protein expression compared to the CTR (Figure 20). These results also seem to be confirmed by the earlier mono-treatment experiments with regorafenib and irinotecan in SW-620 cells at equivalent drug concentrations in general, with only a few conflicting findings. There was a lower level of PARP protein and higher total ERK

expression with regorafenib in the mono-treatment experiments compared to the combination experiments. In addition, the mono experiments performed with irinotecan demonstrated no cleaved PARP in any of the treatment groups, while it was observed in the iri. group of the combination experiments. The mono-treatment experiments with irinotecan in SW-620 cells were only performed once though (Figure 10, Figure 14).

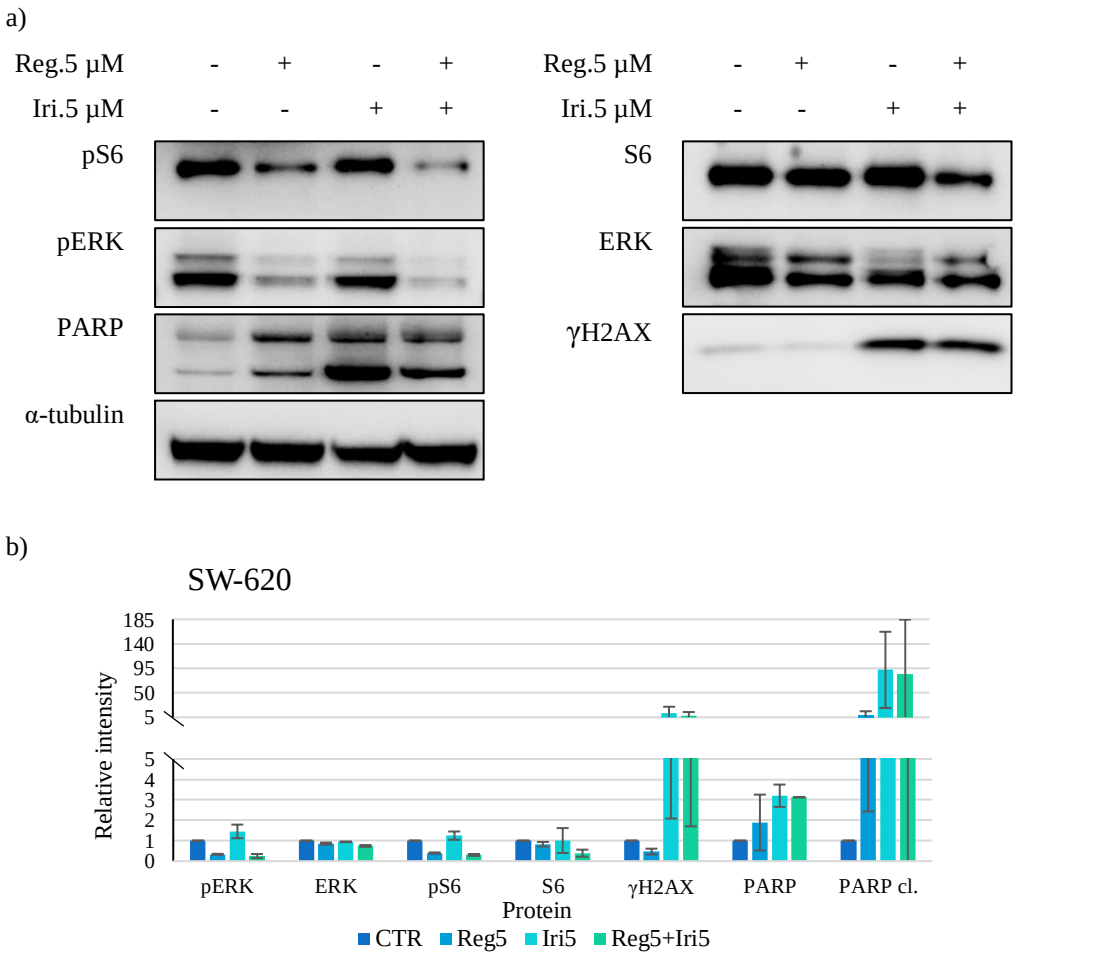

Figure 20: a) Representative Western Blot Immunoassay results for detection of protein expression levels in different signaling pathways in SW-620 cells after 72-hour combination therapy with regorafenib and irinotecan. α-tubulin was used as internal loading control. b) Relative quantification of Western Blot protein bands with Image-Lab that shows relative levels of protein expression in SW-620 cells compared to the CTR after 72-hour combination treatment with regorafenib and irinotecan. Error bars indicate standard deviation (n=2).

4.2.3. Combination treatment with regorafenib and oxaliplatin in HCT-116

Regorafenib was also combined with oxaliplatin in both cell lines. All mono treatments with either regorafenib or oxaliplatin resulted in reduced confluence with increasing drug concentration, except for the ox.0.1 group which did not differ from the CTR (Figure 21). All combination treatment groups with ox.0.5 exerted almost no differences in drug effects on cell confluence. As the regorafenib concentration increased in the combination treatments the confluence curves tended to flatten off (Figure 21). In the HCT-116 cells, the combination experiments with regorafenib and oxaliplatin only showed additive and antagonistic effects in the different groups (Table 6). There was not found synergistic effect in any of the groups and statistical analysis was therefore not included. The combination experiment results with oxaliplatin with each cell line were also compared against MTS measurement results of cell viability and can be seen in table G1 (Appendix G). The oxaliplatin mono-treatment in HCT-116 did not differ much from IncuCyte results, but all combination groups and regorafenib mono-treatment groups were less responsive to the drugs and indicated higher cell survival in general, when using MTS. Even though the viability was higher, the dose-effect patterns remained quite similar with both measurements. The MTS data demonstrated synergistic effect in reg.1+ox.0.1 group and slight synergism in reg.1+ ox.0.25 group though.

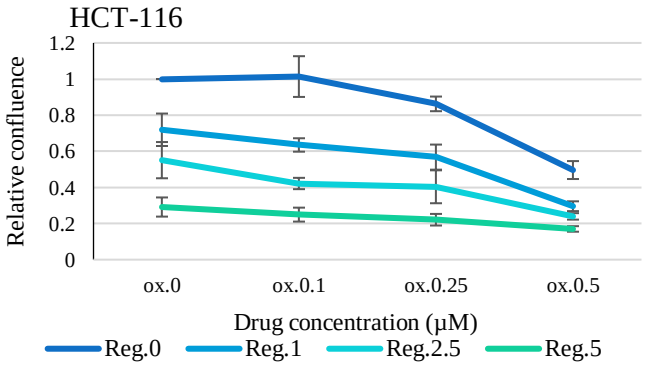

Figure 21: IncuCyte measurement of dose-effect relationship in HCT-116 cells with regorafenib and oxaliplatin as single agent and in combination after 72 hours. Error bars indicate standard deviation (n=3).

Table 6: Calculation of combination index for relative values from HCT-116 combination experiment (Figure 21) by using CalcuSyn software.

	Oxaliplatin 0.1	Oxaliplatin 0.25	Oxaliplatin 0.5
Regorafenib 1	0.908	1.112	1.175
Regorafenib 2.5	0.971	1.242	1.299
Regorafenib 5	0.936	1.111	1.361

4.2.4. Combination treatment with regorafenib and oxaliplatin in SW-620

In SW-620 cells, exposure to regorafenib and oxaliplatin alone reduced confluence with increased drug concentration, except for reg.1, which did not seem to affect the cells differently than the CTR (Figure 22). The reg.1+ox.0.1 combination group exerted a more pronounced reduction in confluence compared to the respective mono-treatment groups. As the oxaliplatin concentration increased above 0.5 μM, the effects on confluence in the combination treatment groups tended to converge (Figure 22). The SW-620 cell line had a slightly more synergistic responses to combination treatment with regorafenib and oxaliplatin than HCT-116 (Table 7). Synergistic effect was only found at the lower drug concentrations in SW-620 (reg.1+ox.0.1 and reg.1+ox.0.5 groups). As the drug concentrations increased, the effect became additive and with the highest concentrations tested the effects were antagonistic. In the two mentioned groups, where synergism was demonstrated, there was a significant difference in confluence compared to regorafenib mono-treatment and the CTR, using ANOVA-tests and Tukey HSD ($p < 0.05$). However, the combination treatment was not significantly better than mono-treatment with oxaliplatin. The same responses were confirmed by MTS measurement, without much variation between the two measurements (Table G2 in Appendix G). The results obtained using MTS did not demonstrate synergistic effect in any of the treatment groups.

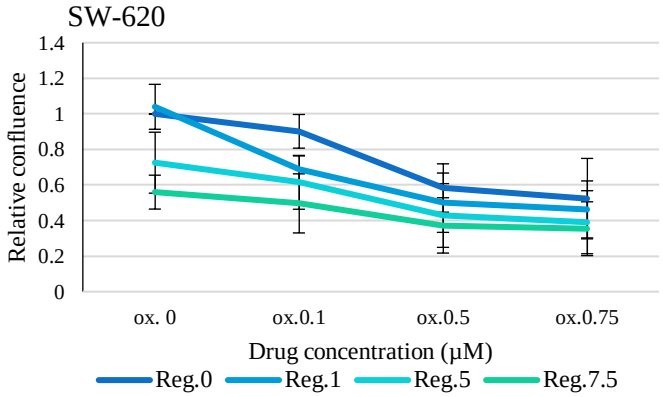

Figure 22: IncuCyte measurement of dose-effect relationship in SW-620 cells with regorafenib and oxaliplatin as single-agent and in combination after 72 hours. Error bars indicate standard deviation (n=3).

Table 7: Calculation of combination index for relative values from SW-620 combination experiment (Figure 22) by using CalcuSyn software. Statistical significance ($p < 0.05$) as obtained from Tukey HSD is indicated with asterisks (** = significant against both mono-treatments or * = significant against one mono- treatment).

	Oxaliplatin 0.1	Oxaliplatin 0.5	Oxaliplatin 0.75
Regorafenib 1	0.441*	0.806*	1.003
Regorafenib 5	0.986	1.173	1.303
Regorafenib 7.5	1.188	1.359	1.504

4.3. Morphological changes in HCT-116 and SW-620 cells induced by drug treatment

The two cell lines differed in growth rate and morphology before and after exposure to the different drugs (Figure 23). Normally, HCT-116 cells were more fast growing compared to SW-620 cells. SW-620 cells tend to form and grow as dense “cell islands”. The HCT-116 grew denser than SW-620 cells and could reach a confluence of 100% if allowed, while the SW-620 cells stopped growing when they reached a confluence of about 80%. The faster growth of the HCT-116 cells can also be observed in figure E (Appendix E), where initial pilot experiments to determine the number of cells to seed in each well are shown. Treatment with regorafenib and irinotecan in HCT-116 cells resulted in cellular differentiation by exhibiting typical apoptotic morphology such as cell shrinkage, whereas oxaliplatin treatment led to less pronounced differences. Both mono and combination treatment with regorafenib and irinotecan led to a higher extent of visualized cytoplasm in addition to nuclear changes in HCT-116. All of the drugs also showed distinct effects in SW-620, where cells exposed to

mono and combination treatment with irinotecan tended to undergo fragmentation and rupture into cell debris, unlike the HCT-116 cells (Figure 23).

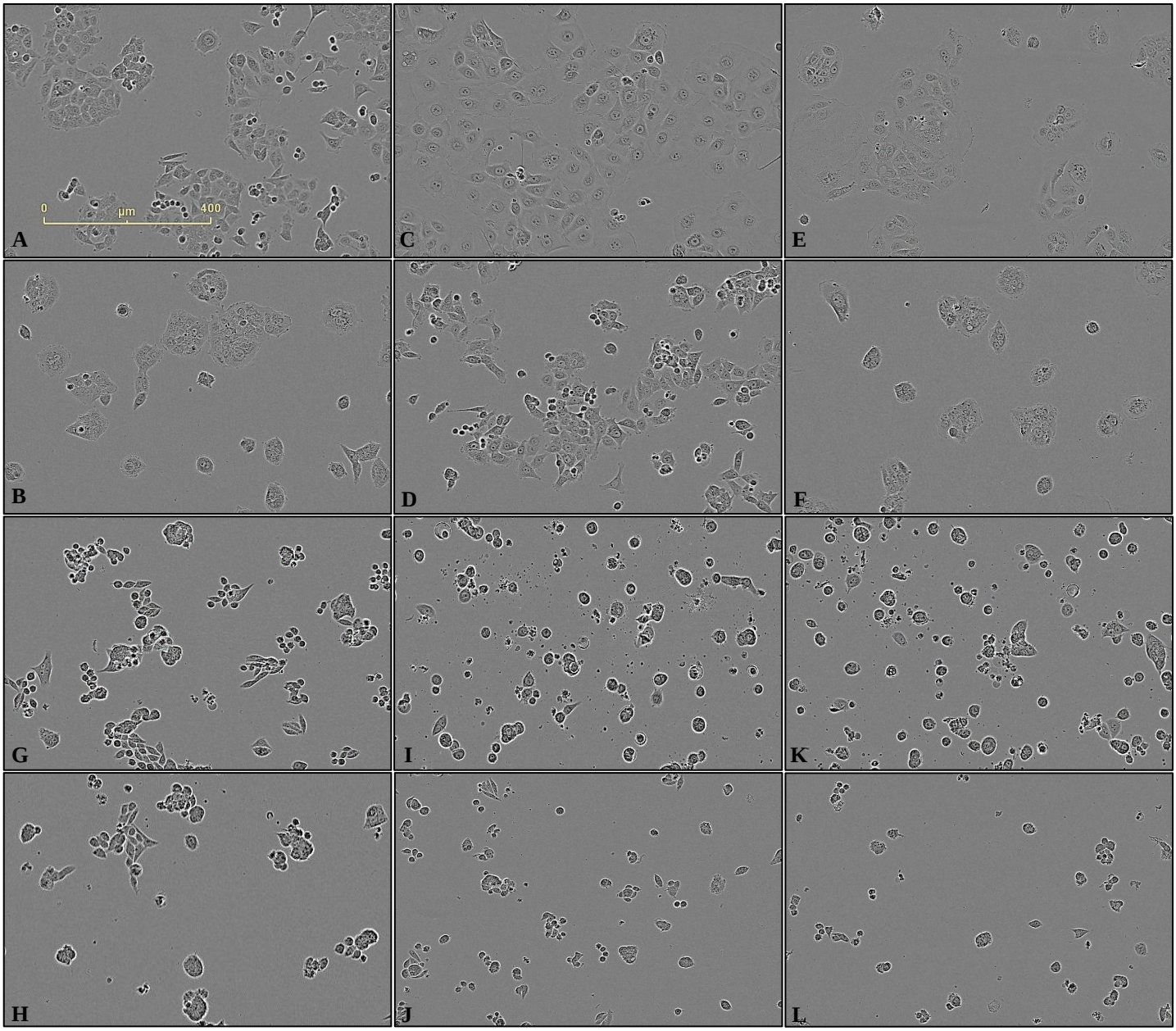

Figure 23: Phase-contrast images from IncuCyte of confluence of HCT-116 and SW-620 cells with and without mono or combination treatment with regorafenib (reg.), irinotecan (iri.) and oxaliplatin (ox.). All images are from day 3 (after 48 hours of drug treatment). The numbers represent the actual concentration of drug in micromolar (µM). A: HCT-116 CTR, B: HCT-116 reg.5, C: HCT-116 iri.10, D: HCT-116 ox.0.5, E: HCT-116 reg.5+iri.10, F: HCT-116 reg.5+ox.0.5, G: SW-620 CTR, H: SW-620 reg.5, I: SW-620 iri.10, J: SW-620 ox.0.5, K: SW-620 reg.5+iri.10, L: SW-620 reg.5+ox.0.5. Scale bar 400 µM.

4.4. Combination experiments in mucinous PDX- models

4.4.1. Combination experiments with regorafenib and irinotecan

The efficacy of the combination treatment with regorafenib and irinotecan was also investigated in two different mucinous PDX-models (PMCA-1 and PMCA-2). The viability measurement of the mucins was only performed with MTS. The MTS measurement show varied responses to drug treatment in the different PDX-models (Figure 24). PMCA-2 had a stronger response at the same drug concentrations than PMCA-1. In PMCA-1, no differences in viability were observed upon treatment with either regorafenib, irinotecan or the combination. The physical appearance of the mucin samples also varied, where PMCA-1 had a much finer consistency and was less lumpy compared to PMCA-2 mucin. This difference was also reflected in the color formation during the MTS assay, where the PMCA-2 sample tended to develop darker brown spots, while PMCA-1 was more unicolored. In PMCA-2, regorafenib did not seem to inhibit tumor growth, while treatment with irinotecan as single agent showed a tendency to reduce viability. None of the reductions in viability after treatment were significant compared to the CTR ($p > 0.05$). Combination treatment tended to have reduced viability compared to irinotecan alone, but there was no significant difference.

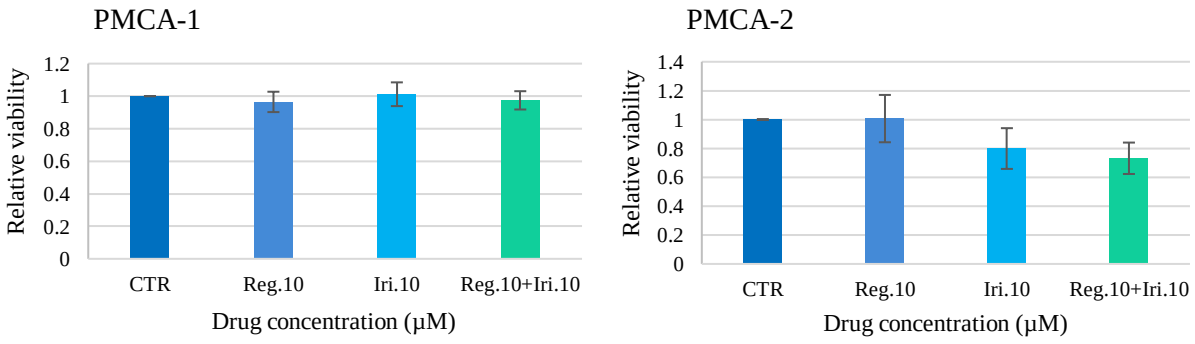

Figure 24: Measurement of viability of treated PMCA-1 mucin (n=3) and PMCA-2 mucin (n=2) with MTS assay after 24-hour mono or combination treatment with a selected dose of regorafenib and irinotecan. The results are presented as relative absorbance at 490 nm relative to the CTR as function of drug concentration. Error bars indicate standard deviation.

Western Blot Immunoassay was also performed as previously described with the PDX-model to detect the same proteins as for the cell lines. The results demonstrated that PMCA-1 treated with regorafenib as single agent led to an increase in phosphorylated STAT3 (Figure 25). This was not observed in samples treated with irinotecan or a combination of the drugs, with similar levels as the CTR. No apparent difference in total STAT3 protein was seen between the treatment groups. The quantification plot demonstrated that there was a reduction in phosphorylated S6 in all treatment groups compared to the CTR and total S6 protein was reduced in the iri. group. Mono-treatment with regorafenib seemed to cause a reduction of pERK in the MAPK signaling pathway, while there were no differences in total ERK protein in all treatment groups. An increase in γH2AX was observed in the iri. group and combination group, but there was no difference in level of phosphorylation between these two groups. PARP cleavage was also observed in the iri. group and combination group, but again there was no difference in expression between these groups. None of the treatments resulted in increased total PARP expression (Figure 25).

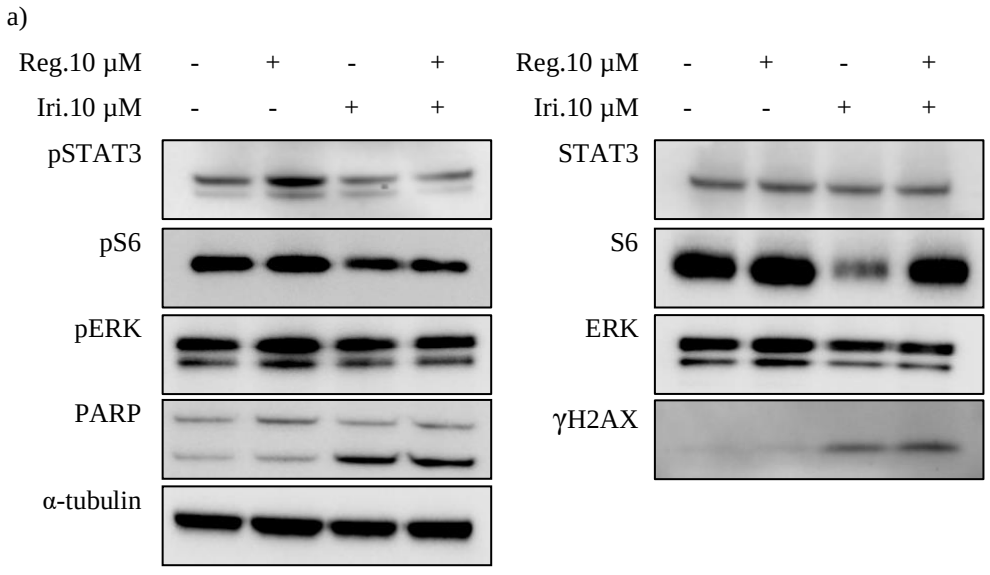

b)

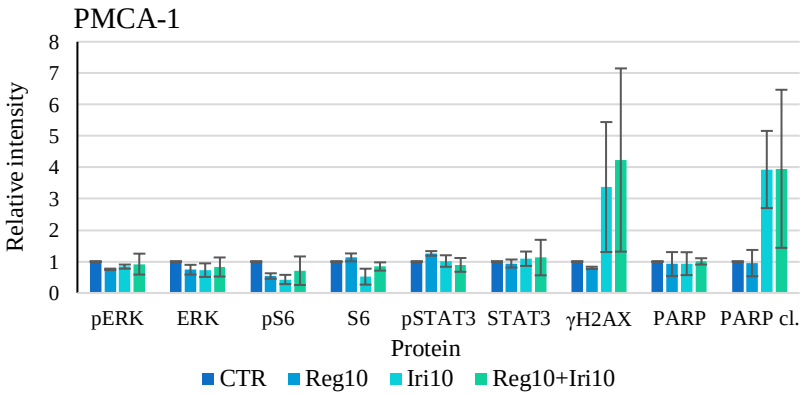

Figure 25: a) Representative Western Blot Immunoassay results for detection of protein expression levels in different signaling pathways in PMCA-1 mucin after 72-hour combination therapy with regorafenib and irinotecan. α-tubulin was used as internal loading control. b) Relative quantification of Western Blot protein bands with Image-Lab that shows relative mean levels of protein expression in PMCA-1 mucin compared to the CTR after 72-hour combination treatment with regorafenib and irinotecan. Error bars indicate standard deviation (n=2).

4.4.2. MUC-2 gene expression in drug exposed mucin

In addition to investigating protein expressions, the levels of MUC-2 in PMCA-1 was determined with RT-qPCR after treatment with regorafenib and irinotecan, to investigate if the treatment would influence expression of mRNA, as these models contain a lot of MUC-2. A significant reduction in MUC-2 levels was found in samples treated with regorafenib compared to the CTR group (Figure 26). Treatment with irinotecan and the combination of the drugs showed significantly lower levels of expression compared to regorafenib as single agent. The data indicated lowest MUC-2 expression in the combination treatment compared to the regorafenib and irinotecan mono-treatment groups. The difference in MUC-2 expression in the combination group and irinotecan group was relatively small, and there was not found statistical significance in expression level between these two treatment groups with ANOVA (Figure 26).

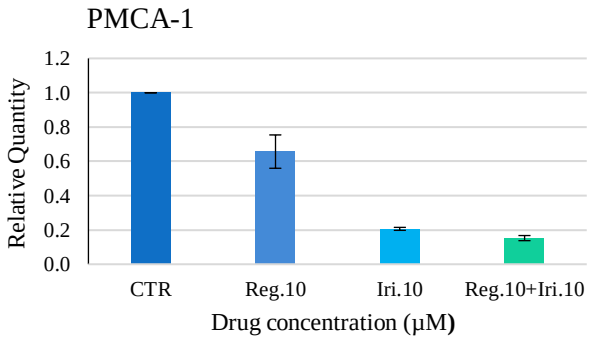

Figure 26: MUC-2 expression in PMCA-1 mucin analyzed with qPCR after 24-hour of drug exposure to regorafenib and irinotecan in combination or as single agents. Error bars indicate standard deviation (n=2).

4.5. Microscopy of tissue sections from mucin

PMCA-1 mucin was stained with H&E to investigate the histology of the sample (Figure 27). Most of the sample consisted of mucinous tissue, which was visualized as light white-pink areas on the images. Clusters of cells, visualized as dark pink spots, were spread among the mucin.

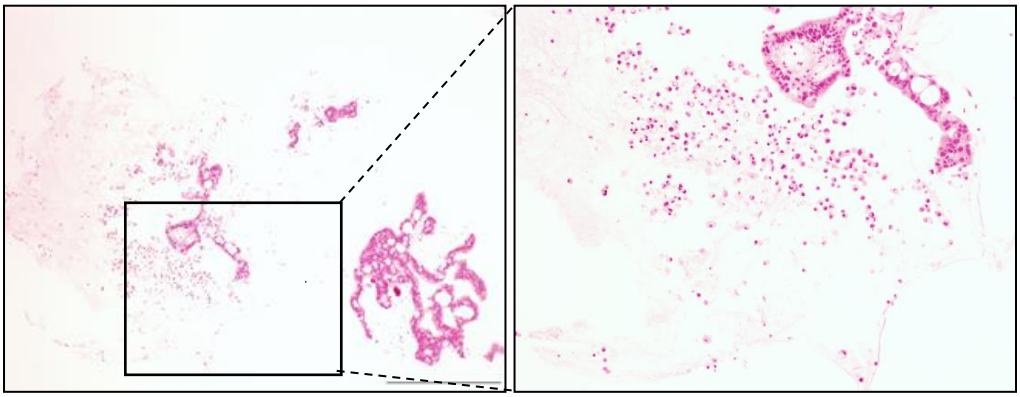

Figure 27: Images of H&E stained PMCA-1 mucin tissue section, obtained by using color brightfield microscopy. The nucleus is stained dark pink and the cytoplasmic components pink. Objective taken with 4x and 10x original magnification. Scale bar 200 µM.

4.6. Nuclear topoisomerase-1 expression visualized by immunofluorescence

The topo-1 enzyme expression level was investigated in HCT-116 and SW-620 cells following treatment with regorafenib and irinotecan. This was done to find out more about the mechanism behind the antitumor activity the combined drugs exert in mCRC. The function of this enzyme is essential for the cells' ability to divide, and irinotecan targets and inhibits its function. Both the HCT-116 and SW-620 cell lines showed clear nuclear expression of topo-1 in the CTR group, but they demonstrated differences in expression levels in the regorafenib mono-treatment group (Figure 28, Figure 29). The nuclear expression of this enzyme was strongly reduced in regorafenib treated HCT-116 cells, while in SW-620 cells, there were some, but less reduction in topo-1. The regorafenib treatment group in HCT-116 cells only had topo-1 expression in some of the nuclei, while the enzyme was expressed in most nuclei in the iri. group. In SW-620 cells, the reg. group showed topo-1 expression in most nuclei present, while the iri. group only had expression in a few. The enzyme tended to be expressed more strongly in the HCT-116 iri. group than in SW-620 cells. Very few viable cells were found in the irinotecan and combination treatment groups for both cell lines. Some single cells may have succeeded in avoiding the drug and exerted nuclear expression of the enzyme. No nuclear expression was visualized in the HCT-116 combination group and the dense green coloring seen is most likely due to dying cells. The enzyme expression in SW-620 cells exposed to combination treatment did not differ much from the iri. group, but in comparison to the reg. group, the expression in these groups was highly reduced. The irinotecan and combination treatments resulted in nuclear fragmentation, an indication of cells undergoing apoptosis. In all negative control groups (images not included) topo-1 was not detected.

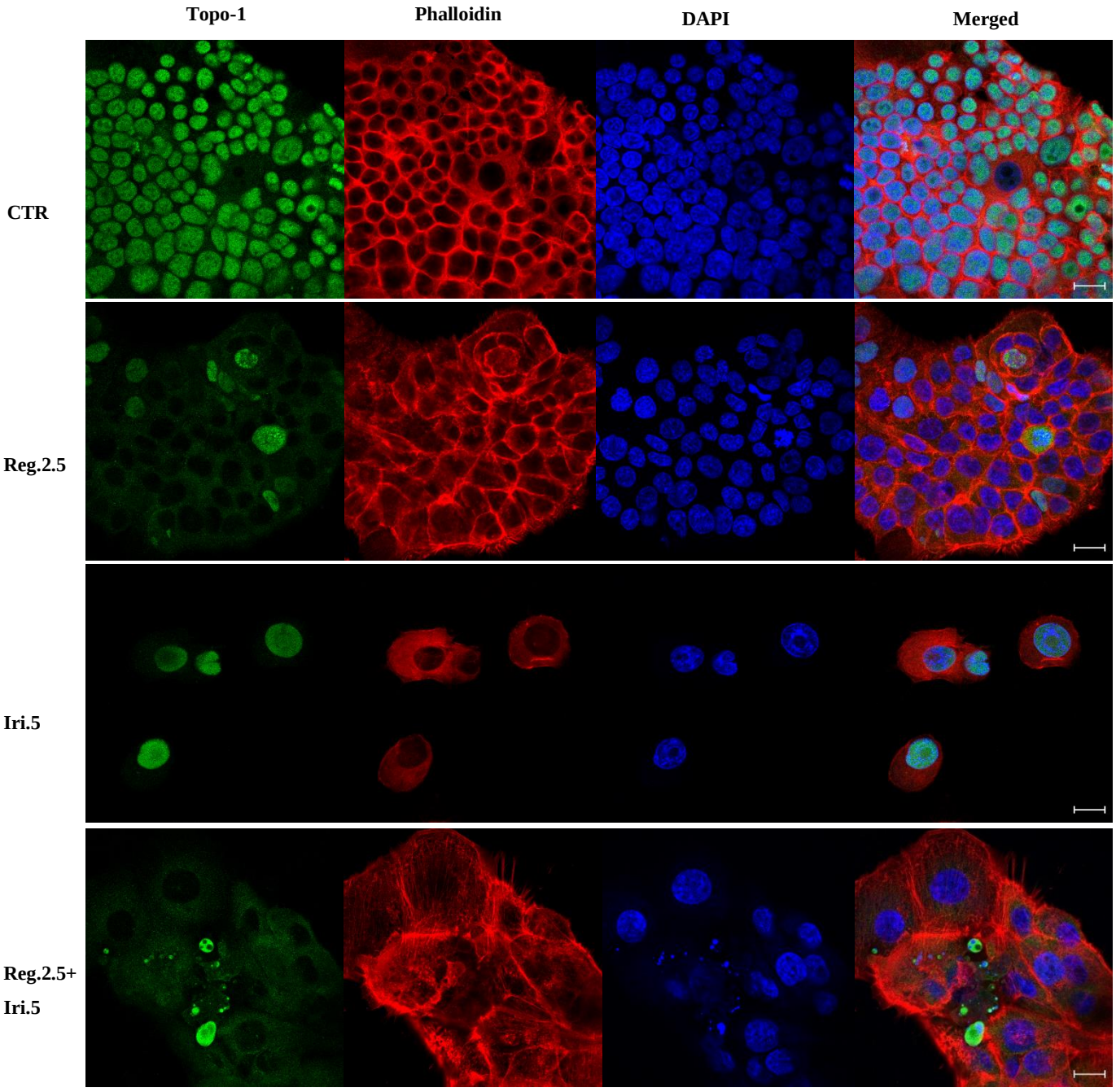

Figure 28: Images obtained from immunofluorescence microscopy of HCT-116 cells treated with regorafenib, irinotecan or the combination for 72 hours. From left to right; anti-topoisomerase, phalloidin (F-actin), DAPI (nucleus), merged images. From top to bottom; CTR, Reg.2.5, Iri.5 and Reg.2.5+Iri.5. Objective taken with magnification of 63x. Scale bar 20 μm.

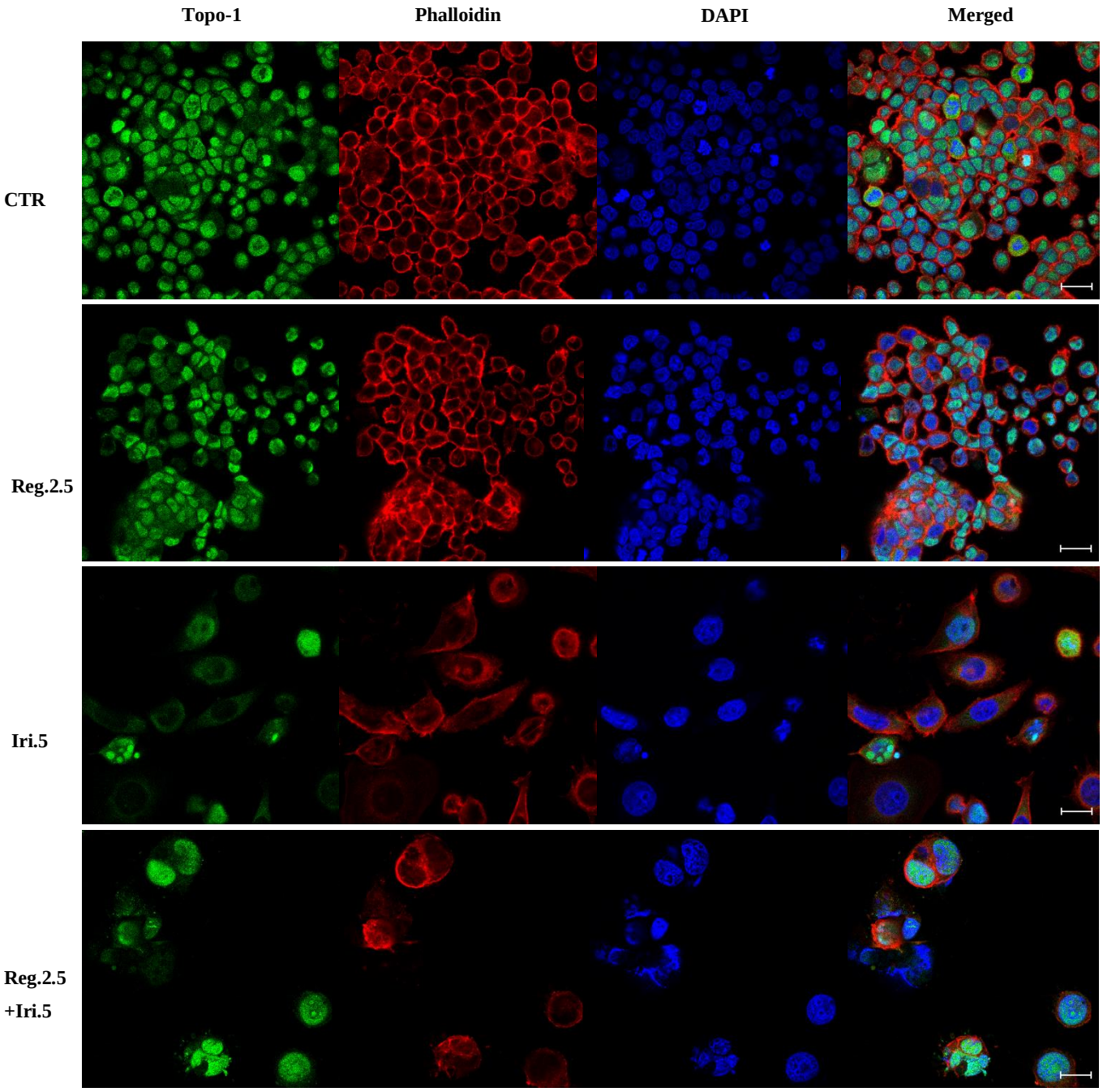

Figure 29: Images obtained from immunofluorescence microscopy of SW-620 cells treated with regorafenib, irinotecan or the combination for 72 hours. From left to right; anti-topoisomerase-1, phalloidin (F-actin), DAPI (nucleus), merged images. From top to bottom; CTR, Reg.2.5, Iri.5 and Reg.2.5+Iri.5. Objective taken with magnification of 63x. Scale bar 20 μm.

5 DISCUSSION

New and improved treatment options which have the potential to be implemented in clinical practice are of major importance for metastatic CRC patients with disease recurrence after treatment failure. In this master project we therefore wanted to investigate a potentially synergistic combination treatment with regorafenib plus irinotecan or oxaliplatin in vitro. Furthermore, proteins and phospho-proteins in relevant signaling pathways in CRC were also studied with Western Blot to look for synergistic effects at the protein level and to improve our understanding of how these drugs exert their actions. Since the patient's response to irinotecan treatment might be associated with topoisomerase, the expression and localization of the enzyme was studied in treated cell lines. In many cases, CRC disease also involves production of mucous, which can lead to treatment difficulties. This is why we wanted to investigate the drug effects on MUC-2 expression in a PDX-model.

5.1. Regorafenib inhibits cell growth in both cell lines and induces apoptosis in SW-620 cells

Prior to combination treatment, the cell lines were exposed to mono therapy with regorafenib, irinotecan and oxaliplatin. In clinical trials where regorafenib has been administered as single agent in refractory mCRC patients, the treatment outcome was only a modest improvement in OS, PFS and disease control [68, 69]. In the present study, we observed a dose dependent inhibition of cell growth in both cell lines following mono-treatment with regorafenib (Figure 7, Figure 9). Regorafenib has earlier been reported to mediate inhibition of proliferation in human CRC cell lines such as HCT-116 and SW-620 in vitro, in a dose dependent manner [22, 70]. Regorafenib targets and inhibits different multi-tyrosine kinases involved in oncogenesis, tumor angiogenesis and tumor microenvironment modulation [20]. Different signaling pathways, which previously have been shown to be affected by regorafenib were also investigated by looking at protein expression [20]. Several mechanisms for the growth inhibitory effect of regorafenib have been suggested. Schmieder R. et al. have demonstrated reduced phosphorylation of ERK with regorafenib in HCT-116, but no effect on total ERK [22], which may contribute to the tumor growth inhibition. Furthermore, the CRC cells' response to regorafenib treatment is suggested to depend on induction of p53-upregulated modulator of apoptosis (PUMA) expression, which is proposed to be activated through ERK inhibition. In addition, this mechanism may play a role in the sensitivity to regorafenib in

combination with other drugs [37]. We did observe a reduction of pERK in both HCT-16 and SW-620 cells exposed to 5 μM regorafenib, but not at lower doses (Figure 8, Figure 10), indicating the ability of regorafenib to inhibit RAF serine/threonine kinase as a possible mechanism for its anti-growth activity. Total ERK protein reduction was only observed in HCT-116 cells. This might suggest a PUMA mediated drug response with regorafenib in HCT-116 cells, but the apoptosis induction indicated by PARP cleavage did not correlate with the ERK inhibition level, possibly due to selected drug concentrations. Regorafenib has earlier been reported to induce apoptosis, indicated by PARP cleavage [70]. We observed induction of apoptosis in HCT-116 with the lowest drug concentration tested and with the two highest concentrations in SW-620 cells. The drug sensitivity to regorafenib has been demonstrated to be lower in SW-620 compared to HCT-116 [12, 22], which is confirmed by our findings. If the regorafenib mediated induction of apoptosis in these cell lines is due to p53 activated PUMA, the lower drug response observed in the SW-620 cells might be dependent on its distinct mutational profile, which encompasses a p53 mutation compared to the HCT-116 cells. Another suggestion is that the antiangiogenic effect of regorafenib could also possibly contribute to its mediation of tumor growth inhibition, giving the drug easier access to the tumor [22].

Furthermore, we also found regorafenib mediated activation of the oncogenic JAK/STAT signaling pathway in HCT-116 cells with all doses tested. Studies with HCT-116 cells have demonstrated association between the apoptotic effects of regorafenib and mediated downregulation of pSTAT3 due to enhanced SH2 domain containing phosphatase 1 (SHP-1) activity [70], but also an in vitro study with hepatocellular carcinoma cells (HCC) has suggested that the effect of regorafenib treatment is determined by inhibition of STAT's related signaling [71], which was not confirmed by our results in HCT-116. However, as mentioned earlier we did not find regorafenib induced apoptosis in most concentrations tested in HCT-116. Napolitano S. et al. showed that exposure to 1 μM regorafenib did not result in any alterations in phosphorylation of protein S6 in both HCT-116 and SW-620 cells [12], which seems to be consistent with our data with the same respective regorafenib concentration, but at higher concentrations, suppression of the PI3K-Akt pathway was observed in both cell lines.

5.2. Regorafenib combined with irinotecan exerted synergistic effects in HCT-116 and SW-620 cells

In an attempt to find potential synergistic drug combinations for treatment in mCRC patients, which can enhance the therapeutic effect, while minimizing the adverse reactions associated with treatment, combination treatment experiments were performed with regorafenib and irinotecan with a range of concentrations in HCT-116 and SW-620 cells. The efficacy of treatment was evaluated after 72 hours of drug exposure. We hypothesized that combining the drugs could achieve an enhanced effect by modulation of effectors in different signaling pathways. Promising effects induced by this combination have previously been observed in vivo [22], but also in clinical studies [72]. Our results demonstrated synergistic effect for the majority of the doses selected in HCT-116, but the effects were more prominent at lower doses (Figure 17). This drug combination also showed synergy at the lower doses in SW-620 cells (Figure 19), but were expected at the highest drug concentrations since most cells were killed, reducing the combined drug efficacy. Sorafenib, an analog of regorafenib, which also targets VEGFR, PDGFR and B-RAF, has previously been reported to enhance the cytotoxic effect of SN-38 in HCT-116 and SW-620 compared to SN-38 as a single agent [73].

We also investigated some proteins in the MAPK, PI3K-Akt and JAK/STAT signaling pathways that are known to be influenced by regorafenib. In addition, we looked into apoptosis and DNA damage in an attempt to elucidate other possible mechanistic reasons for the synergistic effect. The selected proteins are part of different pathways that will influence several mechanisms in the cells, and the wide variety was chosen to get an idea if any of the pathways showed some synergistic effects, and if so, could then be investigated in more detail later. Different mechanistic explanations for this synergistic effect between regorafenib and irinotecan have been suggested. Elucidation of synergistic effects has shown that gefitinib, another tyrosine kinase inhibitor, induced apoptosis (indicated by PARP cleavage), which was enhanced in combination with CPT-11 in CRC cells, suggesting this as a possible mechanism behind the synergistic effect in colorectal cell lines [74]. Gefitinib is a tyrosine kinase inhibitor, just like regorafenib, which inhibits EGFR mediated cell proliferation [46]. In patients SN-38 is metabolized and detoxified by uridine diphosphate glucuronosyl-transferase (UGT) in the liver to its inactive metabolite SN-38G. This enzyme is the main factor determining cytotoxic effect and side effects of irinotecan [75]. Regorafenib inhibits this enzyme in the liver and it has therefore been suggested that this could be the mechanism behind synergism in combination treatment, where regorafenib enhances cytotoxic effects of

irinotecan [72]. In this case, it would lead to more biologically active SN-38 and it is assumed that it would result in a higher expression of γH2AX and cleaved PARP in the combination group compared to treatment with irinotecan as single agent. This was not observable in our in vitro testing, where the combination treatment did not lead to increased PARP cleavage (apoptosis induction) or γH2AX in either cell lines (Figure 18, Figure 20). Furthermore, Mazart T. et al. have suggested that sorafenib overcomes irinotecan resistance by inhibition of the ABCG2 drug-efflux pumps, which leads to intracellular accumulation of SN-38 and increased cell toxicity [73].

Mono-treatment with irinotecan suggested HCT-116 cells as less responsive against irinotecan than SW-620 at the lowest concentrations tested, according to our obtained data (Figure 11, Figure 13). Several previous studies have demonstrated the same response in these cell lines [73, 76]. Elevated levels of γH2AX and cleaved PARP have been detected after treatment with irinotecan in HCT-116 cells, indicating induction of downstream events that cause DNA damage and apoptosis [45], which support our findings (Figure 12). Irinotecan treatment as a single agent has also been reported to induce apoptosis in treated SW-620 cells [76], an effect we also observed with a slight increase in PARP cleavage (Figure 14). The increased levels of cleaved PARP in SW-620 cells following mono-treatment with irinotecan we found were much more pronounced in the combination experiments than in the mono-treatment experiments, most likely due to a lack of replicates in mono-treatment experiments with irinotecan and large variation between experiments. Furthermore, in vitro studies with HCT-116 cells have demonstrated no changes in pS6 or pERK expression following SN-38 exposure compared to the untreated CTR [77]. We found a slight increase of pERK and reduction of pS6 in HCT-116, but these results are only based on a single experiment, so more replicates are needed. When combining irinotecan with regorafenib we did not observed any difference in protein levels compared to the drugs individually.

5.3. Combination therapy with regorafenib and oxaliplatin in HCT-116 and SW-620 cells

The efficacy of combination treatment with regorafenib and oxaliplatin was also investigated in HCT-116 and SW-620 cells (Figure 21, Figure 22). Most of the treatment groups with regorafenib and oxaliplatin from this current study did not demonstrate synergism. Some additive effects were observed, but the majority of the combinations had antagonistic effects. This seems to be consistent with previous studies, where the activity of regorafenib was assessed in a clinical trial, in combination with an oxaliplatin based therapy, and no synergism was observed [78]. Pharmacokinetics of oxaliplatin did not seem to be affected by regorafenib [72]. Oxaliplatin as single agent has demonstrated reduced cell viability in a dose dependent manner in human CRC cell lines like HCT-116 [28]. HCT-116 cells have also indicated less sensitivity to oxaliplatin treatment (50 μM) than SW-620 [79]. Our results showed higher sensitivity in HCT-116 than SW-620 cells at oxaliplatin concentrations below 1 μM, and at higher doses, the cell confluence became asymptotic, most likely due to no remaining living cells (Figure 15, Figure 16). In this present study, any potential mechanistic interaction between regorafenib and oxaliplatin was not investigated, as the viability studies did not show any tendencies towards synergistic interaction.

5.4. Heterogeneous combination therapy response in PDX-models

We also wanted to confirm if similar drug responses to regorafenib and irinotecan as for the cell line experiments could be obtained with different PDX-models. The response to treatment with regorafenib and irinotecan in the PDX-models tested varied, possibly due to the mucin's physical appearance, while individuality of the tumors and the distinct mucinous phenotypes may also have an impact [80]. Mucinous patient material often contains few tumor cells and is mainly dominated by mucinous tissue. Similar results were observed in the PDX-models that were investigated as shown by the IHC images (Figure 27). The majority of the samples was mostly mucin with only some cancerous cells spread throughout. The total amount of cancer cells present in the samples, but also the protective properties of the mucin could have an impact on the drug sensitivity and this might also be a possible explanation to the mucin's varied response observed against the different drug treatments. We did not observe any anti-tumor effect in PMCA-2 following mono-treatment with regorafenib, while irinotecan as single agent tended to reduce the viability (Figure 24). PMCA-2 mucin exposed to the

combination of the drugs tended to show a slight, but not significantly increased antitumor effect than the drugs as single agents, while PMCA-1 mucin did not seem to be affected in any treatment group. In a previous study, mono-treatment with irinotecan resulted in significant growth inhibition in vivo in PDX-model derived from mucinous CRC, while regorafenib only led to minimal antitumor and no antiangiogenetic effect, possibly due to elevated COX-2 concentrations (a promoter of tumor growth in CRC) [22]. The combination of regorafenib and irinotecan was reported to result in tumor growth inhibition of the same model, compared to the control [22], which reflects our results in PMCA-2. In addition to elucidating the viability in drug exposed PDX-models, we also performed protein analysis following regorafenib and irinotecan treatment (Figure 25). The protein analysis results we obtained with the xenograft model tended to confirm the observations we found in the cell line experiments. Our results indicated no difference in induction of apoptosis nor DNA damage in PMCA-1 with regorafenib in combination with irinotecan, compared to irinotecan as single agent at selected drug concentrations, which again indicates that this combination did not lead to higher effect of irinotecan. The same pattern was observed with the other proteins tested, where the combination did not differ from one of the mono-treatments.

5.5. Combination therapy may result in additional reduction of MUC-2 expression in PDX-model

Expression patterns of mucins are associated with development and progression of malignant diseases [81]. MUC-2 is the predominantly secreted mucin in CRC and identifying ways to reduce the MUC-2 production in cancer treatment is therefore desirable. This involves a major challenge because of the complex mucous protective barrier surrounding the epithelium of the tissues. The tumors might use the mucin to create a beneficial microenvironment during growth or metastasis and can result in reduced intracellular uptake of drugs [80]. We therefore wanted to investigate if MUC-2 expression following regorafenib and irinotecan treatment in the PMCA-1 PDX-model would be altered. The obtained results demonstrated that treatment with regorafenib alone led to a significant downregulation of MUC-2 compared to the CTR, while irinotecan as single agent resulted in even higher reduction in expression (Figure 26). Other studies have also reported intestinal mucosal changes and downregulation of MUC-2 expression based on in vivo experiments with irinotecan [82]. Furthermore, we also observed a tendency to downregulated MUC-2 in the combination group compared to the drugs as individual treatments. Dilly A.K. et al. have reported that MUC-2 protein targeting can

happen through MAPK pathway inhibition [83]. As regorafenib targets this pathway as well, it might be through this mechanism that regorafenib exerts its effect on MUC-2. However, in this model no reduction of pERK was seen after regorafenib treatment, thus indicating no inhibition of this pathway. Dilly et.al. have also proposed that inhibition of other pathways can reduce the expression of MUC-2, like the PI3K-Akt signaling pathway [80]. We did observe a reduction of pS6 in this model following treatment with regorafenib, which indicate a suppression of the PI3K-Akt pathway and can possibly be an explanation to the mechanism behind the reduced MUC-2 expression we observed in this model. The reduction in MUC-2 expression seen in this present study following treatment could also be due to cell death, thus leading to fewer cells able to produce MUC-2. Why treated PMCA-1 mucin demonstrates these alterations in MUC-2 expression, while the MTS measurement indicated no difference in viability remains unclear though. A higher dose of regorafenib and irinotecan were chosen in the PDX-model compared to the cell lines, due to an expected lower sensitivity in these models. Inclusion of a positive control with known effects could also have been included to assess the measurement validity. It can be questioned if the selected time of drug exposure is optimal for determining the effects of the drugs or if longer incubation periods are necessary to observe an induced response in these models, but the drug responses observed at protein level and in MUC-2 expression could rule out that the chosen time period was not sufficient.

5.6. Regorafenib combined with irinotecan may results in additional reduction of topoisomerase-1 activity in HCT-116 cells

To further explore the mechanism occurring when combining regorafenib with irinotecan, which led to antitumor activity, immunofluorescence was performed to determine topo-1 expression and location in both cell lines. Irinotecan is an inhibitor of the topo-1 nuclear enzyme, which may serve as a predictive biomarker for the chemotherapeutic response observed with irinotecan [84]. Peleg. R. et al. have elucidated the anticancer effect of combining gefitinib or erlotinib, with camptothecin (CPT) in breast and prostate cancer cells [46]. Like gefitinib, erlotinib is also an EGFR inhibitor. Peleg. R. et al. reported a similar reduction of cellular topo-1 protein level in the combination and irinotecan groups, while gefitinib and erlotinib led to no changes in topo-1 protein level. These findings seems to reflect our findings in SW-620 cells, where mono-treatment with regorafenib only led to a slight reduction in topo-1 expression, compared to the CTR and no differences in topo-1 after the irinotecan and combination treatment (Figure 29). Another expression pattern, possibly

due to cell-specific properties, was observed in the drug exposed HCT-116 cells (Figure 28); A more pronounced reduction of topo-1 was observed in HCT-116 cells compared to SW-620 following regorafenib treatment. In HCT-116 we also observed a tendency to enhanced drug effect with no nuclear topo-1 expression in the combination groups, compared to the mono-treatment. The cell confluence measurements performed in HCT-116 following combination treatment with these drugs did show synergism with the same drug concentrations as used for IF (Figure 17). This result is not necessarily expected, as Desai et al. have previously reported that reduced topo-1 expression can lead to induction of irinotecan resistance [85]. Sharma et al. however have found that sensitivity/resistance to irinotecan does not correlate well with the cellular levels of topo-1 [86] before treatment. An explanation to our synergistic result could be that regorafenib has reduced topo-1 expression, and irinotecan has disabled the remaining enzyme protein. Additional topo-1 activity studies could be performed to determine if this hypothesis is supported. Similarly, gefitinib has been reported to modulate SN-38's ability to inhibit topo-1 and induce apoptosis [46].

Our results also showed that irinotecan as single agent tended to lead to more strongly reduced topo-1 enzyme in the SW-620 compared HCT-116 cells, which could reflect a lower sensitivity to irinotecan in HCT-116 cells. This also corroborates with our observation in the cell confluence experiments after exposure with the same respective drug concentrations (Figure 11, Figure 13). An important factor which determines the cells' response to irinotecan is the cells' ability to repair DNA damage and undergo apoptosis [86]. Cellular stress caused by drug exposure trigger p53 in the cells to induce apoptosis. This means that the cells sensitivity to irinotecan also depends on a functional p53 [86]. As mentioned earlier, the SW-620 cells encompass a p53 mutation that could lead to these cells being less prone to undergo apoptosis following irinotecan treatment. This suggests that the p53 mutation in SW-620 does not explain its higher sensitivity to irinotecan that we observed. This immunofluorescence experiment was only preformed once, so additional experiments might be warranted to verify the results. Protein detection with Western Blotting after drug exposure could be interesting to perform with topo-1, to see if these results can support the expression pattern seen with immunofluorescence.

5.7. Methodological discussion

There are both advantages and disadvantages with human derived cell lines in clinical medical research. Cell lines as a model system limit the usage of animals in research and makes it unnecessary to consider the ethical perspectives related to this. They can be produced in unlimited amounts in cell culture, are suitable for genetic modifications, easy to use in the lab and cost efficient. In addition, the cell line must reflect and maintain the functional characteristics as the primary cells which can be a problem. Genotypic and phenotypic modifications can occur and lead to genetic drift, heterogenic cell cultures and cause variation in measurements [87]. To limit this problem, the cell lines were therefore only grown for a limited number of passages before they were discarded, and new cells were defrosted. The cell lines are not growing in 3D with other cells like they do normally in the body, but in 2D. To overcome this challenge, it is possible to grow the cells in 3D or in combination with other cells such as fibroblasts or astrocytes to better mimic the impact of the microenvironment [88]. However, in our experiments this was not deemed necessary and 2D cultures, which are very common, were used. Ex vivo experiments were also conducted with PDX-models, where mucin was extracted from two different animal models, to investigate the role of mucin in drug delivery. Drawbacks of studying these models in isolation are the limitation of tissue availability and the animal to animal variation [89]. The differences in viability in the two PDX-models tested in the present study varied strongly, which highlights the importance of using multiple models in research, as different models respond differently.

Cell viability and cytotoxic assays are frequently used in vitro for oncological research to evaluate cell growth inhibition. Even though these assays provide a valuable tool in research, it is important to address their limitations. MTS colorimetric assay and IncuCyte instrument were selected for cell viability determination, but since the results from IncuCyte for each cell line were more consistent compared to MTS assays, this was the preferred method to use further in the project. IncuCyte is able to efficiently track cell proliferative effects of drug treatment, but cannot discriminate between contrasting cellular densities at full growth confluency or if the cells are alive or dead [90]. It is also highly dependent on seeding in the wells, as it will take images of certain spots of the well, and uneven distribution could skew the results. In an attempt to reduce this potential error, two images of each well were taken instead of just one, to better show the true distribution and response to treatment. MTS provides a quick, precise and reliable viability measurements in vitro which favors this method against many other assays. However, the MTS assay may lead to variation in results

and wrong estimates of cell viability since metabolic activity of the cells may be changed by certain conditions or when exposed to drugs [91], because of the background absorbance corrections of the measurements. Another drawback is that absorbance levels measured are dependent on selected incubation time with the reagent [92]. In the initial experiments, the MTS results varied strongly between different experiments, while in experiments performed later, the results became more consistent, indicating that more experience with this method improved the results.

One-way ANOVA was used for statistical analysis for the data obtained in this thesis. This was the preferred statistical analysis compared to the Student's t-test because the t-test only estimates the variances between two groups. The t-test gives p-values which are not corrected for multiple testing. The one-way ANOVA test will tell if there is a difference in means between groups, but not which of the groups are different from each other. Therefore, an ad-hoc test was performed post ANOVA, in this case the Tukey's Honest Significant Difference (HSD) method, to get significance levels for pairwise treatment groups. Tukey HSD also corrects for type I errors. In statistical hypothesis testing, a type I error is the wrongful rejection of the null hypothesis (e.g. there is no difference in cell viability between treatment groups.)

6 CONCLUDING REMARKS

New and improved treatment for mCRC patients is necessary to establish, where treatment with regorafenib might be a possibility. However, its effect on survival in patients is limited and is also associated with toxicity. This study was performed to investigate if the combination of regorafenib with other commonly used drugs for treatment of mCRC might be beneficial for these patients.

In this master thesis we have shown that

- Regorafenib, irinotecan and oxaliplatin exhibit anti-proliferative effects as single agents in HCT-116 and SW-620 cells, where regorafenib and irinotecan target signaling pathways such as MAPK, PI3K-Akt, JAK/STAT and DNA damage pathways.
- Combination treatment with regorafenib and irinotecan demonstrated to have synergistic effect in HCT-116 and SW-620 cells.
- Regorafenib in combination with oxaliplatin did not show any potential benefit, where most of the concentrations tested were antagonistic.
- The observed synergistic effects to regorafenib combined with irinotecan in HCT-116 and SW-620 also tended to be reflected in the PMCA-2 model.
- No explanation for the synergistic effect when combining regorafenib and irinotecan was found by using protein analysis. The expression levels of the selected proteins did not show any differences between the mono and combination treatments; thus, we were not able to further elucidate the mechanism for the observed synergy.
- Both HCT-116 and SW-620 cells demonstrated nuclear expression of topoisomerase-1, but exhibited a cell type dependent reduction of the enzyme after drug treatment.

In summary, the results support the already published clinical trials and previous studies, where regorafenib in combination with irinotecan shows an improved effect compared to mono-treatments. However, regorafenib in combination with oxaliplatin did not show any potential benefit, and most of the concentrations tested had antagonistic results, which also supports previous studies. Further studies are needed in order to better understand the synergistic effect observed with regorafenib and irinotecan.

7 REFERENCES

1. GM C. The Cell: A Molecular Approach. 2nd ed: Sunderland (MA): Sinauer Associates; 2000.
2. You JS, Jones PA. Cancer genetics and epigenetics: two sides of the same coin? Cancer Cell. 2012;22(1):9-20.
3. Hanahan D, Weinberg RA. Hallmarks of cancer: the next generation. Cell. 2011;144(5):646-74.
4. Lodish H BA, Zipursky SL, et al. Molecular Cell Biology. 4th edition. New York: W. H. Freeman; 2000.
5. Ballinger AB, Anggiansah C. Colorectal cancer. Bmj. 2007;335(7622):715-8.
6. Simon K. Colorectal cancer development and advances in screening. Clin Interv Aging. 2016;11:967-76.
7. Jasperson K, Burt RW. The Genetics of Colorectal Cancer. Surg Oncol Clin N Am. 2015;24(4):683-703.
8. Haggar FA, Boushey RP. Colorectal cancer epidemiology: incidence, mortality, survival, and risk factors. Clin Colon Rectal Surg. 2009;22(4):191-7.
9. Munteanu I, Mastalier B. Genetics of colorectal cancer. J Med Life. 2014;7(4):507-11.
10. Ahmed D, Eide PW, Eilertsen IA, Danielsen SA, Eknæs M, Hektoen M, et al. Epigenetic and genetic features of 24 colon cancer cell lines. Oncogenesis. 2013;2(9):e71.
11. Guinney J, Dienstmann R, Wang X, de Reyniès A, Schlicker A, Soneson C, et al. The consensus molecular subtypes of colorectal cancer. Nat Med. 2015;21(11):1350-6.
12. Napolitano S, Martini G, Rinaldi B, Martinelli E, Donniacuo M, Berrino L, et al. Primary and Acquired Resistance of Colorectal Cancer to Anti-EGFR Monoclonal Antibody Can Be Overcome by Combined Treatment of Regorafenib with Cetuximab. Clin Cancer Res. 2015;21(13):2975-83.
13. Virk GS, Jafri M, Mehdi S, Ashley C. Staging and survival of colorectal cancer (CRC) in octogenarians: Nationwide Study of US Veterans. J Gastrointest Oncol. 2019;10(1):12-8.
14. James D. Brierley MKG, Christian Wittekind. TNM classification of Malignant tumours. Eighth ed: John Wiley & Sons; 2017.
15. Bray F, Ferlay J, Soerjomataram I, Siegel RL, Torre LA, Jemal A. Global cancer statistics 2018: GLOBOCAN estimates of incidence and mortality worldwide for 36 cancers in 185 countries. CA Cancer J Clin. 2018;68(6):394-424.
16. Larsen I. MB, Johannesen T., Robsahm T., Grimsrud T., Larønningen S., Jakobsen E., Ursin G. Cancer incidence, mortality, survival and prevalence in Norway. 2018.
17. Zhou G, Yang J, Song P. Correlation of ERK/MAPK signaling pathway with proliferation and apoptosis of colon cancer cells. Oncol Lett. 2019;17(2):2266-70.
18. Vatandoust S, Price TJ, Karapetis CS. Colorectal cancer: Metastases to a single organ. World J Gastroenterol. 2015;21(41):11767-76.
19. Vassos N, Piso P. Metastatic Colorectal Cancer to the Peritoneum: Current Treatment Options. Current Treatment Options in Oncology. 2018;19(10):49.
20. Grothey A, Van Cutsem E, Sobrero A, Siena S, Falcone A, Ychou M, et al. Regorafenib monotherapy for previously treated metastatic colorectal cancer (CORRECT): an international, multicentre, randomised, placebo-controlled, phase 3 trial. Lancet. 2013;381(9863):303-12.
21. Lemoine L, Sugarbaker P, Van der Speeten K. Pathophysiology of colorectal peritoneal carcinomatosis: Role of the peritoneum. World J Gastroenterol. 2016;22(34):7692-707.
22. Schmieder R, Hoffmann J, Becker M, Bhargava A, Muller T, Kahmann N, et al. Regorafenib (BAY 73-4506): antitumor and antimetastatic activities in preclinical models of colorectal cancer. Int J Cancer. 2014;135(6):1487-96.
23. Franko J, Shi Q, Meyers JP, Maughan TS, Adams RA, Seymour MT, et al. Prognosis of patients with peritoneal metastatic colorectal cancer given systemic therapy: an analysis of individual

patient data from prospective randomised trials from the Analysis and Research in Cancers of the Digestive System (ARCAD) database. Lancet Oncol. 2016;17(12):1709-19.
24. Winder T, Lenz HJ. Mucinous adenocarcinomas with intra-abdominal dissemination: a review of current therapy. Oncologist. 2010;15(8):836-44.
25. Lugli A, Zlobec I, Baker K, Minoo P, Tornillo L, Terracciano L, et al. Prognostic significance of mucins in colorectal cancer with different DNA mismatch-repair status. J Clin Pathol. 2007;60(5):534-9.
26. Luo C, Cen S, Ding G, Wu W. Mucinous colorectal adenocarcinoma: clinical pathology and treatment options. Cancer Commun (Lond). 2019;39(1):13.
27. Fernandes GDS, Braghiroli MI, Artioli M, Paterlini A, Teixeira MC, Gumz BP, et al. Combination of Irinotecan, Oxaliplatin and 5-Fluorouracil as a Rechallenge Regimen for Heavily Pretreated Metastatic Colorectal Cancer Patients. J Gastrointest Cancer. 2018;49(4):470-5.
28. Chen W, Lian W, Yuan Y, Li M. The synergistic effects of oxaliplatin and piperlongumine on colorectal cancer are mediated by oxidative stress. Cell Death Dis. 2019;10(8):600.
29. Ma CJ, Huang CW, Yeh YS, Tsai HL, Hu HM, Wu IC, et al. Regorafenib Plus FOLFIRI With Irinotecan Dose Escalated According to Uridine Diphosphate Glucuronosyltransferase 1A1 Genotyping in Patients With Metastatic Colorectal Cancer. Oncol Res. 2017;25(5):673-9.
30. Spiliotis J, Halkia E, de Bree E. Treatment of peritoneal surface malignancies with hyperthermic intraperitoneal chemotherapy-current perspectives. Curr Oncol. 2016;23(3):e266-75.
31. van der Zee J. Heating the patient: a promising approach? Annals of Oncology. 2002;13(8):1173-84.
32. Longley DB, Harkin DP, Johnston PG. 5-Fluorouracil: mechanisms of action and clinical strategies. Nature Reviews Cancer. 2003;3(5):330-8.
33. Bajetta E, Beretta E, Di Bartolomeo M, Cortinovis D, Ferrario E, Dognini G, et al. Efficacy of Treatment with Irinotecan and Oxaliplatin Combination in FU-Resistant Metastatic Colorectal Cancer Patients. Oncology. 2004;66(2):132-7.
34. Gramont Ad, Figer A, Seymour M, Homerin M, Hmissi A, Cassidy J, et al. Leucovorin and Fluorouracil With or Without Oxaliplatin as First-Line Treatment in Advanced Colorectal Cancer. Journal of Clinical Oncology. 2000;18(16):2938-47.
35. Li J, Qin S, Xu R, Yau TC, Ma B, Pan H, et al. Regorafenib plus best supportive care versus placebo plus best supportive care in Asian patients with previously treated metastatic colorectal cancer (CONCUR): a randomised, double-blind, placebo-controlled, phase 3 trial. Lancet Oncol. 2015;16(6):619-29.
36. Bijnsdorp IV, Giovannetti E, Peters GJ. Analysis of Drug Interactions. In: Cree IA, editor. Cancer Cell Culture: Methods and Protocols. Totowa, NJ: Humana Press; 2011. p. 421-34.
37. Chen D, Wei L, Yu J, Zhang L. Regorafenib inhibits colorectal tumor growth through PUMA-mediated apoptosis. Clin Cancer Res. 2014;20(13):3472-84.
38. Fondevila F, Mendez-Blanco C, Fernandez-Palanca P, Gonzalez-Gallego J, Mauriz JL. Anti-tumoral activity of single and combined regorafenib treatments in preclinical models of liver and gastrointestinal cancers. Exp Mol Med. 2019;51(9):109.
39. Krishnamoorthy SK, Relias V, Sebastian S, Jayaraman V, Saif MW. Management of regorafenib-related toxicities: a review. Therap Adv Gastroenterol. 2015;8(5):285-97.
40. Goel G. Evolution of regorafenib from bench to bedside in colorectal cancer: Is it an attractive option or merely a "me too" drug? Cancer Manag Res. 2018;10:425-37.
41. Marks EI, Tan C, Zhang J, Zhou L, Yang Z, Scicchitano A, et al. Regorafenib with a fluoropyrimidine for metastatic colorectal cancer after progression on multiple 5-FU-containing combination therapies and regorafenib monotherapy. Cancer Biol Ther. 2015;16(12):1710-9.

42. Bekaii-Saab TS, Ou FS, Ahn DH, Boland PM, Ciombor KK, Heying EN, et al. Regorafenib dose-optimisation in patients with refractory metastatic colorectal cancer (ReDOS): a randomised, multicentre, open-label, phase 2 study. Lancet Oncol. 2019;20(8):1070-82.
43. Dhillon S. Regorafenib: A Review in Metastatic Colorectal Cancer. Drugs. 2018;78(11):1133-44.
44. Fujita K, Kubota Y, Ishida H, Sasaki Y. Irinotecan, a key chemotherapeutic drug for metastatic colorectal cancer. World J Gastroenterol. 2015;21(43):12234-48.
45. Haug K, Kravik KL, De Angelis PM. Cellular response to irinotecan in colon cancer cell lines showing differential response to 5-fluorouracil. Anticancer Res. 2008;28(2a):583-92.
46. Peleg R, Bobilev D, Priel E. Topoisomerase I as a target of erlotinib and gefitinib: efficacy of combined treatments with camptothecin. Int J Oncol. 2014;44(3):934-42.
47. Douillard JY, Cunningham D, Roth AD, Navarro M, James RD, Karasek P, et al. Irinotecan combined with fluorouracil compared with fluorouracil alone as first-line treatment for metastatic colorectal cancer: a multicentre randomised trial. The Lancet. 2000;355(9209):1041-7.
48. Graham J, Muhsin M, Kirkpatrick P. Oxaliplatin. Nature Reviews Drug Discovery. 2004;3(1):11-2.
49. Comella P, Casaretti R, Sandomenico C, Avallone A, Franco L. Role of oxaliplatin in the treatment of colorectal cancer. Ther Clin Risk Manag. 2009;5(1):229-38.
50. de Gramont A, Vignoud J, Tournigand C, Louvet C, André T, Varette C, et al. Oxaliplatin with high-dose leucovorin and 5-fluorouracil 48-hour continuous infusion in pretreated metastatic colorectal cancer. European Journal of Cancer. 1997;33(2):214-9.
51. Hassan B, Akcakanat A, Holder AM, Meric-Bernstam F. Targeting the PI3-kinase/Akt/mTOR signaling pathway. Surg Oncol Clin N Am. 2013;22(4):641-64.
52. Koveitypour Z, Panahi F, Vakilian M, Peymani M, Seyed Forootan F, Nasr Esfahani MH, et al. Signaling pathways involved in colorectal cancer progression. Cell & Bioscience. 2019;9(1):97.
53. Lin L, Liu A, Peng Z, Lin HJ, Li PK, Li C, et al. STAT3 is necessary for proliferation and survival in colon cancer-initiating cells. Cancer Res. 2011;71(23):7226-37.
54. Fang JY, Richardson BC. The MAPK signalling pathways and colorectal cancer. The Lancet Oncology. 2005;6(5):322-7.
55. Paillas S, Boissière F, Bibeau F, Denouel A, Mollevi C, Causse A, et al. Targeting the p38 MAPK pathway inhibits irinotecan resistance in colon adenocarcinoma. Cancer Res. 2011;71(3):1041-9.
56. Henry JT, Johnson B. Current and evolving biomarkers for precision oncology in the management of metastatic colorectal cancer. Chinese Clinical Oncology. 2019.
57. Liu P, Cheng H, Roberts TM, Zhao JJ. Targeting the phosphoinositide 3-kinase pathway in cancer. Nat Rev Drug Discov. 2009;8(8):627-44.
58. Nair R, Tolentino JH, Hazlehurst L. Role of STAT3 in transformation and drug resistance in CML. Frontiers in oncology. 2012;2:30.
59. Dickey JS, Redon CE, Nakamura AJ, Baird BJ, Sedelnikova OA, Bonner WM. H2AX: functional roles and potential applications. Chromosoma. 2009;118(6):683-92.
60. Morales J, Li L, Fattah FJ, Dong Y, Bey EA, Patel M, et al. Review of poly (ADP-ribose) polymerase (PARP) mechanisms of action and rationale for targeting in cancer and other diseases. Crit Rev Eukaryot Gene Expr. 2014;24(1):15-28.
61. https://web.expasy.org/cellosaurus/CVCL_0547. Cellosaurus SW620 (CVCL_0547). 2020.
62. https://web.expasy.org/cellosaurus/CVCL_0291. Cellosaurus HCT 116 (CVCL_0291). 2020.
63. https://www.lgcstandards-atcc.org/products/all/CCL-247.aspx?geo_country=no#specifications. HCT 116 (ATCC® CCL-247™) In: ATCC, editor.
64. Drexler HG, Uphoff CC. Mycoplasma contamination of cell cultures: Incidence, sources, effects, detection, elimination, prevention. Cytotechnology. 2002;39(2):75-90.

65. Flatmark K, Guldvik IJ, Svensson H, Fleten KG, Florenes VA, Reed W, et al. Immunotoxin targeting EpCAM effectively inhibits peritoneal tumor growth in experimental models of mucinous peritoneal surface malignancies. Int J Cancer. 2013;133(6):1497-506.
66. Riss TL MR, Niles AL, et al. Cell Viability Assays. Bethesda (MD): Eli Lilly & Company and the National Center for Advancing Translational Sciences. 2013.
67. Mahmood T, Yang PC. Western blot: technique, theory, and trouble shooting. N Am J Med Sci. 2012;4(9):429-34.
68. Aljubran A, Elshenawy MA, Kandil M, Zahir MN, Shaheen A, Gad A, et al. Efficacy of Regorafenib in Metastatic Colorectal Cancer: A Multi-institutional Retrospective Study. Clin Med Insights Oncol. 2019;13:1179554918825447.
69. Li J, Qin S, Xu R, Yau TCC, Ma B, Pan H, et al. Regorafenib plus best supportive care versus placebo plus best supportive care in Asian patients with previously treated metastatic colorectal cancer (CONCUR): a randomised, double-blind, placebo-controlled, phase 3 trial. The Lancet Oncology. 2015;16(6):619-29.
70. Fan L-C, Teng H-W, Shiau C-W, Lin H, Hung M-H, Chen Y-L, et al. SHP-1 is a target of regorafenib in colorectal cancer. Oncotarget. 2014;5.
71. Tai W-T, Chu P-Y, Shiau C-W, Chen Y-L, Li Y-S, Hung M-H, et al. STAT3 Mediates Regorafenib-Induced Apoptosis in Hepatocellular Carcinoma. Clinical Cancer Research. 2014;20(22):5768.
72. Schultheis B, Folprecht G, Kuhlmann J, Ehrenberg R, Hacker UT, Köhne CH, et al. Regorafenib in combination with FOLFOX or FOLFIRI as first- or second-line treatment of colorectal cancer: results of a multicenter, phase Ib study. Ann Oncol. 2013;24(6):1560-7.
73. Mazard T, Causse A, Simony J, Leconet W, Vezzio-Vie N, Torro A, et al. Sorafenib overcomes irinotecan resistance in colorectal cancer by inhibiting the ABCG2 drug-efflux pump. Mol Cancer Ther. 2013;12(10):2121-34.
74. Koizumi F, Kanzawa F, Ueda Y, Koh Y, Tsukiyama S, Taguchi F, et al. Synergistic interaction between the EGFR tyrosine kinase inhibitor gefitinib (?Iressa?) and the DNA topoisomerase I inhibitor CPT-11 (irinotecan) in human colorectal cancer cells. International journal of cancer Journal international du cancer. 2004;108:464-72.
75. Ma C-J, Chang T-K, Tsai H-L, Su W-C, Huang C-W, Yeh Y-S, et al. Regorafenib plus FOLFIRI with irinotecan dose escalated according to uridine diphosphate glucuronosyltransferase 1A1genotyping in previous treated metastatic colorectal cancer patients:study protocol for a randomized controlled trial. Trials. 2019;20(1):751.
76. Guichard S, Arnould S, Hennebelle I, Bugat R, Canal P. Combination of oxaliplatin and irinotecan on human colon cancer cell lines: activity in vitro and in vivo. Anticancer Drugs. 2001;12(9):741-51.
77. Bradshaw-Pierce E, Pitts T, Kulikowski G, Selby H, Merz A, Gustafson D, et al. Utilization of Quantitative In Vivo Pharmacology Approaches to Assess Combination Effects of Everolimus and Irinotecan in Mouse Xenograft Models of Colorectal Cancer. PloS one. 2013;8:e58089.
78. Argilés G, Saunders MP, Rivera F, Sobrero A, Benson A, Guillén Ponce C, et al. Regorafenib plus modified FOLFOX6 as first-line treatment of metastatic colorectal cancer: A phase II trial. European Journal of Cancer. 2015;51(8):942-9.
79. Zheng C, Zhang Y, Mao W, Li Q. Increasing colorectal cancer cell sensitivity to oxaliplatin through hyperthermia and chloroquine treatment. 2016;9:496-508.
80. Dilly AK, Honick BD, Lee YJ, Guo ZS, Zeh HJ, Bartlett DL, et al. Targeting G-protein coupled receptor-related signaling pathway in a murine xenograft model of appendiceal pseudomyxoma peritonei. Oncotarget. 2017;8(63):106888-900.
81. Kesari M, Gaopande V, Joshi A, Babanagare S, Gogate B, Khadilkar A. Immunohistochemical study of MUC1, MUC2 and MUC5AC in colorectal carcinoma and review of literature. Indian journal of gastroenterology : official journal of the Indian Society of Gastroenterology. 2015;34.

82. Thorpe D, Sultani M, Stringer A. Irinotecan induces enterocyte cell death and changes to muc2 and muc4 composition during mucositis in a tumour-bearing DA rat model. Cancer Chemother Pharmacol. 2019;83(5):893-904.
83. Dilly AK, Song X, Zeh HJ, Guo ZS, Lee YJ, Bartlett DL, et al. Mitogen-activated protein kinase inhibition reduces mucin 2 production and mucinous tumor growth. Translational Research. 2015;166(4):344-54.
84. Shaojun C, Li H, Haixin H, Guisheng L. Expression of Topoisomerase 1 and carboxylesterase 2 correlates with irinotecan treatment response in metastatic colorectal cancer. Cancer Biol Ther. 2018;19(3):153-9.
85. Desai SD, Li TK, Rodriguez-Bauman A, Rubin EH, Liu LF. Ubiquitin/26S proteasome-mediated degradation of topoisomerase I as a resistance mechanism to camptothecin in tumor cells. Cancer Res. 2001;61(15):5926-32.
86. Sharma NK, Kumar A, Kumari A, Tokar EJ, Waalkes MP, Bortner CD, et al. Nitric Oxide Down-Regulates Topoisomerase I and Induces Camptothecin Resistance in Human Breast MCF-7 Tumor Cells. PLoS One. 2015;10(11):e0141897.
87. Kaur G, Dufour JM. Cell lines: Valuable tools or useless artifacts. Spermatogenesis. 2012;2(1):1-5.
88. Kapałczyńska M, Kolenda T, Przybyła W, Zajączkowska M, Teresiak A, Filas V, et al. 2D and 3D cell cultures - a comparison of different types of cancer cell cultures. Arch Med Sci. 2018;14(4):910-9.
89. Lock JY, Carlson TL, Carrier RL. Mucus models to evaluate the diffusion of drugs and particles. Adv Drug Deliv Rev. 2018;124:34-49.
90. Single A, Beetham H, Telford B, Guilford P, Chen A. A Comparison of Real-Time and Endpoint Cell Viability Assays for Improved Synthetic Lethal Drug Validation. Journal of Biomolecular Screening. 2015;20.
91. Wang P, Henning SM, Heber D. Limitations of MTT and MTS-based assays for measurement of antiproliferative activity of green tea polyphenols. PLoS One. 2010;5(4):e10202.
92. Aslantürk ÖS. In Vitro Cytotoxicity and Cell Viability Assays: Principles, Advantages, and Disadvantages. In: Larramendy ML, Soloneski S, editors. Genotoxicity - A Predictable Risk to Our Actual World: InTech; 2018.

8 APPENDIX

Appendix A: Materials and equipment

Cell culture	**Producer**	**Cat. number**
Nunc™ Easy Flask™ 75 cm^2 Nunclon™ Delta Surface	Thermo Scientific	-
RPMI-1640 medium	Sigma®Life Science	R0883
L-alanyl-L-glutamine (Glutamax) 2 mM	Sigma®Life Science	G8541
Fetal Bovine Serum (FBS) 10%	Sigma®Life Science	F7524
EDTA (0.02%)	Sigma®Life Science	E8008
Trypsin-EDTA	Sigma Aldrich	T3924
Trypan- blue Stain (0.4%)	NanoEnTek	T10282
CountessII Automated Cell Counter	Invitrogen	-
EVE cell counting slide	NanoEnTek	EVS-050
96 weils plates	Falcon	353072
IncuCyte®Live Cell analysis	Essen Bioscience	-
Rely + On Virkon tablets	Lanxess	-
DMSO (Dimethylsulfoxide)	Sigma Aldrich	D2650
Regorafenib	Bayer	-
Oxaliplatin (5 mg/mL)	Hospira	137110
Irinotecan hydrochloride trihydrate (20 mg/mL)	Accord	55866
MTS assay	**Producer**	**Cat. number**
CellTiter 96®AQueous One Solution Cell Proliferation assay (MTS)	Promega	G3581
VIKTOR™ X3 Multimode plate reader	PerkinElmer	-
Protein analysis	**Producer**	**Cat. number**
Dulbecco's Phosphate Buffered Saline	Sigma Aldrich	D8537
Nunc™ Easy Flask™ 25 cm^2 Nunclon™ Delta Surface	Thermo Scientific	-
Pierce™ BCA protein assay kit	Thermo Scientific	23225
Western Blot Immunoassay	**Producer**	**Cat. number**
Supersignal® West Dura Extended Duration Substrate	Thermo Scientific	34076
SeeBlue® Plus2 Prestained standard	Invitrogen	LC5925
LDS Sample Buffer (4x)	Invitrogen	NP0009
NuPAGE® Sample reducing agent (10x)	Thermo Fisher Scientific	NP0009
NuPAGE MOPS SDS running buffer (20X)	Invitrogen	NP001-02
iBlot® 2NC Regular Stacks	Invitrogen by Thermo Fisher Scientific	IB23001
NuPAGE™ 4-12% Bis-Tris Midi gel	Invitrogen by Thermo Fisher Scientific	WG1402BOX
Bovine Serum Albumin Fraction V	Roche	10735086001

Polyclonal Goat Anti Rabbit Immunoglobulins/HRP	Dako	P0448
Polyclonal Rabbit Anti-Mouse Immunoglobulins HRP	Dako	P0260
Phospho-STAT3 (Tyr705) (D3A7) XP® Rabbit mAb	Cell signaling technology	9145S
STAT-3 124H6 Mouse mAb	Cell signaling technology	9139S
PARP Rabbit Antibody	Cell signaling technology	9542S
Phospho-p44/42 MARPK (ERK (1/2) (Thr202/Tyr204) (D13.14.4E) XP® Rabbit mAb	Cell signaling technology	4370P
Phospho-S6 Ribosomal Protein (Ser235/236) (D57.2.2E) XP® Rabbit mAb	Cell signaling technology	4858P
S6 Ribosomal protein Rabbit mAb	Cell signaling technology	2217S
Phospho-H2AX mouse Ab	Millipore	05636
p44/42 MAPK (ERK1/2) (137F5) rabbit mAb	Cell signaling technology	4695S
Ultrapure™ 1M Tris-HCl pH7.5	Gibco® Life technologies	15567-027
Tween 20	Sigma Aldrich	S6740684 336
Glyserol (87%)	GE Healthcare Life Science	17 1325 01
1 M NaF	Sigma	7681-49-4
5M NaCl	Millipore	K45393104410
10% Nonidet P-40	VWR	9036-19-5
Protease Inhibitor cOmplete Tablets, Mini EASYpack	Roche	05056489001
Phosphatase inhibitor PhosSTOP EASY pack	Roche	04906837001
Mycoplasma testing	**Producer**	**Cat. number**
Mycoplasma Detection Kit Venor®GeM Classic	Minerva biolabs	11-1250
c1000 Touch™ Thermal cycler	BioRad	-
MultiDoc-it Digital Imaging System UVP	-	-
Ex vivo culture	**Producer**	**Cat. number**
Penicillin Streptomucin	Sigma Aldrich	P4458
RNA extraction	**Producer**	**Cat. number**
Trizol	Ambion	15596026
Chloroform	Millipore	K44888645337
Linear Acrylamid (5mg/ml)	Ambion	00429066
Isopropanol (2-propanol)	VWR	20842312
70% EtOH	Antibac	SE10065860
Sterile water	Braun	180128091
cDNA synthesis	**Producer**	**Cat. number**
qScript™ cDNA Synthesis Kit	QuantaBio	95047-100
qPCR	**Producer**	**Cat. number**
PerfeCTa® qPCR Supermix	QuantaBio	95050-500

Primermix	EuroGenTec	4721522 4121523
Universal Probe Library 35	Roche	192781
MUC-2	BioRad	12001950
Immunofluorescence	**Producer**	**Cat. number**
Prolong™ Gold Antifade Reagent with DAPI	Invitrogen	P36935
Lab Tek-II chamber Slide	Thermo Fisher Scientific	154534
Alexa Fluor™ 546 Phalloidin	Thermo Fisher Scientific	A22283
Anti- topoisomerase antibody (1 mg/mL)	Abcam	ab85038
Saponin	Sigma Aldrich	S7900
Secondary antibody donkey anti -rabbit	Thermo Fisher Scientific	A21206
Paraformaldehyde 32%	Electron microscopy sciences	15714

Appendix B: Reagent preparation

TBST buffer solution	**Volume (mL)**
Tween-20	5
5M NaCl	30
1M Tris -HCl	25
ddH_2O	940
Lysis buffer	**Volume (mL)**
1M Tris- HCl pH 7.5	1
5M NaCl	1.37
1M NaF	5
Glyserol (87%)	5
10% NP-40	5
ddH_2O	32.63
NuPAGE MOPS SDS Running Buffer	**Volume (mL)**
ddH_2O	1900
MOPS (20X)	100
Loading buffer (gel electrophoresis)	**Volume (mL)**
NuPAGE LDS Sample Buffer (4x)	0.075
Sample reducing agent (10x)	0.030
BCA solution (BCA assay)	**Volume (mL)**
Reagent A	9.8
Reagent B	0.2
5% nonfat dry-milk solution	**Volume (g, mL)**
Nonfat dry milk	2.5 g

TBST	50
BSA solution	**Volume (mL, g)**
BSA	2.5 g
TBST	50
Tween-20 solution	**Volume (mL)**
Tween- 20	100
ddH_2O	400

Appendix C: Antibodies used for Western Blotting

Antibody	Secondary antibody	Diluting agent	Western Blot concentration	Molecular weight (kDa)
Phospho-ERK	Anti-Rabbit	BSA	1:1000	42/44
Total ERK	Anti-Rabbit	BSA	1:1000	42/44
α-tubulin	Anti-Mouse	Nonfat dry milk	1:5000	50
Phospho-S6	Anti-Rabbit	BSA	1:2000	32
Total S6	Anti-Rabbit	BSA	1:1000	32
Phospho-H2AX	Anti-Mouse	Nonfat dry milk	1:500	17
Gamma-Histone 3 (H3)	Anti-Rabbit	Nonfat dry milk	1:2000	17
Phospho-STAT3	Anti-Rabbit	BSA	1:2000	79.86
Total STAT3	Anti-Mouse	Nonfat dry milk	1:1000	79.86
PARP	Anti-Rabbit	Nonfat dry milk	1:1000	112/89
Secondary antibody (Anti-Rabbit)	-	BSA	1:3000	-
Secondary antibody (Anti-Mouse)	-	Nonfat dry milk	1:5000	-

Appendix D: Results from ID testing of cell lines

Table D1: ID testing for HCT-116 cell line. The top row shows the result from the ID testing performed by Genetica, while the bottom row is the previously published STR results for HCT-116 from ATCC.

	Sample reference nbr	LabCorpSpecNbr	LabCorpCaseNbr	D3S1358	THO1	D21S11	D18S51	Penta E	D5S818	D13S317	D7S820
	HCT-116 parental	97C90660	CX4007255	12,16,17	8,9	29,30	17	13,14	10,11	10,12	11,12
ATCC	-	-	-	12,18,19	8,9	29,30	16,17	13,14	10,11	10,12	11,12

	Sample reference nbr	LabCorpSpecNbr	Lab Corp Case Nbr	D16S539	CSF1PO	PentaD	vWA	D8S1179	TPOX	FGA	AMEL (amelogenin)	mouse
	HCT-116 parental	97C90660	CX400072 55	11,13	7,10	9,13	16,17,21	12,14	8	18,23	X	Not detected
ATCC	-	-	-	11,13	7,10	9,13	17,22	12,14	8,9	18,23	X, Y	-

*The upper row are specific loci where amelogenin is gender determining locus, the lower row are specific alleles.

Table D2: ID testing for SW-620 cell line. The top row shows the result from the ID testing performed by Genetica, while the bottom row is the previously published STR results for SW-620 from ATCC.

	Sample reference nbr	LabCorpSpecNbr	LabCorpCaseNbr	D3S1358	THO1	D21S11	D18S51	Penta E	D5S818	D13S317	D7S820
	SW-620	-	-	16	8	30	12,16	10	13	12	25
ATCC	-	-	-	16	8	30,30.2	13	10	13	12	8,9

	Sample reference nbr	LabCorpSpecNbr	LabCorpCaseNbr	D16S539	CSF1PO	PentaD	vWA	D8S1179	TPOX	FGA	AMEL (amelogenin)
	SW-620	-	-	9,13	13,14	8	15,16	8,15	11	10	X
ATCC	-	-	-	9,13	13,14	9,15	16	13	11	24	X

*The upper row are specific loci where amelogenin is gender determining locus, the lower row are specific alleles.

Appendix E: Determination of cell density for experiments

a)

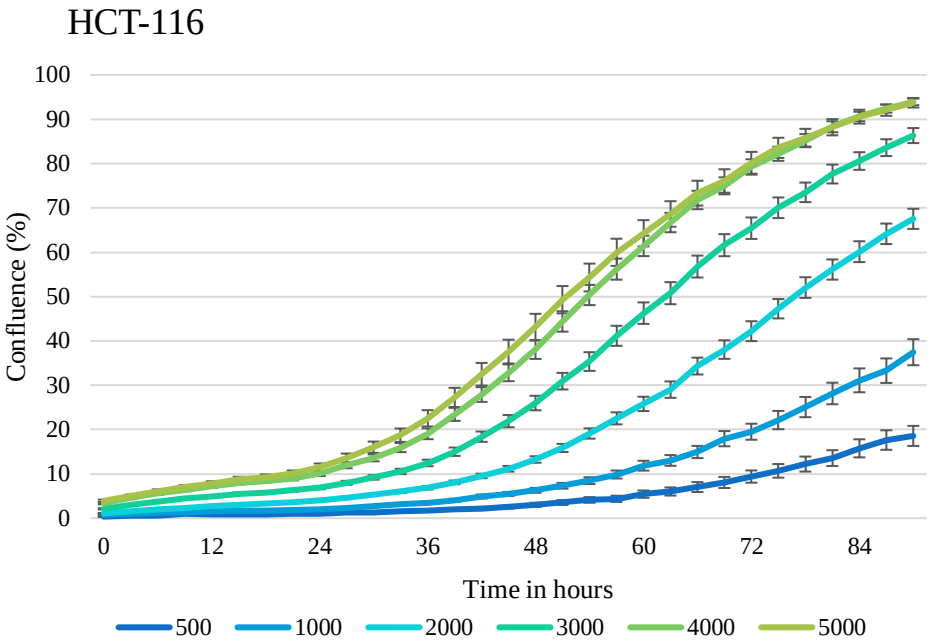

b)

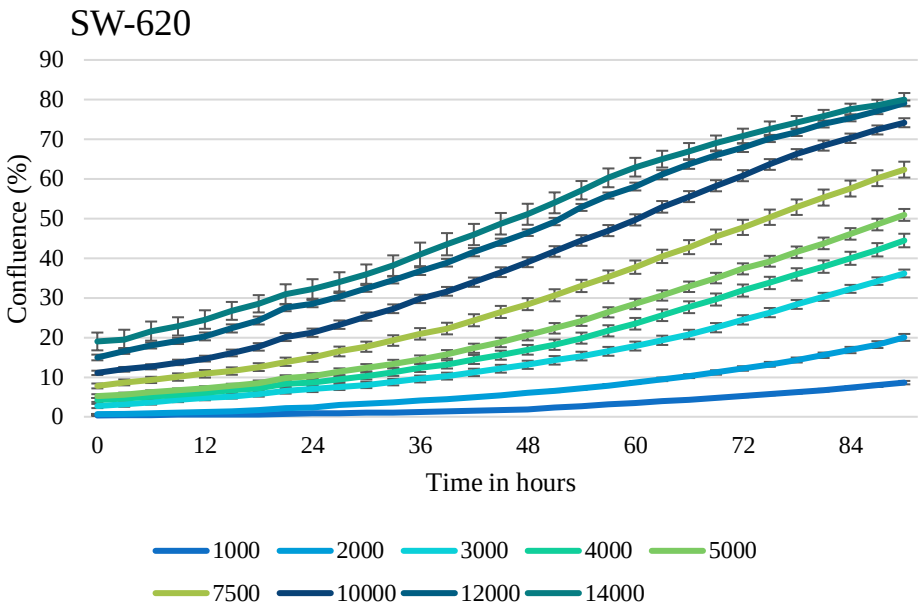

Figure E: a) IncuCyte results for determination of HCT-116 cell quantities to be used in the experiments. Error bars indicate Standard Error of the Mean (SEM). Cells 500 (n =2), 1000-5000 (n =4). b) IncuCyte results for determination of SW-620 cell quantities to be used in the experiments. Error bars indicate Standard Error of the Mean (SEM). Cells 1000-2000 (n =2), 3000-10.000 (n =3), 12.000-14.000 (n =1).

Appendix F: Combination index and cut-off values

Table F: Overview of cut-off values for combination index calculations and their indications [36].

Effect	Cutoff values
Very strong synergism	< 0.1
Strong synergism	0.1-0.3
Synergism	0.3 -0.7
Moderate synergism	0.7-0.85
Slight synergism	0.85-0.9
Nearly additive	0.9-1.1
Slight antagonism	1.1-1.2
Moderate antagonism	1.2-1.45
Antagonism	1.45-3.3
Strong antagonism	3.3-10
Very strong antagonism	> 10

Appendix G: Cell viability measurement with MTS

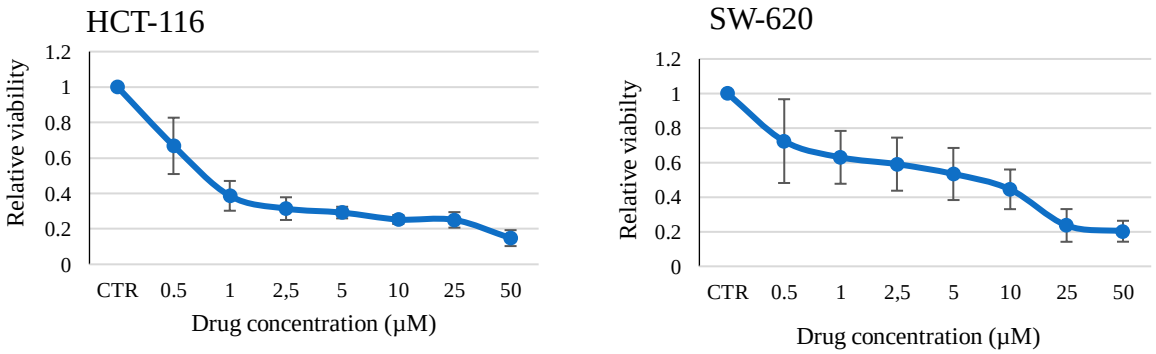

Figure G1: Measurement of viability of HCT-116 and SW-620 cells with MTS assay after 72-hour mono-treatment with different concentration of oxaliplatin. The error bars indicate standard deviation (n=2).

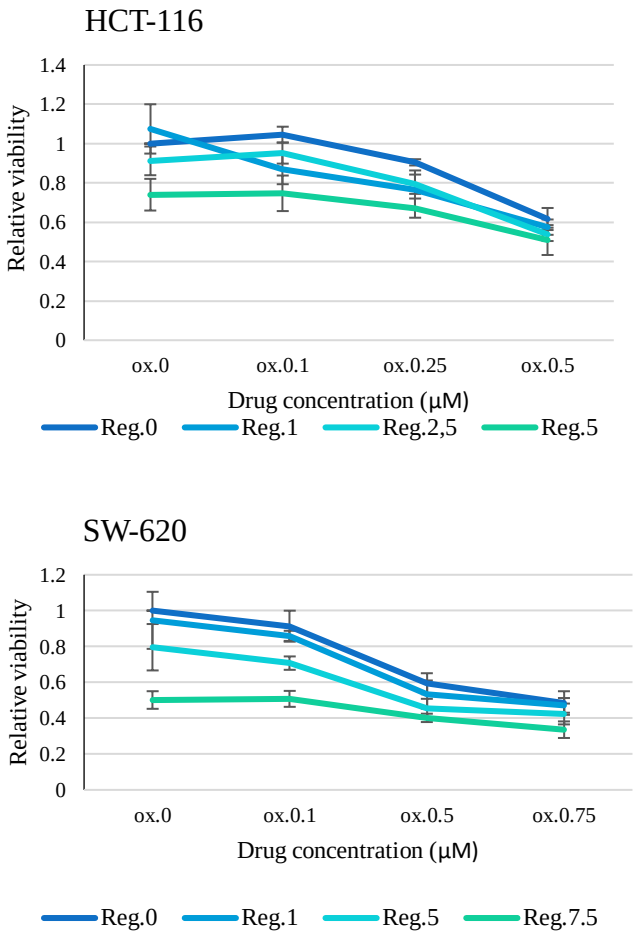

Figure G2: MTS assay measurement of dose-effect relationship in HCT-116 and SW-620 cells with regorafenib and oxaliplatin as single agent and in combination after 72-hour, to determine if a given treatment gain synergistic effect. The error bars indicate standard deviation (n=3).